

THESIS FOR THE DEGREE OF DOCTOR OF PHILOSOPHY

**Mercury cycling in the global marine
environment**

MICHELLE NERENTORP MASTROMONACO



CHALMERS

Department of Chemistry and Chemical Engineering
CHALMERS UNIVERSITY OF TECHNOLOGY
Gothenburg, Sweden 2016

Mercury cycling in the global marine environment

Michelle Nerentorp Mastromonaco

© Michelle Nerentorp Mastromonaco, 2016.

ISBN 978-91-7597-478-1

Doktorsavhandlingar vid Chalmers tekniska högskola
Löp nr. 4159
ISSN 0346-718X

Department of Chemistry and Chemical Engineering
Chalmers University of Technology
SE-412 96 Göteborg
Sweden
Telephone +46 (0)31 772 1000

Author email: michelle.nerentorp@chalmers.se

Cover Picture: Global cycling of mercury in the marine environment showing locations of measurements presented in this thesis (Picture created by Donnie Mastromonaco).

Printed by Chalmers Reproservice
Göteborg, Sweden 2016

Abstract

Mercury is a globally distributed contaminant that exists in the atmosphere in its elemental form as a stable monoatomic gas. Having a residence time of around one year in air allows it to be transported far from emission sources and end up in polar ecosystems. Gaseous elemental mercury (GEM) can in air be oxidized by photo-induced processes which produce water soluble oxidized forms of mercury which are more easily deposited. Deposited mercury can in the environment be transformed to organic and bio-accumulating compounds which are neurotoxic, making mercury a global concern.

Deposited oxidized mercury into the sea can be reduced back to the elemental form (GEM) and be re-emitted to air. This re-evasion constitutes of around 30% of the total emissions of mercury to air and originates from both natural and anthropogenic sources. Models have estimated that the yearly mercury emission from global sea surfaces is between 2000 and 3000 tonnes. The mercury flux rate at the interphase between air and water depends on the Henry's law constant, the concentration gradient and the gas transfer velocity. How to properly account for weather parameters such as wind speed, and how to accurately adjust the flux model to mercury (originally developed for CO₂) has been debated in the literature and have resulted in diverse results of mercury flux rates.

In this work, mercury has been measured in air and in seawater during several campaigns in Antarctica, the Mediterranean Sea, the west coast of Sweden, Northern Finland and in the Arctic. From measured concentrations of mercury, the mercury flux rates from the studied areas were calculated using the gas exchange model described in Johnson (2010). Large spatial and seasonal variations of measured mercury concentrations were found which resulted in similar variations in calculated flux rates.

In Antarctica and the Arctic, high concentrations of mercury were also measured in the sea ice environment. Seasonal variations in mercury concentrations were found and a correlation between solar radiation and the photo-production of elemental mercury in sea ice was discovered. The sea ice was suggested to affect the global marine cycling of mercury in several ways: acting as a cap preventing elemental mercury to evade from sea surfaces in Polar Regions, acting as barrier against direct atmospheric deposition and being a significant reservoir of mercury.

Climate change will likely affect the cycling of mercury in global marine environments due to an increase in temperature, leading to enhanced mercury evasion, and diminishing and melting sea ice causing an increased input of mercury into polar oceans. Results presented in this thesis bring new insights about how mercury is cycling in the global marine environment and the new collected mercury data from remote and inaccessible areas are valuable for future modeling. However, more research is needed to further understand and quantify the accumulation of mercury in vulnerable marine ecosystems.

Keywords: Mercury cycling, mercury flux, seawater, air, sea ice, snow, seasonal and spatial variation

List of appended papers

This thesis is based on the following papers:

I. Antarctic winter mercury and ozone depletion events over sea ice

Nerentorp Mastromonaco, M.; Gårdfeldt, K.; Jourdain, B.; Abrahamsson, K.; Granfors, A.; Ahnoff, M.; Dommergue, A.; Méjean, G.; Jacobi, H.-W.
Atmospheric Environment, **129**:125-132 (2016)

II. Seasonal flux of mercury over West Antarctic Seas

Nerentorp Mastromonaco, M.; Gårdfeldt, K.; Langer, S
In press. Marine Chemistry

III. Speciation of mercury in identified Antarctic water masses

Nerentorp Mastromonaco, M.; Gårdfeldt, K.; Assman, K. M.; Langer, S.; Delali, T.; Shlyapnikov, Y.M.; Zivkovic, I.; Horvat, M.
Submitted to Marine Chemistry

IV. Seasonal study of mercury species in the Antarctic sea ice environment

Nerentorp Mastromonaco, M.; Gårdfeldt, K.; Langer, S.; Dommergue, A.
Submitted to Environmental Science & Technology

V. Seasonal and spatial evasion of mercury from the western Mediterranean Sea

Nerentorp Mastromonaco, M.; Gårdfeldt, K.; Wängberg, I.
Submitted to Marine Chemistry

Contribution to appended papers

I. I performed the air measurements of mercury, prepared figures, wrote the first draft and participated in the development of the article.

II. I performed the air and water measurements of mercury during winter and spring in Antarctica, performed the flux calculations, wrote the first draft and participated in the development of the article.

III. I participated during seawater sampling during winter and spring in Antarctica, performed the majority of dissolved gaseous mercury analyses, collected samples for methyl- and total mercury analyses. I wrote the first draft of the paper and participated in the development of the article.

IV. I participated during sampling on sea ice during winter and spring in Antarctica. I did analyses of elemental mercury in the samples and collected samples for total mercury analysis. I wrote the first draft of the paper and participated in the development of the article.

V. I participated during the two campaigns to the Mediterranean Sea and carried out the air and water measurements of mercury together with my supervisors. I performed the flux calculations of mercury and wrote the first draft of the paper. I participated in the development of the article.

Related publications not included in this thesis

VI. Airborne mercury species at the Råö background monitoring site in Sweden: Distribution of mercury as an effect of long range transport

Wängberg, I.; Nerentorp Mastromonaco, M.; Munthe, J.; Gårdfeldt K.

Atmospheric Chemistry and Physics, Discussion, doi:10.5194/acp-2016-526, accepted, 2016.

VII. Photo-reduction of mercury in Antarctic Sea ice

Nerentorp Mastromonaco, M.; Gårdfeldt, K.; Mattsson, E.

In prep.

VIII. Comparison of two measurement methods of dissolved gaseous mercury concentrations and estimations of supersaturation grade and mercury fluxes during a research campaign at the Mediterranean Sea

Nerentorp Mastromonaco, M.; Gårdfeldt, K.; Wängberg, I.

Proceedings of the 16th International Conference on Heavy Metals in the Environment (2267-1242. Vol 1 (2013).

IX. Speciation measurements of airborne mercury species in northern Finland; evidence for long range transport of air masses depleted in mercury

Nerentorp Mastromonaco, M.; Kyllönen, K.; Wängberg, I.; Kuronen, P.

Proceedings of the 16th International Conference on Heavy Metals in the Environment (2267-1242. Vol 1 (2013).

X. Chemical cycling and deposition of atmospheric mercury in Polar Regions: review of recent measurements and comparison with models

Angot, H.; Dastoor, A.; de Simone, F.; Gårdfeldt, K.; Gencarelli, C.N.; Hedgecock, I.M.; Langer, S.; Magand, O.; Nerentorp Mastromonaco, M.; Nordtrom, C.; Pfaffhuber, K.A.; Pirrone, N.; Ryjkov, A.; Selin, N.E.; Skov, H.; Song, S.; Sprovieri, F.; Steffen, A.; Toyota, K.; Travnikov, O.; Yang, X.; Dommergue, A.

Atmospheric Chemistry and Physics, Discussion, doi:10.5194/acp-2016-509, in review, 2016.

XI. Atmospheric mercury concentrations observed at ground-based monitoring sites globally distributed in the framework of the GMOS network

Sprovieri, F.; Pirrone, N.; Bencardino, M.; D'Amore, F.; Carbone, F.; Cinnirella, S.; Mannarino, V.; Landis, M.; Ebinghaus, R.; Weigelt, A.; Brunke, E-G.; Labuschagne, C.; Martin, L.; Munthe, J.; Wängberg, I.; Artaxo, P.; Morais, F.; Cairns, W.; Barbante, C.; del Carmen Diéguez, M.; Elizabeth Garcia, P.; Dommergue, A.; Angot, H.; Magand, O.; Skov, H.; Horvat, M.; Kotnik, J.; Alana Read, K.; Mendes Neves, L.; Manfred Gawlik, B.; Sena, F.; Mashyanov, N.; Arckadievich Obolkin, V.; Wip, D.; Bin Feng, X.; Zhang, H.; Fu, X.; Ramachandran, R.; Cossa, D.; Knoery, J.; Maruszczak, N.; Nerentorp Mastromonaco, M.; Nordtrom, C.

Atmospheric Chemistry and Physics, Discussion, doi:10.5194/acp-2016-466, in review, 2016.

Populärvetenskaplig sammanfattning

Kvicksilver är ett globalt spridat miljögift som existerar i luft i elementär form som en stabil monoatomär gas. Det har en uppehållstid i luft på ca 1 år vilket gör att det kan spridas till avlägsna platser långt från naturliga och antropogena utsläppskällor. Gasformigt elementärt kvicksilver kan oxideras i luft genom foto-inducerade processer som producerar vattenlösliga oxiderade former av kvicksilver som lättare deponeras till land och vattenytor. Deponerat kvicksilver kan omvandlas i naturen till organiska och bioackumulerande former som verkar som ett nervgift. Detta gör att kvicksilver är ett globalt problem.

Kvicksilver som deponerats i havsvatten kan reduceras tillbaka till sin elementära form och återemitteras till luft. Denna åter-emission bidrar globalt till ca 30 % av de totala årliga utsläppen av kvicksilver till luft och består ursprungligen av kvicksilver som tidigare släppts ut från både naturliga och industriella källor. Globala modeller har uppskattat att de årliga åter-emissionerna av kvicksilver från havsytor uppräknas till mellan 2000 och 3000 ton. Fluxhastigheten av kvicksilver i gränsskiktet mellan luft och vattenytan bestäms av Henrys lags konstant, koncentrationsgradienten och gasöverföringshastigheten. Hur man bäst tar hänsyn till olika väderparametrar såsom vindhastighet och hur man bör justera redan existerande fluxmodeller (som först designades för gaser som CO₂) till kvicksilver har diskuterats i litteraturen och har resulterat i varierande resultat av beräknad fluxhastighet.

I detta arbete har kvicksilver mätts i luft och i havsvatten under olika kampanjer utförda i Antarktis, Medelhavet, Sveriges västkust, i norra Finland och i Arktis. Utifrån mätta koncentrationer av kvicksilver så har fluxhastigheten beräknats för de olika studerade havsytorerna med hjälp av fluxmodellen som beskrivs i Johnson (2010). Stora geografiska skillnader och säsongvariationer av kvicksilverkoncentrationer hittades, vilket resulterade i liknande variationer i beräknade fluxhastigheter.

I Antarktis och i Arktis mättes höga koncentrationer av kvicksilver i havsismiljön. Kvicksilverkoncentrationerna i havsis uppvisade säsongvariationer och en korrelation mellan solljus och photo-produktion av elementärt kvicksilver i havsis upptäcktes. Här föreslås att havsis påverkar the globala kretsloppet av kvicksilver i havsmiljöer på flera sätt: genom att fungera som en kapsyl som hindrar emissioner av elementärt kvicksilver från polara havsytor, genom att fungera som en barriär mot direkt atmosfärisk deposition och genom att vara en signifikant reservoar av kvicksilver.

Klimatförändringar kommer troligtvis påverka kretsloppet av kvicksilver i havsmiljöer genom att en ökad temperatur leder till ökade åter-emissioner från havsytor och en minskande och smältande havsisutbredning resulterar i ökad input av kvicksilver till polarhaven. Resultat presenterade i denna avhandling bidrar till nya insikter om hur kvicksilver cirkulerar i globala havsmiljöer och de nya samlade data från avlägsna och svårtillgängliga platser är värdefulla för framtida globala modelleringar. Mer forskning behövs dock för att fullt förstå och kunna kvantifiera hur stor ackumulation av kvicksilver är i våra ömtåliga marina ekosystem.



KVICKSILVER OCH DÖD

i floderna som förgiftas
kvicksilver och död

i lektiden som stympats
kvicksilver och död

i det vatten som är de fördömdas
kvicksilver och död

i fiskarna som svälter
kvicksilver och död

i skorstenarna i staden
kvicksilver och död

i lungorna hos de eländiga
kvicksilver och död







i spädbarnen utan huvud
kvicksilver och död

i regnets bittra droppar
kvicksilver och död

i orden som gör dikten
kvicksilver och död

-Eliakin Rufino

Table of Contents

List of appended papers	iv
Abbreviations	x
Preface	
Background	1
My contribution to mercury research	2
Aim and research questions	2
Chapter 1 Mercury – The element	
Properties	3
Mercury species	3
Toxicity	4
Historic and Modern uses	5
Emissions and regulations	6
Chapter 2 Mercury – The behaviour	
Reactions in air	9
Reactions in water	12
Exchange between air and water	14
Reactions in snow and ice	14
Chapter 3 Mercury – The measurements	
Mercury detection techniques	17
Air measurements	19
Water measurements	21
Snow and ice sampling	25
Mercury flux and the gas transfer velocity	27
Chapter 4 Mercury – Measurements in the marine environment	
Measurements in Antarctica	29
Measurements in the Mediterranean Region	34
Measurements in Sweden	38
Measurements in Finland	41
Measurements in the Arctic	43
Chapter 5 Mercury – The global picture and climate change	
Global comparisons	51
Implications for future modelling	53
Climate change – changing mercury cycle	55
Chapter 6 Mercury – The conclusions and future work	
Research questions – the answers	59
Outlook	62
Acknowledgements	63
References	65
Appended papers I-V	

Abbreviations

Hg	Mercury
GMOS	Global mercury observation system
Hg(0)	Elemental mercury (oxidation number=0)
Hg(II)	Oxidized mercury (oxidation number=II)
GEM	Gaseous elemental mercury
TGM	Total gaseous mercury
GOM	Gaseous oxidized mercury
HgP	Particulate mercury (oxidized mercury bound to particles)
AMDE	Atmospheric mercury depletion event
ODE	Ozone depletion event
DGM	Dissolved gaseous mercury, (dissolved elemental mercury)
HgTot	Total mercury (elemental mercury plus oxidized forms)
MeHg	Methyl mercury species
MMHg	Monomethylmercury
DMHg	Dimethylmercury
UIW	Under ice water
DMSP	Dimethylsulfoniopropionate
AAS	Atomic absorption spectroscopy
AAF	Atomic fluorescence spectromoter
CV-AFS	Cold vapor atomic fluorescence spectrometer

Preface

Background

Mercury is a toxic pollutant, that due to its long residence time in atmosphere can be dispersed long distances around the world.¹ Both anthropogenic and natural sources are important for the release of mercury to air and 60% of the total emissions are believed to be due to re-emission of mercury from sea surfaces on a global scale. Most of the mercury originate from mercury previously deposited into the oceans.² Previous global models have estimated the yearly mercury evasion from sea surfaces to be around 2700 tonnes.^{3,4} The estimated numbers, however, hold large uncertainties such as unaccounted for seasonal and spatial variations.³ There also exist several different methods to estimate the flux of mercury between air and sea surfaces which have been found to lead to substantially diverse results. Since the global re-emission of mercury from sea surfaces accounts for the majority of the annual emissions of mercury to air, these uncertainties must be addressed and acknowledged when studying the global cycle of mercury in the environment.

Several international conventions have reported about mercury as a global pollutant including UNEP, UNECE-LRTAP, HELCOM, MERSA and AMAP, and international projects such MAMCS, AME, MOE and MERCYMS have been focused on to measure and study mercury in the environment.

The work presented in this thesis was accomplished within the framework of the Global Mercury Observation System project (GMOS, www.gmos.eu), funded by the European Commission 7th Framework Programme. The project was active between year 2010 and 2015 and involved 23 partner organizations from 18 different countries, also including eight external partners. The aims of the GMOS project included to:

- Establish a global monitoring system for mercury observations over land, water and on aircraft.
- Improve and validate regional and global scale models for atmospheric mercury.
- Develop models to evaluate and identify source-receptor relationships, temporal trends and scenarios.
- Develop systems and tools for sharing output data produced by GMOS for policy development and research.



Within the GMOS project several monitoring stations around the world were engaged in common measurement programs including e.g. Ny-Ålesund (Svalbard), Pallas Matorova (Finland), Alert (Canada), Råö/Rörvik (Sweden), Mace head (Ireland), Cape Point (South Africa), Amsterdam Island (Indian Ocean), Cape Grim (Australia). Several over-water campaigns and aircraft measurements have also been performed within the GMOS project and have together provided a unique set of high resolution mercury data presented in numerous publications and databases.

My contributions to mercury research

During my PhD studies I have measured mercury species in air and measured Hg(o) concentrations in the marine environment at diverse latitudes and climate zones in order to study global and seasonal variations of mercury in air- and in the water phase.

I have participated in several oversea campaigns in Antarctica (papers I-IV, VII, VIII), the Mediterranean Sea (paper V) and in the Arctic (ongoing project).

I measured mercury species in air during a one month long field campaign at the Pallas Matorova station in northern Finland where a mercury depletion event was detected in air masses originating from the Arctic and transported to the Pallas site (paper IX). I have also been responsible for the maintenance of the air measurements of mercury species in air at the GMOS master site Råö/Rörvik, located on the west coast of Sweden (paper VI). At this site I have also worked with the development of an automatic method for measuring Dissolved Gaseous Mercury (DGM) in surface seawater using an in situ purging system together with my supervisor at IVL – Swedish Environmental Research Institute.

Aim and research questions

This thesis presents a summary of mercury measurements performed in the marine environment at various locations from the far South to the far North. The aim of this work was to study how mercury is transported between different marine media such as air, seawater, sea ice, snow and brine and investigate how spatial and seasonal variations influence the mercury cycling in the marine environment globally.

The stated research questions were:



What are the concentrations of mercury species in air in different parts of the world?



Are there any spatial or seasonal variations of elemental mercury (Hg(o)) in surface seawater? Is surface seawater generally over-saturated or under-saturated with respect to Hg(o)?



What is the estimated mercury flux between the air-seawater interphase and how is this varying with season and location?



How does the choice of flux model affect the estimate of mercury re-evasion from sea surfaces in global modelling?



Which parameters influence the distribution of different mercury species in seawater columns?



How is the sea ice environment affecting the global budget of mercury?



How is the cycling of mercury in marine environments affected by climate change?



Chapter 1

“A night with Venus, a lifetime with Mercury.”

(Mercury was for centuries used to treat syphilis.)

-Anonymous, saying. In Michael J. O'Dowd and Elliot Philipp, The history of obstetrics and gynaecology (2000), 227.

Mercury – The Element

Properties

Mercury (Hg) is a chemical element belonging to the heavy metals in the periodic table of elements (^{80}Hg , d-block). The chemical symbol Hg originates from the Greek word *hydrargyrum* (“liquid silver”) which hints as to why mercury sometimes is referred to as quicksilver. Mercury has a higher molar mass than gold ($200.59 \text{ g mol}^{-1}$) and is a metal with many fascinating properties. For example, mercury is the only metal that exists as a stable monoatomic gas in air and is also the only metal that is liquid at standard temperature and pressure, being a heavy (density $\sim 13.5 \text{ g cm}^{-3}$) silver-white liquid, see Figure 1. It has a boiling point of 356.73°C and a freezing point of -38.83°C , which can be explained by its unique electron configuration, behaving almost like a noble gas. Mercury has a poor heat-, and a moderate electrical conductivity, and is known to form alloys with other metals such as gold, silver, copper and tin which are called amalgams.^{5,6}



Figure 1. Liquid elemental mercury at standard temperature and pressure.

Mercury species

Mercury exists naturally in the environment as the red mineral cinnabar (HgS , as Hg(II)), often found in volcanic regions.⁵ Mercury exists in three different oxidation states: 0, +I and +II where 0 and +II are the two most common oxidation states in the environment.^{7,8} Hg(I) compounds are rare and are believed to include the dimeric cation Hg_2^{+I} , found in for example the compound Hg_2Cl_2 .⁹ Examples of common inorganic mercury(II) compounds are mercury halides such as HgCl_2 , HgBr_2 and mercury oxide (HgO).⁶

Organic mercury compounds (MeHg) are often written with the general formula CH_3HgX and are all toxic. The most common MeHg species in the environment are monomethyl mercury (CH_3Hg^+) and dimethylmercury ($(\text{CH}_3)_2\text{Hg}$).¹⁰



The predominant form of mercury in air is Hg(0), also called gaseous elemental mercury (GEM).^{11,12} Different types of gaseous oxidized divalent mercury may also occur in the atmosphere. This far only indirect methods exist for measurements of these species and the measurement appears to be dependent of the methods used, i.e. be operational defined. To some extent is also particulate bound mercury dependent on the method of measurement. These species/fractions of airborne mercury will further be referred to as gaseous oxidized mercury (GOM) and particulate mercury (HgP) in this thesis and will further be described in more detail in Chapter 3, page 19.

Toxicity

Inorganic gaseous elemental mercury (Hg(0)) are toxic when inhaled in high concentrations in combination with long-term exposure. It can cause neurological symptoms such as sleeping problems, emotional instability or peevishness and in higher concentrations it can also cause more severe symptoms such as respiratory distress, kidney problems, bronchitis and interstitial pneumonitis; problems that could lead to death.¹³ Hg(0) was in 1989 (at the time being used in teething powder) acknowledged to be the cause of the pink disease, acrodynia, which showed symptoms such as insomnia, rashes, loss of hair and numbness.⁵

Another toxic inorganic compound is the salt mercury chloride (HgCl₂) that exists in some antiseptics and in dry cell batteries and that was previously used to treat syphilis. It is toxic when ingested in high concentrations. However, cases of high dose ingestions are rare.

The toxic effects of dental fillings have been debated for many years, causing a concern among the public. Dental amalgam normally consists of mercury (50%), silver (20-30%), tin (~14%) and copper (~8%) and has been used globally as a dental filling due to its manageability and durability once hardened.¹⁴ The earliest records of the use of dental amalgam date as early as during the Tang Dynasty (618-907) and have also been mentioned in texts from 1505. It was introduced to the Western World in the 1830's where it has been regularly used since, until it got banned in many countries (banned in Sweden 2009 and in Denmark and Norway 2008).¹⁵⁻

¹⁷

Health concerns regarding the use of dental amalgam containing elemental mercury have been raised both for the patients and for the dentists. A recent study found elevated mercury concentrations in the urine of children having more than one amalgam filling.¹⁸ In a literature review by Mutter (2005) it was suggested that the release of elemental mercury from dental fillings could cause problems such as nephrotoxicity, neurological conditions, autoimmunity and autism. Other studies have also shown a link between low-exposure levels of elemental mercury and the development of Alzheimer's disease and Multiple Sclerosis.¹⁹ However, in a Swedish study no elevated risks of neurological symptoms or illnesses could be found among children of mothers working as dentists during the 1960s-1980s.²⁰

The organic Hg(II) compounds such as mono- or dimethyl mercury (CH₃Hg or (CH₃)₂Hg) are the most toxic forms of mercury. Methyl mercury is bio accumulating in food chains resulting in high concentrations ending up in top predators.

Organic mercury compounds are more dangerous due to their ability to cross the blood-brain barrier and reach the central nervous system. Organic mercury has a strong affinity for sulphur atoms in cysteine residues and can therefore interfere with the functions and structures of



proteins.^{21,22} High exposure to MeHg could lead to a disturbed nervous system with sense losses and mental disturbances, which are symptoms of the Hunter-Russell syndrome. High levels of MeHg poisoning can also lead to death. People living near the coasts existing primary on a marine diet are at higher risk. Special caution is addressed to pregnant women since MeHg can cross the placenta and cause intellectual disability and neurological damage to the unborn child.^{2,23}

Some severe events of mercury poisoning exist in history. One well-known example is what happened to a small factory town in Minamata Bay, Japan. The Chisso factory in the town was producing acetaldehyde using mercury sulfate as a catalyst between 1932 and 1968. As a byproduct of the reaction, MeHg was produced which was directly released to the bay via the wastewater. In total around 80 tonnes of MeHg was released into the seawater, parts of which entered and bio accumulated in the local food web, ending up in fish and shellfish which were the population's most important food sources. Neurological symptoms were first found among local rats and cats, and later also among humans. The disease that gained the local name "The Minamata disease" was first suspected to be contagious, leading to people showing symptoms being moved to a distant treatment house. In 1959 it was discovered that the symptoms were the cause of MeHg poisoning. A total of around 2200 people suffered from the poisoning whereof around 1700 died. It has also been shown to affect succeeding generations, causing infertility among women.²⁴

Another example of mercury poisoning in history is the grain disaster in Iraq in 1971. Seed grains for planting were treated with a fungicide containing MeHg and sent from Mexico to Iraq. Poor labelling resulted in the unawareness of the fungicide treatment leading to that the rural people believed the grains could be directly consumed. The ingestion of the seeds resulted in severe neurological damage. Around 6500 people were hospitalized and more than 500 people died.^{25,26}

In nature MeHg bio-accumulates in food webs and is a threat to ecosystems. For every increasing trophic level in a food chain, the MeHg concentration increases around 2-7 times. If a food chain is very long, the increases of MeHg concentrations per trophic level at the end of the food chain can be even higher. Ingested MeHg is stored in the kidneys of land living mammals and in the liver of marine mammals and birds. MeHg can be excreted over time as feces, urine and in growing fur. For mammals without fur, such as toothed whales, the excretion of MeHg is not as high as in other mammals with fur, therefore whales tend to accumulate higher levels of MeHg in their bodies, especially in muscle and brain tissues.

MeHg has similar neurotoxic effects for mammals as for humans. For predatory fish higher up in the food chain the toxicity of MeHg can cause difficulties in spawning, that is to say difficulties in egg production and fertilization. For birds, MeHg can cause eggs that do not hatch, smaller clutches and deformed embryos. The levels of MeHg in top predators in the Arctic are today 10 times higher than before the industrialization.²³

Historic and Modern uses

The first evidence that mercury was used as a material by humans was found in 3500 year-old Egyptian tombs. It is however suspected that mercury was used much earlier than that in



China.^{5,27}

The red mineral cinnabar is known to have been used as a color pigment since prehistoric times and at around 1000 BC cinnabar was mined to extract mercury. The mineral was placed on windy and warm places proposedly leading to degassing of the sulphur in the mineral. What was left on the spot was liquid mercury. This liquid metal certainly attracted people's interest and it was even believed to have magical properties. At around 200 BC the Chinese emperor Shi Huangdi thought that drinking liquid mercury would give him eternal life. This was obviously not the case.

The knowledge that mercury is toxic already existed in 50 BC.²⁷ During the Roman imperium era, slaves were used to mine mercury. Unfortunately the slaves did not usually survive more than 6 months of working in the mines, possibly an effect of mercury poisoning.⁵ The demand for mercury increased during medieval times when mercury started to be used as a reflective media in mirrors. It was also used in medicines and was used to extract gold. From the end of the 15th century until the 20th century mercury was used as a treatment for syphilis.²⁶

During the industrialization hat makers used the metal to strengthen the fabric used to make hats. Rumor has it that the crazy hat maker in *Alice in Wonderland* was an icon of the mental disturbances hat makers often showed due to mercury poisoning.

Modern uses of mercury (also counting already banned uses) include applications such as in cosmetics, medicines (in vaccines), fluorescent lamps, thermometers, manometers, electronics, chloralkali-production, dental fillings and gold mining.^{5,26,27}

Emissions and regulations

Mercury is cycling between different natural reservoirs such as surface soils (1 005 000 tonnes), deep and surface waters (350 000 tonnes), the atmosphere (5600 tonnes) and vegetation. It is more easily transported between different reservoirs in its oxidized form and the highest transportation of mercury in nature occurs between surface soils, surface oceans and deep oceans. The fastest transportations, however, occur in the atmosphere due to that atmospheric reactions are fast. The main sink for mercury is in deep ocean sediments, a transportation that takes around 3000 years.²⁸ The increased anthropogenic emissions since the industrialization have disrupted the natural equilibrium of the mercury cycle, leading to changes in the different natural reservoirs.^{23,29}

The total annual emissions of mercury into the atmosphere were estimated in 2013 to be between 5500 to 8900 tonnes. These numbers include natural and anthropogenic sources as well as the re-emission of previously emitted mercury deposited into natural waters. Natural sources of mercury include for example volcanic and geothermal activities, weathering of rocks and account for around 10% of the total yearly emissions.^{2,23}

Anthropogenic sources accumulatively account for around 30% of the total annual emissions and include (in the order of magnitude) gold mining, burning of fossil fuels, metal production, cement production, waste incineration, contaminated sites, chloralkali industries and the production and end-use of dental amalgam. The global anthropogenic mercury emissions



estimated for 2010 are presented in Figure 2, showing that Asia is a large contributor to atmospheric mercury.

The re-emission of mercury from oceans and lakes is accounting for around 60% of the total annual emissions of mercury to air. It is often put in a separate group due to that the origin of the re-emitted mercury could be either natural or anthropogenic.^{2,23} The re-emission of mercury from sea surfaces will be further discussed in Chapter 2, 3, 4 and 5.

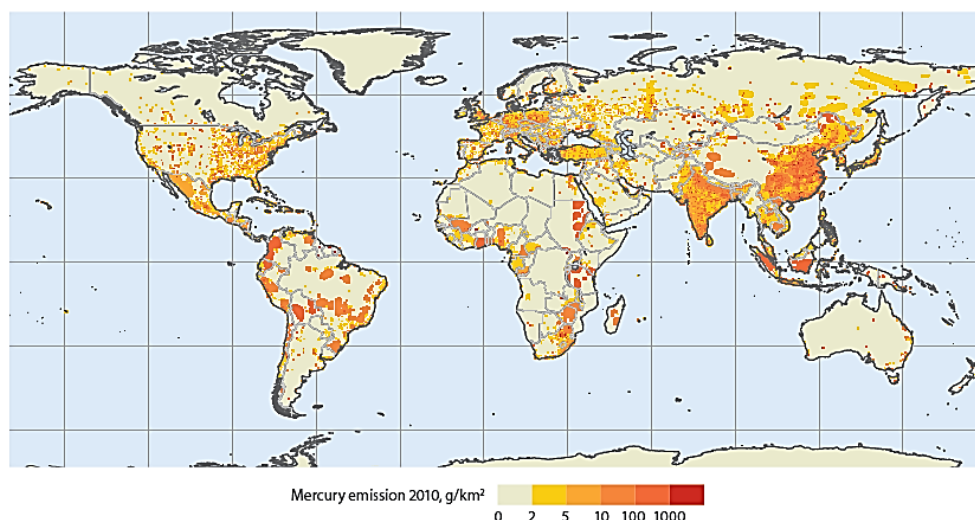


Figure 2. Global anthropogenic mercury emissions estimated for 2010.²

In the 1990's, Sweden's wildlife received in around 5.4 tonnes of transported and deposited mercury, of which one third was believed to originate from European countries. The European implementation of the *Large Combustion Plants Directive*, adopted in 1987, led to an improvement of industrial techniques and resulted in the installation of efficient particulate filters and desulphurization equipment in coal combustion plants. The improved cleaning techniques installed in Europe have shown to be efficient. In 2011 the total mercury deposition in Sweden was estimated to have been reduced to 4 tonnes. However, this includes an increased input of mercury from countries outside Europe. Of mercury deposited in Sweden around 1.5% was estimated to originate from Swedish sources, 10.5% from European sources and 86% from global sources.

Since the acknowledgement of mercury being a risk to humans and wildlife due to its toxicity and global distribution, many policy agreements have been initiated in different parts of the world, aiming to decrease the use and fabrication of mercury-containing products. In Europe a legislation for the use and transportation of mercury was signed in October 2008 and initiated in March 2011.³⁰ In the US, *The Mercury Export Ban Act* was signed in October 2008 aiming to stop all exports of mercury after the 1st of January 2013. The act also prohibits sales and transfers of mercury and includes a plan for the long-time storage of elemental mercury.³¹

The use of mercury amalgams as a dental filling was banned in Norway and Denmark in 2008 and in Sweden in 2009.³² In memorial of the mercury catastrophe in Minamata Bay, and the awareness of the environmental risks with mercury pollution that has been evident since then, the 25th Governing Council of UNEP initiated a Minamata Convention aiming to phase out the mercury mining and use of mercury and to control anthropogenic mercury emissions globally. The Minamata Convention was agreed on in January 2013 and to date, 102 countries have signed it including the US, UK, Sweden and Japan.³³

Chapter 2

“[Mercurial medicines] affect the human constitution in a peculiar manner, taking, so to speak, an iron grasp of all its systems, and penetrating even to the bones, by which they not only change the healthy action of its vessels, and general structure, but greatly impair and destroy its energies; so that their abuse is rarely overcome. When the tone of the stomach, intestines, or nervous system generally, has been once injured by this mineral ... it could seldom be restored.”

-Thomas Graham, quoted in Wooster Beach, A Treatise on Anatomy, Physiology, and Health (1848), 177.

Mercury – The Behaviour

Reactions in air

Mercury in the atmosphere consists of up to 90-99% of the gaseous elemental form (GEM), Hg(O).¹² GEM is a stable and monoatomic gas that has a residence time in the atmosphere of between 6 months to 2 years. Due to its long lifetime it can be transported long distances and end up far away from emission sources.⁸ The long lifetime also leads to GEM concentrations in the atmosphere being relatively well-mixed within the two hemispheres.

In the Northern hemisphere the monitoring of mercury in air started in the middle of the 1990's at Mace Head, Ireland, measuring a background concentration of total gaseous mercury (TGM) of 1.8 ng m⁻³.⁸

Recent measured averages recorded at stations within the GMOS project showed background concentrations in the Northern hemisphere of 1.55 ng m⁻³ in 2013 and 1.51 ng m⁻³ in 2014. This indicates that the concentrations of mercury in air have decreased in the Northern hemisphere since the 1990's.¹²

In the Southern hemisphere the average background concentration of TGM showed a maximum of 1.5 ng m⁻³ in the beginning of the 1990's, decreasing to around 1.1 ng m⁻³ in 2005.³⁴ At Southern GMOS sites average concentrations of 0.93 and 0.97 ng m⁻³ were measured in 2013 and 2014, respectively. The highest background concentrations of GEM/TGM within the GMOS project were found in the Tropical Zone. In 2013 and 2014 average concentrations of 1.23 and 1.22 ng m⁻³ were measured, respectively.¹² The in general higher concentrations of mercury in air found in the Northern hemisphere are mainly due to higher numbers of emission sources.²⁸

Even though dry deposition of GEM has been found to be significant, the major pathway for mercury to be deposited from the atmosphere to the environment is through oxidation, leading to oxidation products such as gaseous oxidized mercury (GOM) and particulate mercury (HgP). Oxidized forms are more water soluble and deposit faster (days to weeks) and closer to the emission source through wet and dry deposition.^{28,35}

Figure 3 summarizes the mercury cycle in the environment and its fate in Polar Regions. The mercury is released from anthropogenic and natural sources as Hg(O), Hg(II) and as particulate mercury (HgP).

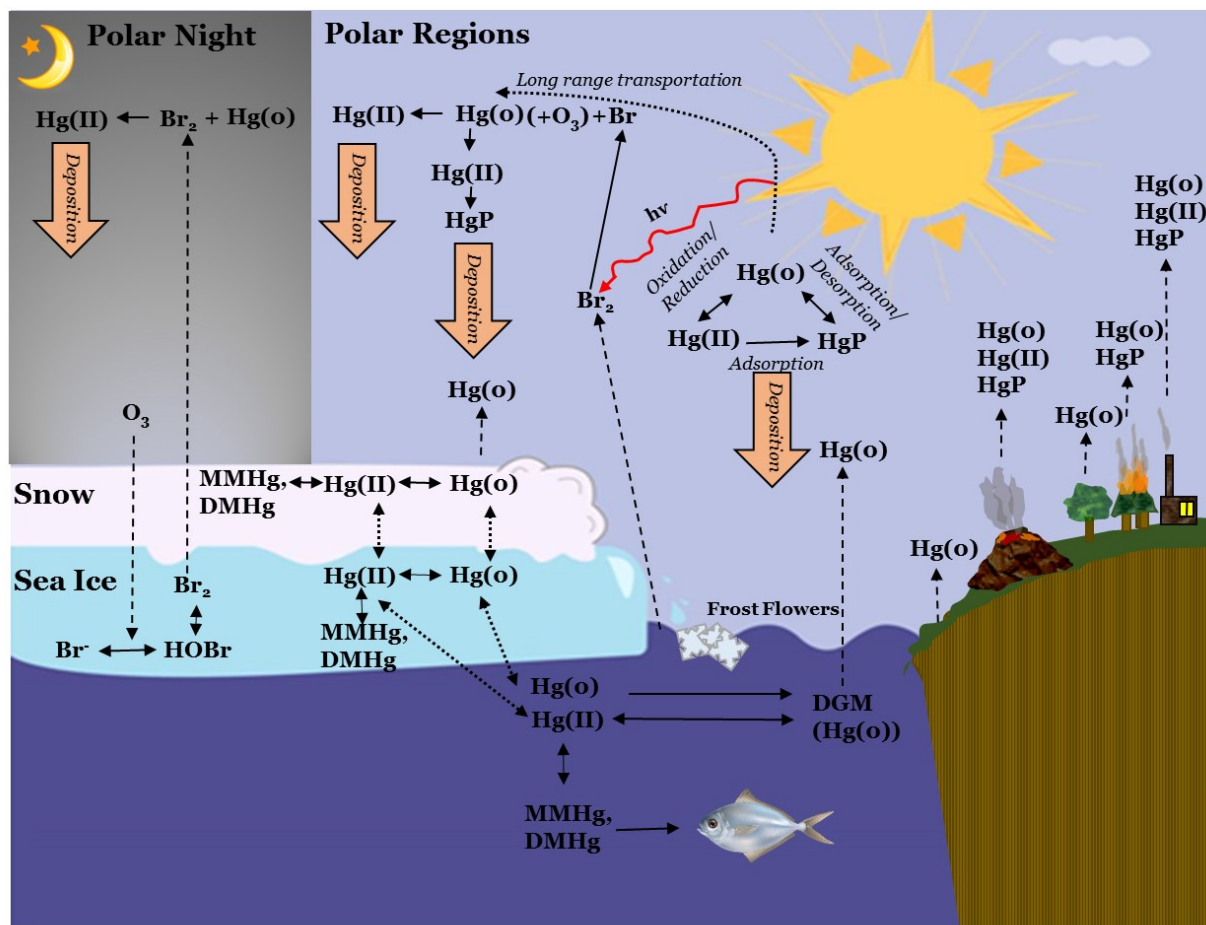
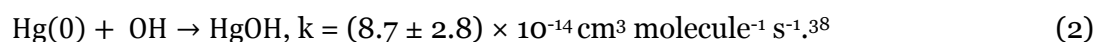
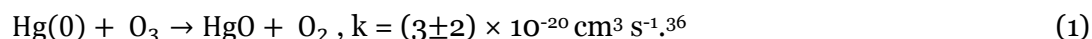
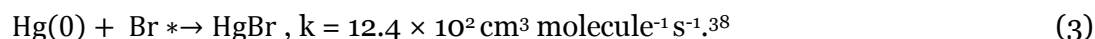


Figure 3. The major pathways and reactions of elemental and oxidized forms of mercury in the marine and polar environment.

In the atmosphere Hg(o) can get oxidized to Hg(II) or be adsorbed onto particles. Possible oxidants in the atmosphere have been suggested in the literature to be primarily ozone and OH-radicals, oxidizing Hg(o) according to reactions 1 and 2, respectively.^{36,37}



These reactions have however been found to be unlikely during atmospheric conditions, as concluded from kinetic and enthalpy change calculations.³⁹ The major oxidant for Hg(o) in the atmosphere has also been suggested to be bromine. Measurements and chemical box models have shown that halogen radicals can oxidize Hg(o) at mid-latitudes according to reaction 3.⁴⁰



Other suggested oxidants for Hg(o) in the atmosphere found in the literature are Cl, NO₃, BrO and H₂O₂. Confirming the main oxidant of Hg(o) in the atmosphere through laboratory experiments has been problematic, as the oxidation products formed are often hard to detect and due to problems with reactor wall condensation.⁴¹



Small fractions of organic mercury species also exist in air, in the form of dimethylmercury (DMHg) and monomethylmercury (MMHg). However they are not of toxicological importance since they only exist in such low concentrations. The existence of these organic forms of mercury in air is mainly due to their formation and release in gas phase from for example oceans and landfills.⁴¹ It has also been shown that they can be formed in the atmosphere from Hg(II) and acetic acid.⁴² MMHg can be found in rain, possibly due to a formation in the atmosphere or due to the decomposition of DMHg.⁴¹⁻⁴³

Atmospheric mercury depletion events in Polar Regions

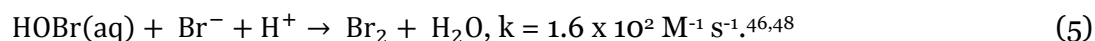
The environmental conditions in Polar Regions are different from the rest of the world regarding climate and solar conditions, switching from 24 hours of sunlight during summer to 24 hours of darkness in winter.²³

In 1988, Barrie et al. (1988) reported that during springtime in the Arctic tropospheric ozone concentrations were depleted or completely destructed. The phenomenon they named 'ozone depletion events' (ODE) was found to occur in the surface boundary layer, around 2 km above the Arctic sea ice. It was suggested to be caused by photo produced halogen radicals formed by early sunlight that just returned after the long dark winter.⁴⁴

Bromine radicals are formed via photolysis (reaction 4) from Br₂ released from sea salt, see Figure 3.

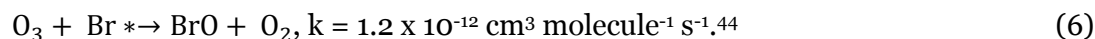


During springtime in Polar Regions the so called 'bromine explosion' is initiated by the uptake of gaseous HOBr in the quasi-liquid layer of sea ice and in surface snow, producing Br₂ according to reaction 5 (see also Paper I).⁴⁶⁻⁴⁸



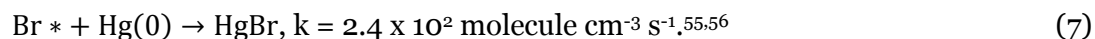
Br₂ can also be produced in the dark by the absorption of tropospheric ozone in surface sea ice brine which reacts with bromine ions to form HOBr, producing Br₂ via reaction 5 (see Figure 3 and paper I).⁴⁹

The bromine radicals produced in reaction 4 are highly reactive and destruct tropospheric ozone via reaction 6.



When measuring GEM at Alert, Canada in early spring 1995 the concentrations of GEM suddenly dropped under the detection limit, simultaneously to a detected ODE.¹ Since their discovery, atmospheric mercury depletion events (AMDE) have been observed during springtime at several polar sites in the Arctic and in Antarctica.^{1,50-53}

The bromine radicals formed in reaction 4 and BrO formed in reaction 6 are the two most likely oxidants for GEM during AMDEs.⁵⁴ Bromine radicals can oxidize GEM during AMDEs according to equation 7.



The reaction between BrO and GEM can form several products according to reactions 8-10,



which have been confirmed in laboratory studies.⁷



BrO concentrations in air can be measured by satellite (e.g. the SCIAMACHY UV-vis-NIR spectrometer onboard the European Environmental Satellite (ENVISAT)) or by measurements with multi axis differential optical absorption spectroscopy (MAX-DOAS). The detection of BrO can serve as evidence that reaction 6 has occurred, hence showing evidence of where an ODE and possibly a simultaneous AMDE have occurred.

AMDEs are influencing the mercury cycle in Polar Regions due to the sudden formation of oxidized mercury in large quantities, which deposits more quickly into the Polar environment. Despite that around 60-80% of the deposited Hg(II) onto surface snow has been estimated to be reduced back to Hg(0) and re-emitted to air as GEM within 2 weeks after the deposition. It has been estimated that around 100 tonnes of mercury are accumulated per year in the Arctic solely due to the AMDEs. These events are therefore believed to play an important role for the cycling of mercury in Polar Regions.^{51,57,58}

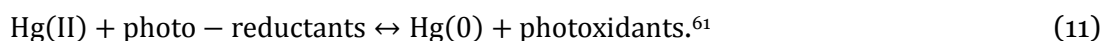
Reactions in water

The residence time for mercury in the ocean water column has been estimated to be 350 years and the majority of mercury exists as Hg(II) in inorganic and organic compounds.⁵⁹⁻⁶¹ Inorganic aqueous mercury species have been suggested to principally be different complexes with OH ($[\text{Hg}(\text{OH})]^+$, $\text{Hg}(\text{OH})_2$, $[\text{Hg}(\text{OH})_4]^{2-}$) and chloride ($[\text{HgCl}]^+$, HgCl_2 , $[\text{HgCl}_3]^-$, $[\text{HgCl}_4]^{2-}$, $\text{HgCl}(\text{OH})$).⁶¹ Halogen ions in the aquatic environment are important as stabilizers acting as ligands for mercury.⁶²

Redox reactions and reactions that are too slow to be relevant in the atmosphere could occur in the water phase, such as reactions involving electron transfer that are important for free radicals.⁶³ For example, reaction 2 is about 50 times faster in water than in the atmosphere.⁶⁴

Oxidized mercury deposited into waters can be reduced to Hg(0), forming dissolved gaseous mercury (DGM), see Figure 3. Reduction of Hg(II) species in water could occur due to photo-reduction and it has been shown that the formation of Hg(0) in surface water has a positive correlation to solar radiation.^{65,66} Reduction can also occur during dark conditions due to biotic reduction involving heterotrophic bacteria and algae. However, the rates of the reactions are about 2-20 times lower than during light conditions.⁶¹ In freshwater only around 40% of Hg(II) complexes have been estimated to be reducible and dissolved organic carbon has been suggested to be important for the reduction.^{67,68} In seawater there exist more chloride Hg(II) complexes that are not as easily reduced photo-chemically.⁶⁹ It has been hypothesized that for the reduction of Hg(II) complexes in aquatic systems, Hg(II) possibly needs to be complexed with dissolved organic matter due to the electron transfer from the organic ligand to the mercury atom.⁷⁰

The general formation of Hg(0) in seawater is described by reaction 11.



This redox reaction is reversible as also presented in Figure 3. However, it has been found that reaction 11 might involve an intermediate specie Hg^* , which is produced by the oxidation of Hg(0) .⁶²



The intermediate specie Hg^* can become either Hg(0) or Hg(II) , via two pathways that have different rate constants. However, from experiments it was not possible to distinguish which pathway is more likely. UV-A (315-400 nm) and UV-B (280-315 nm) are the most important wavelengths for mercury redox reactions of which UV-B has been found to be more important for the reducible form of mercury.⁶²

Dissolved gaseous mercury (DGM) in seawater consists mainly of gaseous Hg(0) and DMHg and makes up 10-30% of the total mercury in the water column.⁷¹ Of the DGM in the water DMHg is mostly found in deeper water columns. In the surface layers higher shares of Hg(0) are found due to photo-reduction processes.⁷² DGM concentrations in seawater, measured at different geographical positions during different seasons, found in the literature are presented in Table 4 in Paper II.

Hg(0) can also be oxidized in the water column by photochemical processes. The main oxidant has been suggested to be the OH radical that can be formed via photolysis of nitrate/nitrite or organic acid coordination compounds with the involvement of halides.^{61,64} Dark oxidation of Hg(0) also occurs in water and was shown to have higher rates in the presence of chloride ions, particles and colloids. However, the dark oxidation was found to be dependent on previous light exposure in order to photo-produce hydrogen peroxide, and was also found to have a rate about 10 times lower than photo-oxidation.⁶¹ Mercury oxidation rate constants found in the literature are equal or greater compared to found reduction rates, indicating that the oxidation of Hg(0) occurs in equal or greater magnitudes than the reduction of Hg(II) .⁶¹

Hg(II) species can in aquatic environments be transformed to DMHg or MMHg either abiotically (by photochemical reactions) or biotically (by microbial metabolism), involving organic matter.⁴³ An abiotic reaction is referred to whenever a reaction occurs outside a living organism, even though organic material is needed. MMHg is the most toxic form of mercury in aquatic environments due to its ability to bio-accumulate and bio magnify in food chains. The biotic formation of MMHg is believed to be the most important and is occurring both in aerobic and anaerobic conditions. Abiotic methylation has been found to be not as important and is primarily due to photolytic processes occurring in the presence of suitable methyl donors such as acetic acid or small alcohols. In sediments the production of MMHg is believed to involve sulfate-reducing bacteria.⁶¹

The methylation rate depends on several factors such as the concentrations of Hg(II) , sulfide, total organic carbon and chloride complexes and the redox potential. In Polar Oceans the methylation rate has also been observed to correlate with chlorophyll a. The production of MMHg has been found to be more efficient in acidic conditions and high mercury concentrations, while the production of DMHg was found to be higher in more basic conditions and lower mercury concentrations. Of organic mercury concentrations the share of DMHg is often higher in intermediate and deeper water compared to MMHg where the share is often higher in the surface waters. The production of MeHg has been indicated to vary seasonally



due to higher rates having been observed at higher water temperatures and high nanoplankton concentration.

A demethylation of MeHg species in aqueous system occurs with time and transportation distance. The demethylation is believed to be mediated by biological and abiotic pathways during both dark and light conditions via redox processes. Results have shown that around 90% of produced MeHg is demethylated at a distance of 20-2000 km from source. This indicates that the bioaccumulation of MMHg likely occurs locally where it was produced.⁶¹

Exchange between air and water

Dissolved gaseous mercury (DGM) is volatile and if surface waters gets supersaturated with respect to Hg(o) and DMHg it can partly be re-emitted to air, which consequently decreases the load of mercury in the water compartment, see Figure 3 (Figure 3 does not present the cycling of DMHg).^{23,73}

The re-emission of Hg(o) from sea surfaces to the atmosphere is a significant source of GEM to air. Global models show estimations of yearly emissions of mercury from sea surfaces varying between 2600 and 2800 tonnes.^{3,4} Due to different existing methods and approaches to calculate the flux rate of mercury between the air and the water interphase, large differences in results can be found in the literature leading to uncertainties in global models, further discussed in Paper II and V. A literature survey of measured Hg flux in various geographical areas and seasons are presented in Table 4, Paper II.

Reactions in snow and sea ice

In Polar Regions the deposition of Hg(II) onto surface snow is enhanced during AMDEs due to a large and fast production of Hg(II) in air. A large part of the deposited Hg(II) is generally reduced via biotic and abiotic processes to Hg(o) and re-emitted to air.^{1,51,52,58,74} If deposited mercury is trapped by precipitated or blowing snow, the reduction and re-emission of deposited Hg(II) could be hindered and mercury could possibly be transported further down into the snow column and reach the sea ice.^{75,76}

Reduction of Hg(II) in snow has been found to be possible in the dark through photolytic induced reactions or via total dark mechanisms.^{75,76} However, the majority of the reduction has been found to occur in the presence of solar radiation where UV-B has been found to be more efficient than UV-A.^{1,51,52,58,74} The photo-reduction in snow was also found to possibly be dependent on the presence of reductants such as H₂O₂, HO₂^{*}, oxalic acid, humic acids and sulphite based compounds.^{75,76} Also oxidation of Hg(o) has been found to occur in the polar snowpack via proposed oxidants such as H₂O₂, bromine radicals (in light conditions), Br₂ (in dark conditions), ozone and OH.⁷⁶

Hg(II) in the snowpack has been found to be able to methylate via proposed aerobic and anaerobic processes with the involvement of a substrate used during dimethylsulfoniopropionate (DMSP) cycling.⁷⁷ Sulphate-using bacteria survive at low oxygen levels and temperatures and have been found in Arctic snow and ice. The bacteria are believed



to be able to convert inorganic Hg(o) to MeHg in snow and sea ice.²³

Brine is a solution of sea water and salt that forms during the freezing process of sea ice when the salt is pushed out into cavities in the ice. The brine solution is very saline and is gathered in ice pockets that can connect to each other to form brine channels.⁷⁸ The permeability of sea ice depends on the brine volume and the microstructure of the ice. The dynamics and presence of brine pockets and drainage channels are believed to be important for the transportation of mercury in polar sea ice.^{75,79}

Mercury can enter the sea ice either from the atmosphere or from the underlying sea water. There are three major processes by which mercury can enter the sea ice: freeze rejection from seawater, scavenging of airborne mercury by non-snow covered ice surfaces and downward leaching from the overlying snow cover. During freeze rejection, dissolved species within the ice are rejected together with the sea salt and form a crystal matrix in the ice. This rejection could lead to an enrichment of mercury in brine. When new sea ice is formed and the top-layer is directly exposed to the atmosphere, the sea ice can take up mercury from the surrounding atmosphere. This atmospheric uptake is however more important and significant when frost flowers are formed.⁷⁵

Once in the ice, mercury can likely undergo transformations to other compounds, such as MeHg or can be transported further within the ice.⁷⁵ Similar reactions as in seawater have been suggested to also occur in sea ice, especially in the saline environments such as in brine channels. Hg(o) within brine could oxidize in the presence of solar radiation and chloride ions. In brine, which is an anaerobic environment, methylation of Hg(II) could occur with the involvement of sulfate-reducing bacteria.⁷⁵ Methylation has been suggested to occur in the lower part of sea ice involving methylation bacteria.⁷⁹



Chapter 3

“The mercury light doesn't show red. It makes the blood in your skin look blue-black. But see how splendidly it brings out the green in the plants.”

-Charles Proteus Steinmetz, From George MacAdam, 'Steinmetz, Electricity's Mastermind, Enters Politics', New York Times (2 Nov 1913), SM3. Answering the reporter's question about why he lit the cactus collection in his conservatory with the blue light from a mercury lamp, which makes a man look like a corpse.

Mercury – The Measurements

Mercury detection techniques

Mercury is known to form alloys and amalgams with noble metals, a property that is used in for example the gold industry to extract gold from ore.^{23,80} This property can also be used to collect and trap mercury for detection. A gold trap used for mercury collection generally consists of a heat resistant tube (e.g. quartz glass) that is packed with small beads of gold, see Figure 4.



Figure 4. Picture of a gold cartridge from Tekran Instruments Cooperation[©] used for collecting GEM/TGM in air.

The collection of GEM and TGM in air is mainly performed by using gold traps and the principle is to let a known amount of air pass through the gold trap. The mercury in the air passing through the gold will form an amalgam with the gold and gets trapped. The gold trap is then heated up to around 500°C, which will release the trapped mercury due to desorption. A mercury-free carrier gas flowing through the gold trap will transport the released mercury to a detector. This method has been proven to be an easy and reliable method for air sampling of mercury.^{8,11,81–83}

For detection of mercury two main detection techniques are used: atomic absorption spectroscopy (AAS) and atomic fluorescence spectroscopy (AFS).⁵⁸

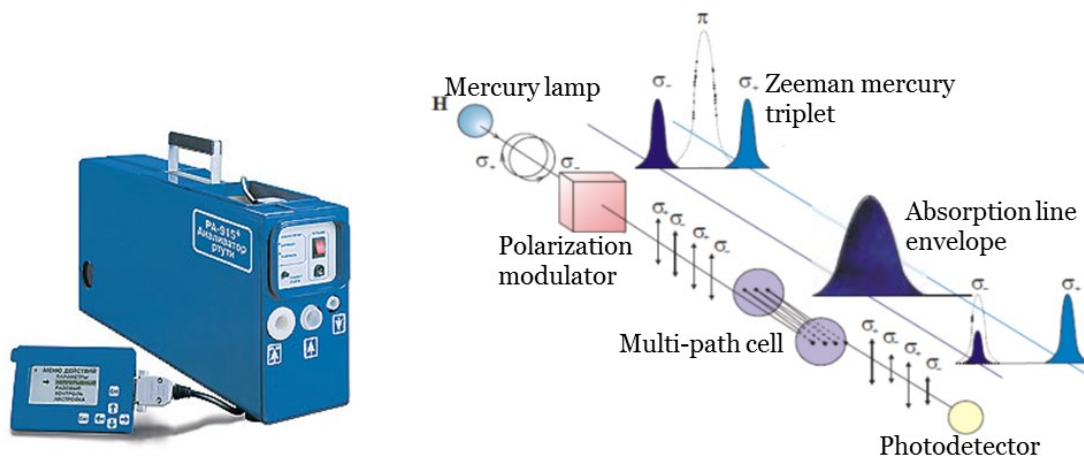


Figure 5. The Lumex RA-915+ mercury analyzer and the principle of Zeeman atomic absorption spectrometry (picture adapted from the Lumex manual).⁸⁴

The general principle of Zeeman AAS used in the Lumex RA-915+ mercury analyzer is presented in Figure 5. A mercury lamp is placed in a magnetic field which makes the resonance line for mercury split into three Zeeman components; two σ components and one π component, which remains at the same position as the original absorption line. The three components will propagate along the magnetic field. The π component is removed using a polarization modulator and the signal from the σ component, that has the proper absorbance line for mercury, will be absorbed by the mercury atoms in the sample, making this component smaller than before entering the multi-path cell. The photodetector detects the magnitudes of the two σ components and the mercury concentration is then proportional to the difference between the two components, calculated based on Beer-Lamberts law. The multipath cell of the Lumex RA-915 + instrument has an optical length of 9.6 m and a cell volume of 0.7 L. Zero corrections are performed automatically by the instrument to set the baseline for the measurements using mercury-free air. The detection limit of the instrument was estimated to be around 0.5 ng m^{-3} during measurements. Some advantages of the Lumex instrument are the mobility due to the low weight and the low cost compared to other analyzers.

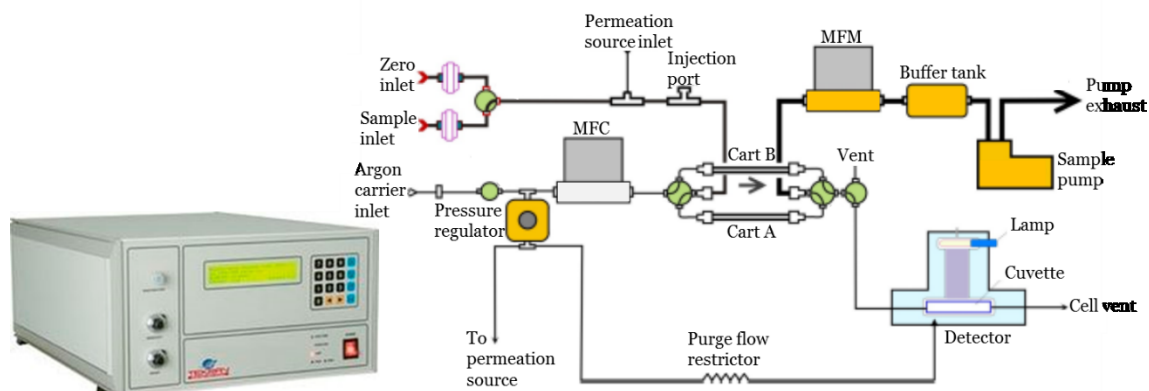


Figure 6. The Tekran 2537A mercury analyzer and the different components of the instrument (picture adapted from the Tekran manual).⁸⁵



Also widely used within the GMOS project for GEM and TGM measurements is the Tekran 2537A/B/X mercury analyzer, see Figure 6. It uses the technique of cold vapor atomic fluorescence spectrometry (CV-AFS) for detecting mercury. It uses dual subsequent gold cartridges which allow continuous measurements of mercury in air. While the first gold trap is collecting mercury from air, the second one is heated for desorption and analysis. After the sample period is finished the gold traps switch and mercury starts collecting on the second trap, whilst the first one is heated. The CV-AFS technique is based on a mercury lamp emitting light at 253.7 nm (the absorbance line for mercury). The mercury atoms in the desorbed sample air absorb the light, and the re-emitted light (the fluorescence) is detected by a detector consisting of a photodiode.

The Tekran instrument generally costs more than the Lumex instrument and uses argon gas as a carrier gas during desorption. However it has the advantage of having a higher sensitivity ($<0.1 \text{ ng m}^{-3}$) which makes it able to detect mercury species in air at pg range.⁸⁵ Calibration of the Tekran instrument is performed by injecting a known amount of mercury from either an external source or using the internal permeation source that is kept at constant temperature.

When measuring mercury in air using the Tekran 2537 instruments the gold traps are not only collecting gaseous elemental mercury (GEM). It has been shown in some studies that gold traps are also collecting some oxidized forms of mercury.^{52,86-88} Hence, without a PTFE filter at the sample air inlet of the Tekran instrument, total gaseous mercury (TGM) is measured.⁸⁹

Air measurements

To be able to measure oxidized forms of mercury in air, fractionation of the oxidized forms existing in air is needed. The fractionation of mercury species in air was performed using the Tekran 1130/35 speciation unit in addition to the Tekran 2537 analyzer. The Tekran 1130/1135 system is shown in Figure 7. The system is measuring three mercury species in air; GEM (Hg(0)), GOM (Hg(II)) and HgP (Hg(II)) which are operationally defined. GOM is collected in the denuder module (the 1130 system) and HgP is collected in the re-generable particulate filter system (the 1135 system).

The 1130 denuder module has an impactor at the sample air intake which will remove particles larger than $2.5 \mu\text{m}$. The air then passes through an annular quartz glass denuder coated with potassium chloride (KCl). The Hg(II) species in air that are not attached to particles (HgP) are trapped by the chloride ions and are trapped and collected on the walls of the denuder. It is not certain exactly what Hg(II) species are collected using this method but they could comprise of HgCl_2 , HgBr_2 , HgO , HgSO_4 , $\text{Hg(NO}_2)_2$ and Hg(OH)_2 .^{8,39,90-92} Air is then passed through a column with embedded quartz chips and a quartz re-generable filter that collects Hg(II) on particles (HgP) smaller than $2.5 \mu\text{m}$.^{11,93}

Since GOM and HgP exist in much lower concentrations than GEM in air longer sampling times are needed to be able to collect enough to exceed the detection limit. The sampling time can be adjusted and should be at least 1 hour when having a total sampling flow rate of 10 L min^{-1} (Tekran analyzer pumps air at 1 L min^{-1} and the pump module pumps air at 9 L min^{-1}).

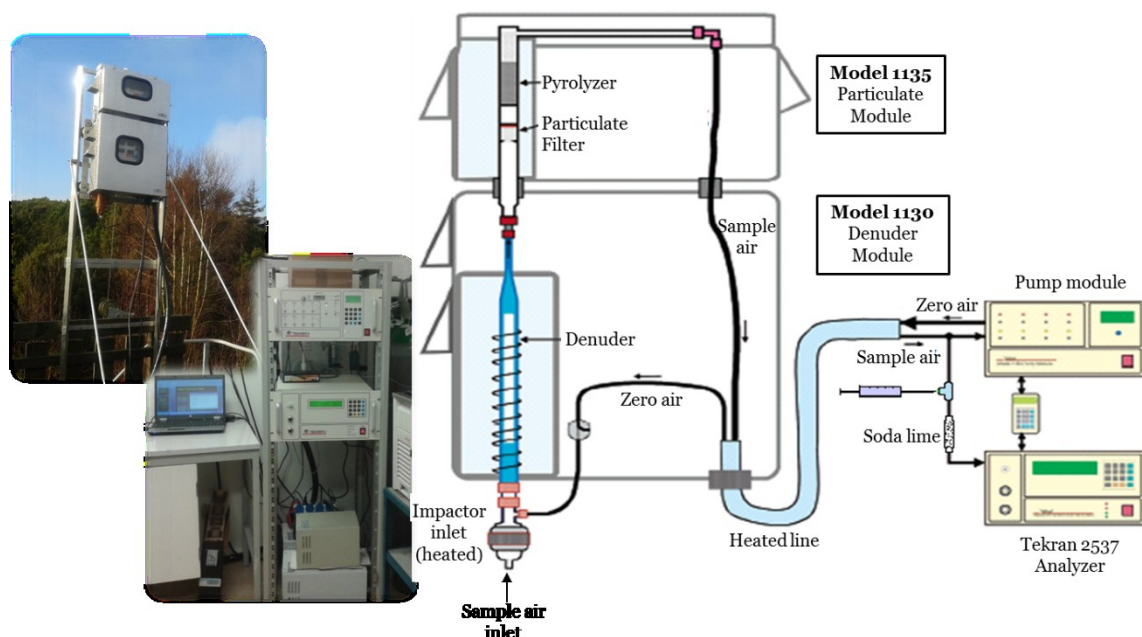


Figure 7. The Tekran 1130/1135 mercury fractionation unit used to measure oxidized species in air. Pictures of the system installed at the Råö/Rörvik station and a picture of the components showing the principle of the system.

Longer sampling time is needed at locations with very low concentrations.⁹³ A sampling time of three hours was chosen when measuring mercury species in air in Antarctica, at the Råö/Rörvik station, in Finland and in the Arctic. GEM that is not trapped in the fractionation unit is measured every 5 min with the Tekran analyzer during the sampling cycle of GOM and HgP.

After three hours of sampling, the pump module switches from pumping 9 L min^{-1} to flush 7 L min^{-1} of zero air through the system instead (Figure 7). Zero air is produced from indoor air that first has been dried and then passed through several coal canisters that absorb mercury in the air. After 15 min of flushing the pyrolyzer oven is heated to thermally destruct organic compounds. The particulate filter is heated to 800°C to decompose collected HgP to GEM. The GEM released is then following the zero air stream to the Tekran analyzer for analysis. The obtained concentration is recalculated using a conversion factor to represent the average 3 hours value. Then the denuder oven is heated to 500°C to decompose the collected GOM to GEM while the pyrolyzer oven is still heated. The decomposed GOM is following the zero air stream and is analyzed in the analyzer as GEM, recalculated by the conversion factor. After desorption of HgP and GOM zero air is flushing through the system for another 10-15 min. When the analysis cycle is finished, the pump module starts to pump air through the inlet again at 9 L min^{-1} and another 3 hours sampling period starts. During sampling, the denuder and particulate filter are kept warm at a temperature of 50°C .

Every second week the denuder needs to be cleaned and re-coated with new KCl. The particulate filter needs to be cleaned and replaced once per month. Glassware and plastic connectors inside the outdoor equipment need to be cleaned and sample filters and soda lime filters need to be replaced every second week.

When measuring in cold places (for example in Polar Regions) extra care should be taken to



ensure the correct air flow volumes and sampling times. Since there is a large difference between the outdoor and the indoor temperature there is also a risk of mercury adsorbing on the walls of the heated line.⁹⁴ Other possible problems using this setup for collecting and detecting mercury species in air have been discussed in the literature; the passivation of gold traps with time and the impact of ozone and water vapor when collecting GOM and HgP. The denuder collects some parts of Hg(II) compounds which so far have not been identified.⁹³ Since uncertainties exist using this method, the results of GOM and HgP obtained using the Tekran 1130/35 system are hereafter operationally defined.

Water measurements

Manual method

Seawater samples for dissolved gaseous mercury (DGM) analysis were collected at selected depths in the sea using a CTD/Rosette system, see Figure 8. CTD (conductivity, temperature, density) denotes the measurements performed by the instruments that are sent down to get information about the physical properties of the water column and are often used by oceanographers to be able to identify different water layers. Other measurable parameters could be for example the oxygen concentration and the fluorescence.

A Rosette system consists of a metallic ring holding up to 24 Teflon Niskin bottles that can hold 7-12 L of water. The bottles are initially opened at both ends and the whole CTD/Rosette system is sent into the water. While going down in the water column, seawater is flowing through the open bottles. The bottles are often closed manually on the way up at depths selected by the operator.

Once the CTD/Rosette had returned to the deck the Niskin bottles were gently tapped via a FEP tubing either directly into the analysis flasks (Fenice 2011 + 2012) or into cleaned conditioned glass bottles filled to the rim (ANTXXIX/6&7 + AO16). It is important that the water sampling for DGM analysis is performed from full Niskin bottles. If head space is created some DGM in the water might degas into the air leading to a loss of DGM in the water. Samples collected in the analysis flasks were directly analyzed. The samples collected in glass bottles were kept in a cold temperate bath prior analysis keeping approximately the same temperature as the seawater.

Dissolved gases in seawater can be degassed by purging air through the water. This technique was used to analyze the DGM concentration in the seawater samples by analyzing the samples using a purging system (Figure 9). Approximately 0.4 L of the water sample was gently transferred from the glass bottle to a clean and conditioned analysis flask. A glass frit of pore size 0 or 1 was inserted into the analysis flask, connected to a Tekran 2537A mercury analyzer. A coal canister was installed at the air inlet to create mercury-free air. The pump in the Tekran 2537A analyzer, pumping air with a flow rate of 1 L min⁻¹, was used to suck air through the purging system, creating small gas bubbles that purged the sample.

Once degassed from the water sample, the mercury gases followed the air stream to the analyzer where the mercury concentration was detected.



Figure 8. A CTD/Rosette system used to sample seawater obtaining deep water profiles of DGM concentrations. The system on the picture was used during the Fenice 2011 and Fenice 2012 campaigns.

The results of the analyses were then divided by the measured sample volume. According to calculations by Gårdfeldt et al. (2002), 9 min purging time is enough to allow DGM in the sample to be depleted.⁹⁵ The detection limit for this method was on average 0.3 pg L^{-1} , calculated as the standard deviation of the total blanks.

The precision measured in field was between 1 to 20%, varying between the campaigns. Wängberg et al. (2001)⁹⁶ calculated the statistical reproducibility of the method to be $\pm 6 \%$ for DGM concentrations between 15 to 20 pg L^{-1} . A soda lime trap was used to protect the Tekran analyzer from humidity.

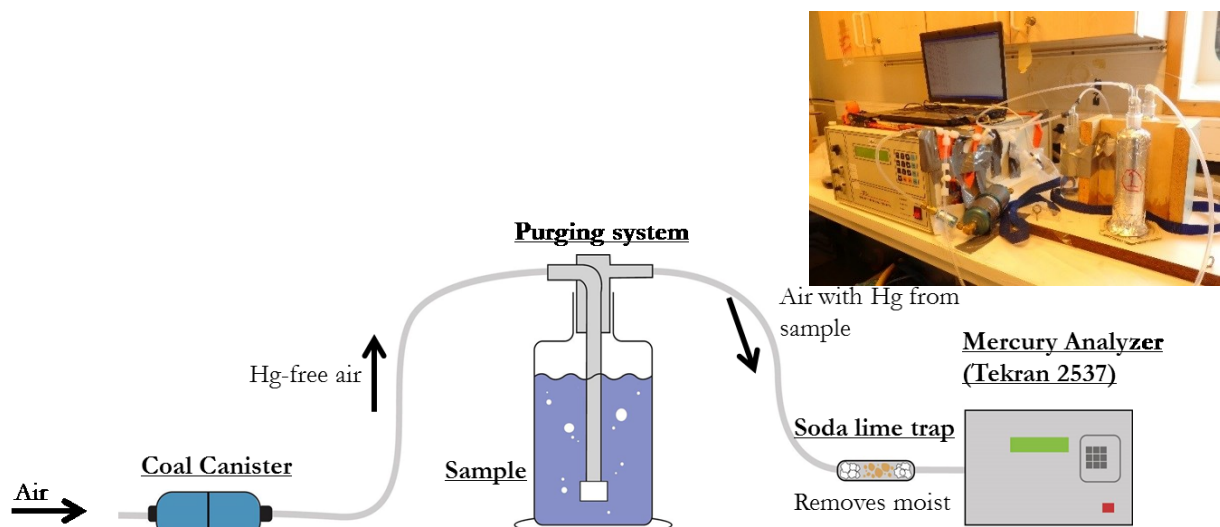


Figure 9. Principle of the purge and trap system used to measure DGM in seawater samples and melted ice and snow samples.

Automated methods

Continuous equilibrium system

DGM can be measured continuously in flowing water in for example seawater using the ship's bow water system. This was obtained by using a similar purging method, see Figure 10.

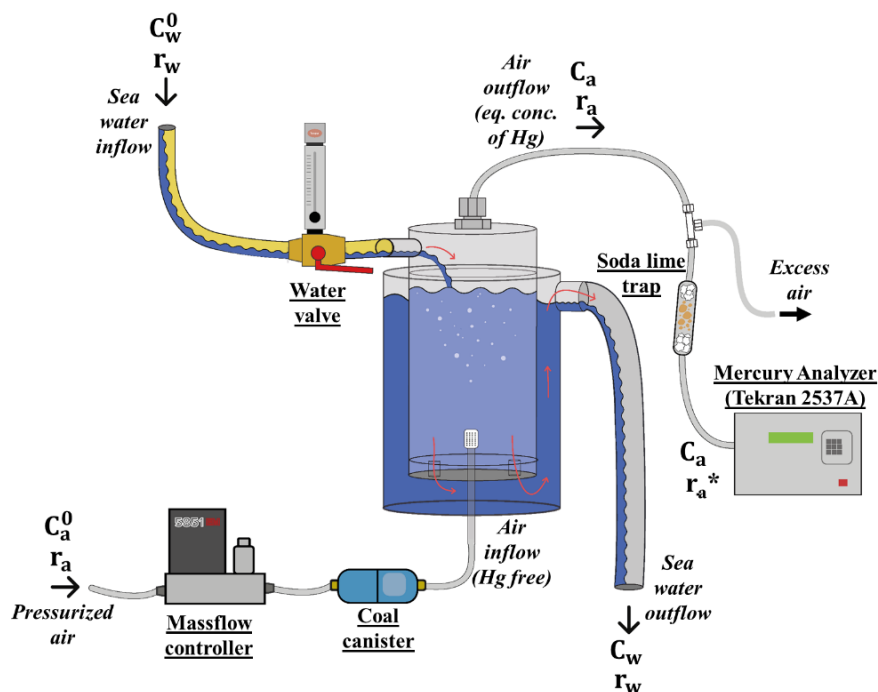


Figure 10. Principle of the continuous equilibrium system and the set up for measuring DGM continuously in surface seawater.

The device was developed by Andersson et al. (2008)⁹⁷ and consists of two cylinders of pyrex glass of which the outer cylinder is used as insulation and as the outflow of water. The seawater enters the device through the inner cylinder from above and flows through the holes in the bottom of the inner cylinder, entering the outer cylinder from below. The water exits at the top of the outer cylinder and is led to a sink. Mercury free air is purged at a controlled air flow rate through a glass frit installed at the bottom of the inner cylinder. Instead of depleting the DGM concentration in the water, an equilibrium concentration of DGM between water and air phase is created. The air exits the system at the top of the inner cylinder, bringing an equilibrium concentration of gaseous mercury to the analyzer. A Tekran 2537A was used for detection during all campaigns. The purging flow rate is set higher than the pump flow rate of the Tekran analyzer (1 L min^{-1}) and the excess air exits through a t-coupling.

In the continuous equilibrium system it is important to ensure that the DGM concentration in the water and air phases are at equilibrium. The flowrates of air and water were chosen according to calculations presented in Andersson et al. (2008)⁹⁷ and Gårdfeldt et al. (2002)⁹⁵.



The concentration of DGM in the water was calculated with equation 13:

$$C_w^0 = \text{DGM} = \frac{C_a}{H'} + (C_a - C_a^0) \frac{r_a}{r_w} \quad (13)$$

where H' is the dimensionless Henry's law constant which describes the partitioning of an atom or compound between the gaseous and aqueous phase. The dimensionless Henry's law constant is described in equation 14:

$$H' = \frac{C_a}{C_w} \quad (14)$$

where for mercury it describes the ratio between the concentration of mercury in the air phase and the concentration of mercury in the aqueous phase. The Henry's law constant for mercury was determined by Andersson et al. (2008)⁹⁸ to be calculated as:

$$H' = e^{-2404.3/T [K] + 6.92} \quad (15)$$

In equation 13, C_a is the equilibrium concentration of mercury in the outgoing air and C_a^0 is the mercury concentration in the incoming air. During all campaigns pressurized air was used to create an air flow for purging. Before the air entered the system it was scrubbed using a zero air canister. Hence, in this study the term C_a^0 was equal to zero. In equation 13, r_a is the purging air flow rate controlled by a mass flow controller and r_w is the water flow rate, adjusted by a water valve.

The continuous equilibrium system is further described in paper II, paper V and in Andersson et al. (2008a).⁹⁷

In situ purging system

A system for in situ purging of DGM in surface seawater was developed and tested at the Råö/Rörvik station in 2015. A funnel in stainless steel was constructed and attached to a life buoy and a stand for tide and wave motion support, see Figure 11. The funnel was installed in the water, and attached to the pier via a rail, in which tubing for inflowing and outflowing air was installed. Mercury free air was pumped at 1-2 L min⁻¹ through a FEP tubing leading to a glass frit installed under the funnel at approximately 20 cm under the sea surface. The air bubbles thus created, purged through the surface seawater leading gaseous mercury into the outgoing air, collected by the funnel. The outgoing air was led to a Lumex RA-914+ analyzer for analysis, installed in a shed ashore (Figure 11).

The DGM concentration in surface water was calculated with equation 14. C_a is adjusted to the prevailing temperature and pressure in the water and measured in the instrument according to equation 16;

$$C_a = \frac{T_{\text{Lumex}} \times P_{\text{Seawater}}}{P_{\text{Lumex}} \times T_{\text{Seawater}}} C_{a, \text{Lumex}} \quad (16)$$

where $C_{a, \text{Lumex}}$ is the concentration of Hg(0) measured by the Lumex instrument.

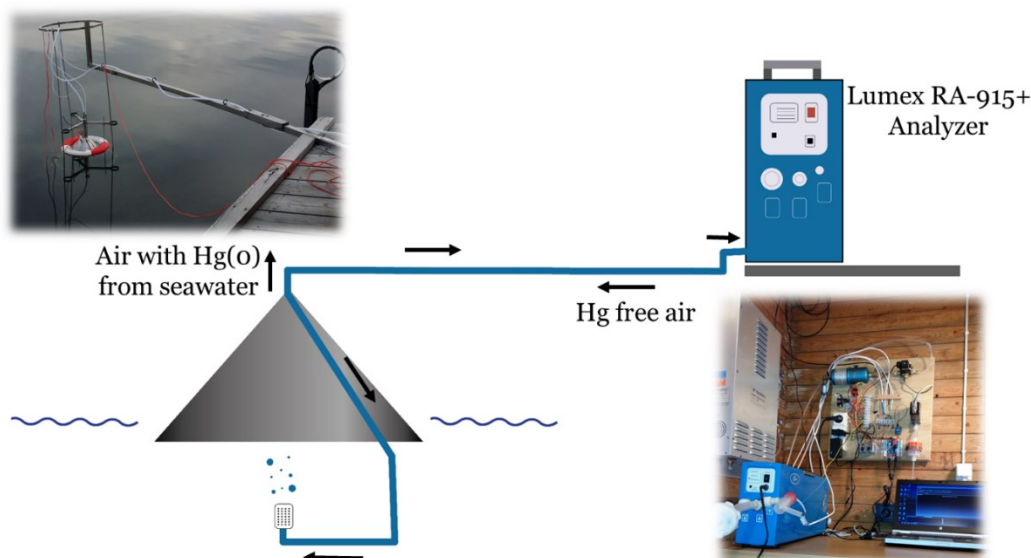


Figure 11. The principle of the in situ purging system for DGM detection in surface seawater. The device consists of a funnel and a glass frit. The gas passing through the glass frit purges the surface seawater, and the outgoing air is collected by the funnel and led to the Lumex RA-915+ analyzer for analysis (pictures: Ingvar Wängberg).

Snow and sea ice sampling

During the campaigns performed in Antarctica and in the Arctic, samples of snow, sea ice, brine and under-ice water were collected during ice stations on ice floes close to the ship and on ice floes reached by helicopter. The nearby ice floes were reached by the gangway or, if the floe was not stable to walk on, by a mummy chair (Figure 12a).

The sampling areas were chosen in clean areas not contaminated by the ship, the helicopter or snow scooters.

Ice cores were sampled from clean areas that were shovelled to remove snow just prior to coring. During the winter and spring campaigns in Antarctica coring was performed using a Mark II coring system from Kovacs Enterprise, consisting of a Teflon coated corer having aluminium cutting shoes and a diameter of 9 cm (Figure 12c). The corer was powered by an electrical drilling machine powered either by a diesel generator or by a battery. When the diesel generator was used it was placed downwind of the sampling site to avoid contamination. During the summer expeditions to Antarctica and the Arctic ice corers made of stainless steel were used with a diameter of 12 cm, powered by a gasoline motor.

The ice core was obtained from inside the corer which had a catch to prevent the core from falling out during coring. The ice core was often cracked into several pieces that were ordered and aligned in blank-tested LD-PE bags for the transportation back to the lab on board the vessels, see Figure 12b. The packed ice cores were put in black plastic bags to reduce the risk of photo-reduction or oxidation within the ice during transportation.

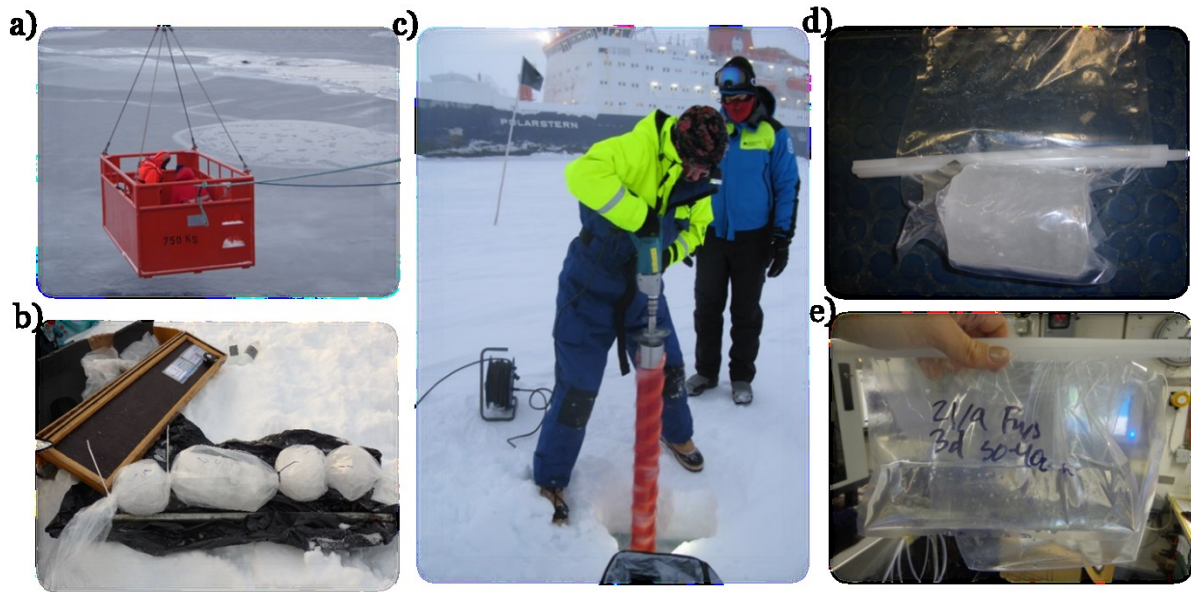


Figure 12. a) Sampling frost flowers using a mummy chair, b) cored ice packed for transportation to the lab, c) drilling an ice core using an electrical drill and a Mark II coring system from Kovacs Enterprise, d) cut section of the ice core, vacuum packed and ready to melt, e) melted ice core sample ready for analysis (pictures: myself and Anna Granfors).

Back in the lab the ice cores were sawn into approximately 10 cm long sections using a stainless steel saw. The surface of the cut ice samples was scraped with a Teflon scraper to remove possible contaminated surfaces. The ice samples were put into gas tight blank-tested LD-PE bags. The bags were sealed airtight and air was removed using a syringe (Figure 12d). This was completed in order to prevent gaseous mercury evading from the sample during melting. The ice samples were left to slowly thaw at room temperature in the dark until totally melted (Figure 12e). The melted ice samples were analysed for Hg(o) concentrations using the manual purge and trap method described on page 21.

The volume of brine within sea ice is a function of the sea ice temperature in °C (T_{Ice}) and the salinity in ppt (S_{Ice}) according to equation 17;

$$V_{Brine} = S_{Ice}(0.0532 - 4.919/T_{Ice})^{0.99} \quad (17)$$

The temperature of the ice was measured in a reference ice core that was cored in conjunction to the sample core. The temperature measurements were performed by drilling small holes every 5 to 10 cm in the reference core and inserting a temperature probe. During the winter campaign in Antarctica and the summer campaign in the Arctic a RTD thermometer with a Pt100 element (precision $\pm 0.1^\circ$ C) was used. An Amadigit (digital thermistor, resolution 0.1° C) was used during the summer campaign in Antarctica. The salinity of the ice was measured in melted and analysed cut sections of the ice. During the winter and summer expeditions to Antarctica the salinity was measured using a WTWCond330i or 3210 instrument having a precision of ± 0.1 . During the summer campaign in the Arctic the salinity was measured using a XS Instruments Cond 70 instrument.



Snow samples were placed in blank-tested LD-PE bags using an acid-cleaned plastic shovel. The snow was sampled at varying depths and was handled and analyzed in the same manner as the ice samples using the manual purge and trap method.

Under ice water (UIW) was sampled in the hole of the sampled ice core. A FEP bottle attached to an elongated bar was quickly inserted through the hole down to the under ice water. When the bottle was filled to the rim it was quickly brought back up. The UIW samples were analysed using the purge and trap method.

Sea ice brine was sampled by drilling partially through the ice with the ice corer to chosen depths varying from 20 to 80 cm. The hole was covered to avoid contamination. When enough brine had leaked from the surrounding ice into the hole yielding enough volume, the brine was sampled using a plastic syringe and put into FEP bottles. At occasions with high brine volume the brine could be collected using the same technique as for UIW. Sea ice brine was analysed using the manual purge and trap method.

Mercury flux calculation and the gas transfer velocity

The transfer of a gas between air and water is limited by diffusion, driven by the solubility of the gas and the concentration gradient according to Henry's law (equation 14). The kinetics of the diffusion is controlled by the gas transfer velocity which is representing the physical turbulence and the diffusivity of the gas.

To estimate the mercury flux at the air-water interphase two different approaches are normally used for mercury, one is the direct flux chamber method and the other is by using gas exchange models. The direct flux chamber method measures the mercury flux in situ using a chamber with a constant air flow passing through. The concentration change of mercury over a fixed water surface inside the chamber is measured, from which the flux rate can be calculated. This method is only applicable during calm weather conditions. A disadvantage of this method is that it creates a closed environment, possibly creating an unnatural environment and an artificial flux rate. It has been discussed in the literature that measuring mercury flux using a flux chamber generally results in lower flux rates than when using gas exchange models.^{100,101}

In studies presented in this thesis a gas exchange model was used to estimate the mercury flux from seawater (Paper II and V). Gas exchange models were first developed for trace gases and are well established for gases such as oxygen and CO₂.¹⁰² The developed models for CO₂ can be adjusted for mercury and the first two-phase film model for mercury was introduced by Liss and Slater (1974).¹⁰³ This model takes into account that the resistance due to the molecular diffusion against gas transfer exists on both sides of the air-water interphase.

In this study the flux of Hg(O) was calculated using equation 18, described in Johnson (2010).¹⁰⁴

$$\text{Hg}_{\text{flux}} = -K_a \times (\text{GEM} - H' \times \text{DGM}) = -K(\text{GEM}/H' - \text{DGM}) \quad (18)$$

K_a and K_w are the total gas transfer velocity constants expressed on the air side and the water side of the interphase respectively [m h^{-1}], GEM is the measured concentration of Hg(O) in air



[ng m⁻³], H' is the Henry's law constant calculated with equation 15 and DGM is the measured concentration of Hg(o) in seawater [pg L⁻¹].

The total gas transfer velocities were calculated by; ¹⁰⁴

$$K_a = \left[\frac{1}{k_a} + \frac{H'}{k_w} \right]^{-1} \quad (19)$$

$$K_w = \left[\frac{1}{k_w} + \frac{1}{H'k_a} \right]^{-1} \quad (20)$$

where k_w and k_a are the gas transfer rates on the water [cm h⁻¹] and air [m s⁻¹] sides, respectively.

The procedures for calculating k_w and k_a are described in papers II and V. The gas transfer rate on the water side (k_w) is a function of the wind speed and the Schmidt number for mercury in seawater.¹⁰⁴ The Schmidt number is a function of the kinematic viscosity, the density of seawater and the diffusivity of mercury in seawater which was calculated according to the equation described in Kuss et al. (2009).¹⁰⁵

The gas transfer rate on the air side (k_a) is a function of the friction velocity, the drag coefficient and the Schmidt number for mercury on the air side, which is a function of the kinematic viscosity and the density of air and the diffusivity of mercury in air.¹⁰⁶ The diffusivity of air is a function of the molar volume of air and mercury, the temperature and the relative molar mass. The dynamic viscosity and the density of air were calculated according to the scheme presented in Tsilingris (2008).¹⁰⁷

Chapter 4

“Satire is a composition of salt and mercury; and it depends upon the different mixture and preparation of those ingredients, that it comes out a noble medicine, or a rank poison.”

-Lord Francis Jeffery, in Tryon Edwards (ed.), A Dictionary of Thoughts (1908), 502.

Mercury – Measurements in the Marine Environment

Measurements in Antarctica

The Antarctic Circle is drawn at 66.5 degrees south and comprises of a total area of 70 million km².^{108,109} The continent is surrounded by the Southern Ocean and the main sea bays are the Weddell Sea and the Ross Sea. The sea ice extent varies with season, having around 20 million km² in winter and 4 million km² in summer. However, the total sea ice extent has in recent years been observed to decrease.^{94,108} Antarctica is a cold continent having an average temperature in winter of -60°C and -28.2°C in summer. It receives limited heating from the surrounding Southern Ocean is the continent with the highest elevation on earth.¹⁰⁹

Antarctica is uninhabited except for around 4000 people working at scientific research stations from all over the world, having no significant emission sources. Air pollutants found in Antarctica have most likely been emitted from countries in the southern hemisphere.^{109,110} Low mercury concentrations were found in marine sediments at Terra Nova Bay in a study by Bargagli et al. (1998). However, Antarctic marine food webs are normally short and mercury has been found in tissues and feathers of many different organisms and animals, at similar levels as found in the northern hemisphere.¹¹¹

The Weddell Sea was visited during two subsequent expeditions onboard the German research vessel and icebreaker Polarstern. The winter campaign (ANTXXIX/6) begun on the 6th of June in Cape Town, South Africa and ended the 12th of August 2013 in Punta Arenas, Chile. The spring expedition (ANTXXIX/7) started 14th of August in Punta Arenas and finished in Cape Town 16th of October 2013. The routes of the two campaigns are presented in Figure 1, Paper I. The analyses were performed onboard by Katarina Gårdfeldt and myself during (ANTXXIX/6) and myself during (ANTXXIX/7).

Another expedition to Antarctica was performed between 8/12 2010 and 14/1 2011 onboard IB Oden during Antarctic summer (OSO 10/11). The study area consisted of the Amundsen and Ross Seas and all Hg(0) analyses were performed by Katarina Gårdfeldt and Sarka Langer onboard the ship. The results of analysis from this campaign have been treated, handled and interpreted by myself and are presented in Paper II, III and IV.

Air measurements

Mercury species in air were measured continuously during the winter and spring campaigns using a Tekran 1130/35 system described on page 19. The outdoor equipment with the air intake was installed on the top deck, on the starboard side in the fore of R/V Polarstern. The results from the air measurements are mainly presented in Paper I. The average concentrations of GEM, HgP and GOM measured during the two campaigns are presented in Figure 32 and in Paper I, and were found to correlate well with earlier measurements in the Southern hemisphere.^{112,113}

Atmospheric mercury depletion events in this study were detected for the first time over sea ice in the Weddell Sea, as early as the middle of July during the Antarctic winter (Paper I). Bromine produced in the dark or photo-induced reactions at early twilight are processes suggested to be involved during the dark oxidation of Hg(O). Reactions suggested to be involved are presented in Figure 3 and in Paper I, beginning with the dark production and release of Br₂. First, ozone is absorbed at the surface layers of the ice and reacts with bromine ions to form OBr⁻ according to reaction 21.⁴⁹



OBr⁻ further reacts with H⁺ in the ice to form HOBr(aq) ($k=10^8$) which forms Br₂ that is released to air (Figure 3 and Paper I). Br₂ has been found in laboratory studies to oxidize Hg(O), forming HgBr₂. It has however been discussed in the literature that this reaction is not important in atmospheric conditions due to it being so slow ($k = 0.9 \times 10^{-16} \text{ cm}^3 \text{ molecule}^{-1} \text{ s}^{-1}$).³⁸ However, if Br₂ exists in great enough concentrations it could play a role in the observed winter depletions. CH₃Br was found in high concentrations in sea ice during Antarctic winter (Paper I) and since HOBr is also the starting material needed to form CH₃Br, this indicates that HOBr probably existed in high concentrations, possibly leading to a high production and release of Br₂.

During the summer expedition onboard IB Oden air measurements of total gaseous mercury (TGM) were performed using a Tekran 2537A. The results are presented in Paper II and the average concentration is presented in Figure 32.

Water column profiles of DGM

During the three campaigns mercury was measured in the water columns of the Weddell, Amundsen and Ross Seas using the CTD/Rosette system onboard the vessels. A total of 63 CTD stations were sampled for DGM (see Paper III).

Seawater samples were also collected and sent to partners at the *Jozef Stefan Institute* in Ljubljana, Slovenia for analysis of MeHg (12 stations) and HgTot (8 stations). The results from the mercury measurements are presented and discussed in Paper III in the context of the different water masses of the Southern Ocean.

Mercury concentrations in the waters of the Southern Ocean were found to vary spatially and seasonally. The average DGM concentrations in the water columns of the Weddell, Amundsen and Ross Seas were found to be higher than the concentrations of MMHg, opposing what has previously been observed on the Eastern side of the Antarctic continent in autumn 2008.¹¹⁵ Significant variations of mercury concentrations were also found in these identified water masses. All results from the measurements are presented in Paper III.

Surface water measurements of DGM

DGM was measured continuously (5 min resolution) during the three Antarctic expeditions using the continuous equilibrium system, described on page 23. The results of the measurements are presented in Paper II, showing 3-5 times higher DGM surface concentrations under sea ice compared to when measuring in open sea. This is due to a 'capping' effect of sea ice, resulting in a build-up of Hg(O) under the ice. This has previously been described by e.g. Andersson et al. (2008).^{116,117}

Mercury flux calculations

By using the measured GEM and surface DGM concentrations together with the ship measurements of wind speed, water and air temperatures and the seawater salinity, the flux of Hg(O) at the air-water interphase could be calculated using equation 18 (procedures are further described on page 27 and in Paper II and V). The results of the mercury flux calculations for the three expeditions are presented in Paper III showing an average net evasion of Hg(O) during winter ($0.4 \text{ ng m}^{-2} \text{ h}^{-1}$) and spring ($1.1 \text{ ng m}^{-2} \text{ h}^{-1}$) in the Weddell Sea and a net deposition during summer ($-0.2 \text{ ng m}^{-2} \text{ h}^{-1}$) in the Amundsen and Ross Seas. Accounting for seasonal changes in sea ice extent and using estimated flux rates for autumn, the total annual mercury evasion from the Southern Ocean was estimated to 30 tonnes.

Hg(O) in the Antarctic sea ice environment

Sea ice, snow, brine, under ice water, pancake ice and frost flowers were collected during the three campaigns at a total of 25 ice stations. The samples were analyzed for Hg(O) onboard the vessels using the methods described on page 21. Samples for HgTot analysis were collected during the campaigns in the Weddell Sea and were sent to partners at *Laboratoire de Glaciologie et Géophysique de l'Environnement (LGGE)* in Grenoble, France for analysis. The results from the mercury measurements in samples collected in the Antarctic sea ice environment are presented in Paper IV. Seasonality of Hg(O) and HgTot concentrations in snow and sea ice was found in this study, and was concluded to be due to varying factors such as solar radiation, atmospheric deposition, temperature and the brine volume of the ice. Spatial variations could also explain the varying mercury concentrations in the sea ice environment in the Southern Ocean.

Solar radiation and Hg(O) in sea ice

A photo-reduction experiment was performed during the three Antarctic expeditions to study how solar radiation influenced the concentration of Hg(O) in sea ice. Cores of one year old sea ice were drilled at different times of the day (usually every 6 hours) to obtain ice cores sampled at varying solar radiation intensities. Solar radiation was measured using sensors installed on the ships. The ice cores were melted and analyzed for Hg(O) (see page 21) and the experiment showed that generally higher Hg(O) concentrations were found in sea ice at higher solar radiation intensity.

Statistical analyses were performed to examine the consistency of the data and to study the correlation between the two parameters. For data set comparisons the radiation intensities were divided into three groups: $0-300 \text{ W m}^{-2}$, $300-600 \text{ W m}^{-2}$ and $600-2000 \text{ W m}^{-2}$. The Hg(O) concentrations obtained in the ice within these radiation spans were divided into three different groups; the average Hg(O) concentrations in the whole ice core, in the top third of the ice core and in the top 10 cm of the ice core. This grouping was chosen in order to study where the influence of solar radiation in the sea ice is largest.

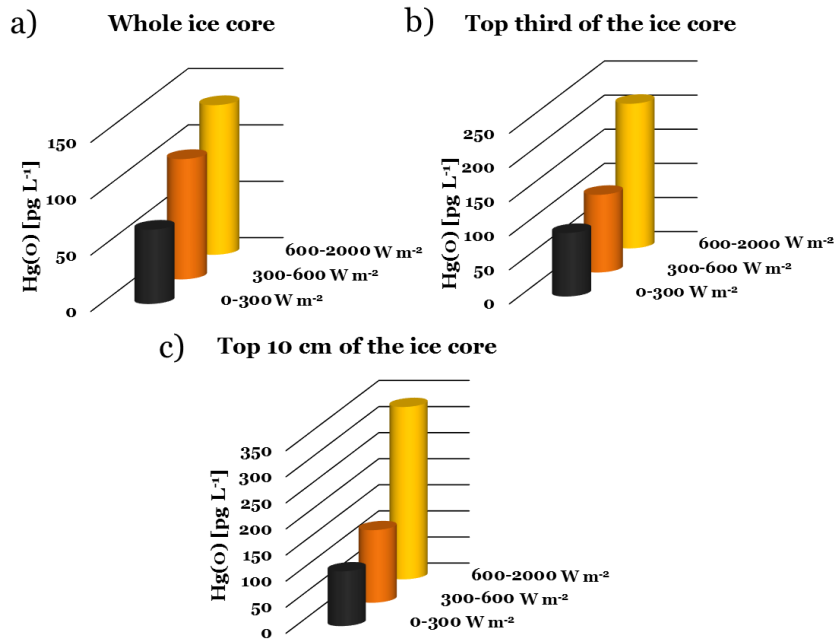


Figure 13. Average $Hg(O)$ concentrations in a) the whole sea ice profile, b) the top third of the sea ice core and c) in the top 10 cm of sea ice cores drilled at solar radiation spans of 0-300 $W m^{-2}$, 300-600 $W m^{-2}$ and 600-2000 $W m^{-2}$.

The results from the photo-reduction experiments are presented in Figure 13 and Tables 1 and 2. Figure 13 shows that the average $Hg(O)$ concentration was highest in the highest radiation span (600-2000 $W m^{-2}$) and that generally higher $Hg(O)$ concentrations were found in the top 10 cm of the ice. The solar radiation is most likely strongest in the top layer of the ice due to the light scattering in air bubbles and brine pockets within the ice. Sea ice is a crystalline material and in one year old ice the crystals in the top part of the ice are small and disorganized, leading to more scattering of incoming light. Further down in the ice the crystals get larger and more ordered and less light is scattered.¹¹⁸

The average and median values and standard deviations of the $Hg(O)$ concentrations in sea ice as a function of solar intensity are presented in Table 1. The Pearson and Spearman correlation coefficients are also presented in Table 1, showing generally low correlation coefficients between $Hg(O)$ and solar radiation. However, by studying the frequency distributions of the data, our data sets were found not to be Gaussian distributed.

For non-Gaussian distributed data sets other statistical analyses than Pearson and Spearman are generally used, such as Student's T-test, ANOVA and Wilcoxon.

A Student's T-test is a hypothesis test where two datasets are compared with respect to the null hypothesis, which is normally stated as "there is no difference between the two studied datasets". ANOVA tests are similar to Student's T-tests but allow comparisons of several datasets in the same statistical analysis. The test yields F-values which are compared to table values that are a function of the degrees of freedom. A Wilcoxon test is a non-parametrical test that compares if the values with the middle rank differ between the two test groups.

Table 1. Average, median and standard deviations of Hg(o) concentrations in sea ice sampled during the photo-reduction experiment, divided into the averages of the whole ice core, the top third and the top 10 cm of the ice core. The Pearson and Spearman correlation coefficients for the data sets are also presented.

Solar radiation [W m ⁻²]		N (no. of samples)	Average Hg(o) conc [pg L ⁻¹]	Median Hg(o) conc [pg L ⁻¹]	StDev	Pearson correlation R ²	Spearman correlation R ²
0-300	Hg(o) average	31	66	50	40	0.02	0.16
	Hg(o) Top 1/3	31	93	66	82	0.13	0.31
	Hg(o) Top value	31	105	92	84	0.09	0.31
300-600	Hg(o) average	15	107	73	71	0.02	0.06
	Hg(o) Top 1/3	15	114	107	50	0.03	-0.30
	Hg(o) Top value	15	139	121	92	0.10	-0.36
600-2000	Hg(o) average	8	133	95	74	0.41	0.30
	Hg(o) Top 1/3	8	212	160	141	0.32	0.27
	Hg(o) Top value	8	331	210	326	0.32	0.42

Table 2. Results from the statistical analysis of the correlation between solar radiation and the Hg(o) concentration in sea ice, using Student's T-test, ANOVA and Wilcoxon. The analysis was divided into three test groups; the average Hg(o) concentration in the whole ice core, the top third and the top 10 cm of the ice core.

	Solar radiation [W m ⁻²]	Student's T-test	ANOVA F-value	Wilcoxon p-value
Hg(o) average	Min (0-300)	0.051 Min-Med	*5.90	*0.006 Min-Med
	Med (300-600)	0.429 Med-Max	Min-Med-Max	0.208 Med-Max
	Max (600-2000)	*0.039 Min-Max		*0.012 Min-Max
Hg(o) Top 1/3	Min (0-300)	0.301 Min-Med	*6.07	*0.017 Min-Med
	Med (300-600)	0.092 Med-Max	Min-Med-Max	0.123 Med-Max
	Max (600-2000)	0.050 Min-Max		*0.012 Min-Max
Hg(o) Top value	Min (0-300)	0.216 Min-Med	*8.25	0.100 Min-Med
	Med (300-600)	0.145 Med-Max	Min-Med-Max	0.327 Med-Max
	Max (600-2000)	0.092 Min-Max		*0.012 Min-Max
H ₀ = There is no difference between the two datasets		If p-value < 0.05 H ₀ is rejected	Table F-value: 2,51 40=3.2317 60=3.1504 If F-value > table value H ₀ is rejected	If p-value < 0.05 H ₀ is rejected
*H₀ is rejected				

The results from the statistical evaluations are presented in Table 2. The ANOVA tests showed that there exists a significant difference in the Hg(o) concentration between the three radiation spans. The Wilcoxon tests showed that the largest difference in Hg(o) concentration existed between the ice sampled at minimum (0-300 W m⁻²) and maximum light intensities (600-2000 W m⁻²).

The statistical evaluations show that there exists a link between the Hg(o) concentration in sea ice and solar radiation. This is hypothesized to be due to a photo-reduction, forming Hg(o)



from oxidized Hg(II)-complexes within the ice.

During the spring and summer expeditions a snow layer experiment was also conducted to study how light diffusion through snow affects the photo-reduction of mercury within sea ice. At ice stations of longer duration, one area was shoveled free of snow to expose the ice surface directly to the atmosphere and to direct solar radiation. After a couple of hours a core was sampled from the uncovered area and in conjunction, an ice core from an un-shoveled area was cored for comparison. The sampling of the two ice cores was performed several times at maximum light conditions at midday and during minimum light conditions at midnight. The results of the snow layer experiment are presented in Figure 14.

The highest average Hg(o) concentrations were found in uncovered ice sampled at maximum light during both spring and summer, showing higher values than in ice cored from covered areas. This indicates that the snow cover does influence the light diffusion and is probably affecting the photo-reduction of mercury within sea ice.

An opposite trend was observed during minimum light at midnight with higher Hg(o) concentrations in the snow covered ice than the uncovered ice. This might signify that the evasion of Hg(o) from the uncovered ice surface directly to the atmosphere was larger than the production of Hg(o).

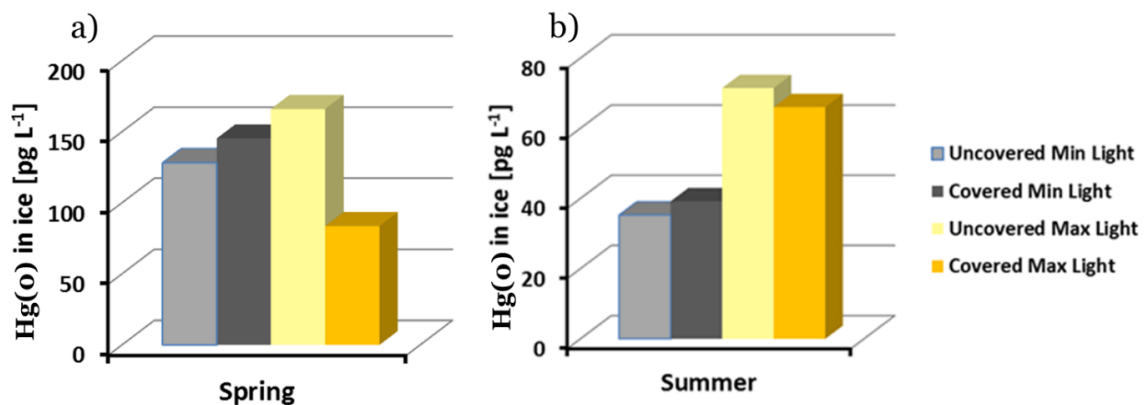


Figure 14. Results from the snow layer experiment showing average Hg(o) concentrations in the whole ice profile of ice cored from an uncovered areas and snow-covered areas under minimum and maximum light intensities during a) the spring expedition and b) the summer expedition.

Measurements in the Mediterranean Region

Around 132 million people live along the Mediterranean Sea which is a region having many natural and industrial emission sources. The area is known to have a high volcanic and tectonic activity and has historically been used for mercury mining due to the large cinnabar deposits. The Mediterranean seawater consists of four major water masses which originate from the Atlantic Ocean via the narrow strait of Gibraltar and the Black Sea via the Dardanelles/Marmara Sea/Bosporus system. Increased levels of mercury have been found in soil, fish and vegetation in the area.^{119,120} The average measured air temperature in autumn 2011 was $19 \pm 1.4^{\circ}\text{C}$ and during summer 2012, $26 \pm 2.2^{\circ}\text{C}$.

Two overwater campaigns were conducted in the Mediterranean Region aboard the Italian Research vessel Urania. The first campaign was performed in the Tyrrhenian Sea during autumn from 25/10 to 8/11 2011 (Fenice 2011). The second expedition Fenice 2012 (11/8 to

29/8 2012) was carried out during summer in the Mediterranean Sea, passing through the Strait of Gibraltar to the Atlantic Ocean. The routes of the two expeditions are presented in Paper V.

Air measurements

GEM in air was measured during the two Mediterranean campaigns using a Lumex RA-915+ analyzer, see page 18. The instrument was installed on the bridge deck on the starboard side of R/V Urania during both expeditions to avoid influences from the ship's exhaust funnel. The measurements were performed with 5 second resolution and the results of the air measurements are presented in Paper V, showing higher average values during autumn (1.7 ng m^{-3}) than during summer (1.5 ng m^{-3}). These measurements are in good agreement with what has previously been measured in the Mediterranean Sea.^{101,121–123}

Water column profiles of DGM

Deep water profiles of DGM concentrations were obtained during the two campaigns by collecting seawater samples using the ship's CTD/Rosette system, see Figure 8. A total of 8 CTD stations were sampled during Fenice 2011 with results presented in Figure 15. The two deeper stations So2_b and So2_3 showed generally higher DGM concentrations in the deeper water column (>100 m) with highest concentrations found close to the bottom.

The strong tectonic activity and volcanism in the area could lead to a degassing and upwelling of Hg(0) from the sea bottom, possibly explaining the higher concentrations of DGM observed close to the bottom.⁷² Enhanced DGM concentrations were also found in the bottom layers of the So5_05 station located close to the volcanic Island Stromboli, which is probably due to similar upwelling processes.

During Fenice 2012 a total of 12 CTD stations were sampled, see Figure 16. Generally higher DGM concentrations were found in the water columns during the summer campaign of Fenice 2012, with an average of $51 \pm 38 \text{ pg L}^{-1}$, compared to during the autumn campaign of Fenice 2011, with an average of $36 \pm 24 \text{ pg L}^{-1}$. This is mainly due to that deeper water columns were sampled during the summer campaign and generally higher DGM concentrations are found in deeper waters.⁷²

The highest DGM concentrations during Fenice 2012 were found at stations So7, So8 and So9. The observed variations could be due to the water circulation of the four different water masses in the Mediterranean Sea.^{72,124}

Surface water measurements of DGM

DGM concentrations were measured every 5 min in the ship's bow water having a seawater intake at a depth of 4 m. The continuous equilibrium system (described on page 23) was used for the sampling and a Tekran 2537A was used for the analysis.

The average DGM concentrations obtained during the two campaigns were found to correlate well with values presented in the literature (see Table 2, Paper V). Substantial spatial variations of surface DGM concentrations were found in the Mediterranean Sea, with the highest concentrations in the surface waters of the Tyrrhenian Sea. Seasonality of DGM concentrations was also found in this study and in the literature, showing highest values in autumn and lowest during winter.

The results of the surface DGM measurements performed during the two expeditions are presented in Paper V.

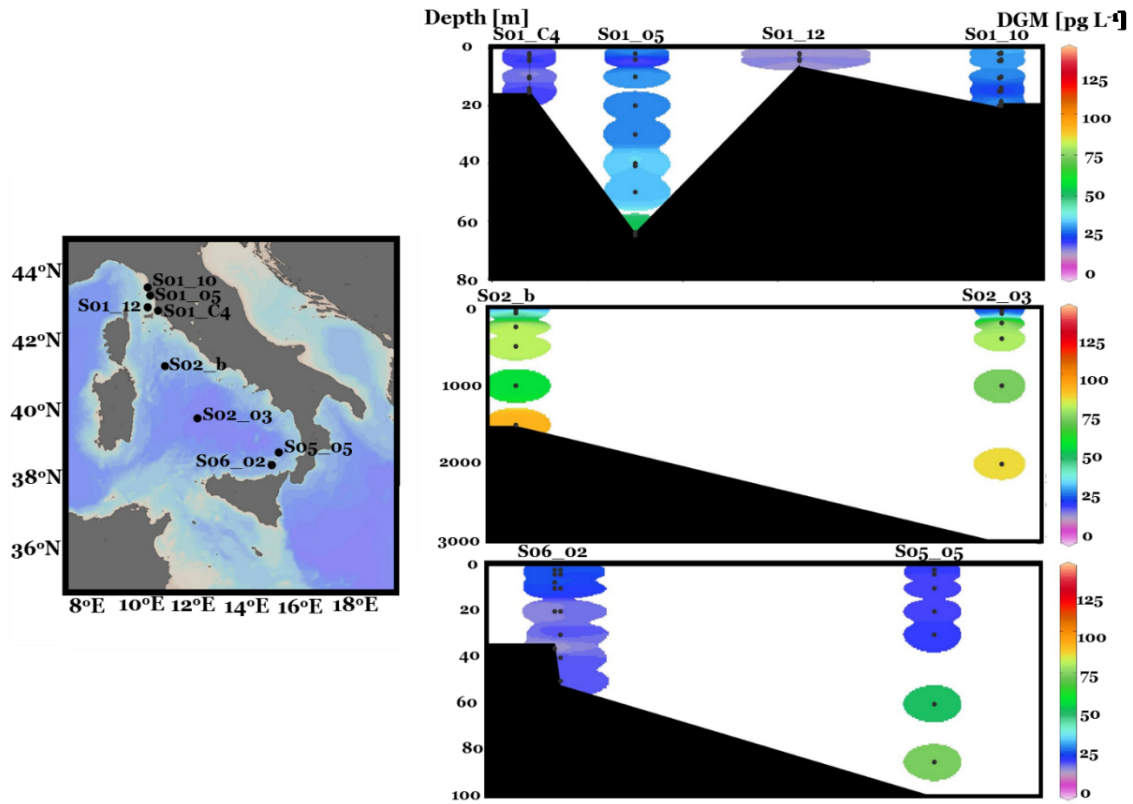


Figure 15. Deep water profiles of DGM concentrations sampled at 8 CTD stations during Fenice 2011 (25/10 to 8/11 2011) in the Tyrrhenian Sea.

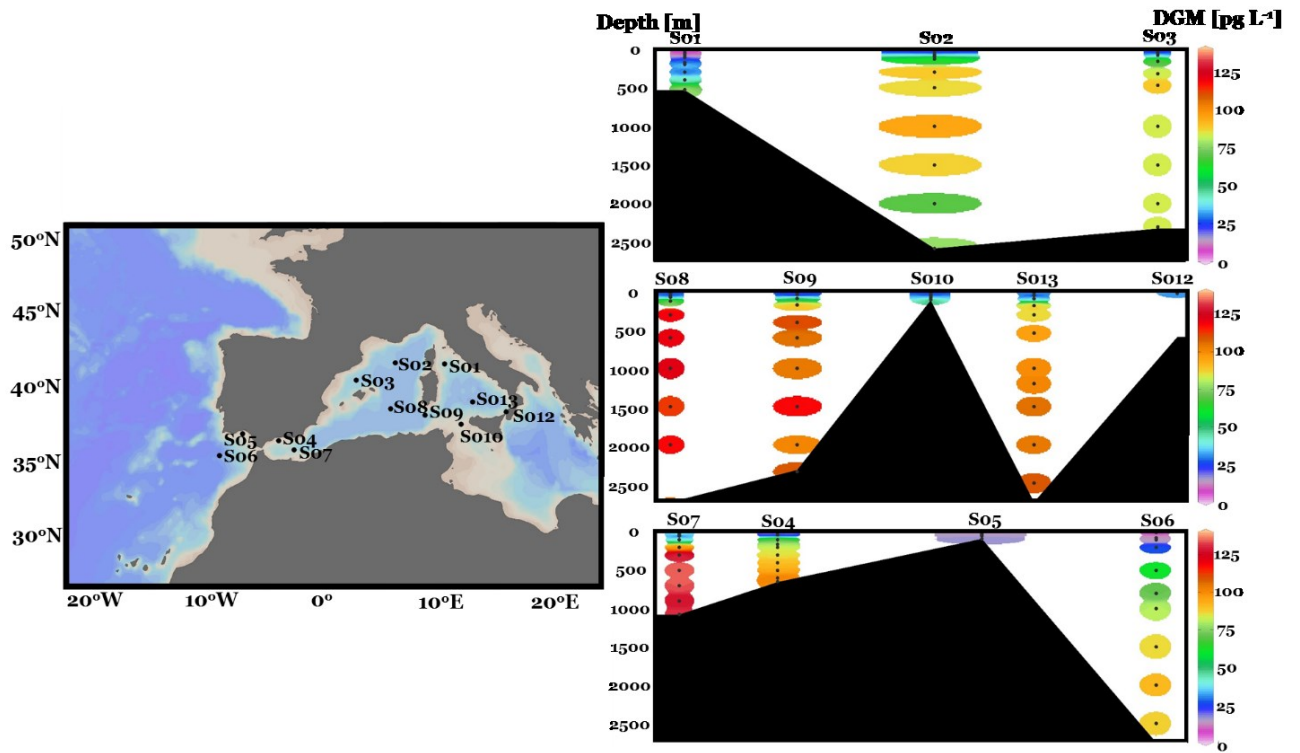


Figure 16. Deep water profiles of DGM concentrations sampled at 12 stations during Fenice 2012 (11/8 to 29/8 2012) in the Mediterranean Sea.

Mercury flux calculations

The results from the GEM and DGM measurements were used to calculate the fluxes of Hg(o) from the Mediterranean Region. The waters of the Mediterranean Sea were found to be supersaturated to around 400-500% with respect to Hg(o), during both autumn and summer. The Hg(o) flux was found to be higher in the Tyrrhenian Sea due to higher surface DGM concentrations. Calculated Hg fluxes in the Mediterranean Sea found in the literature were found to vary substantially. Due to the chosen gas exchange model the estimated Hg flux could vary up to 50%, even at low wind speeds (section 3.5, Paper V).

Solar radiation and Hg(o) in surface seawater

At coastal stations during Fenice 2011, CTD casts were executed down to around 20 m depth at different times of the day in order to study the influence of solar radiation in shallow seawater.

The solar radiation experiment performed at station S01C close to Piombino is presented in Figure 17. No significant variations in DGM concentrations were found in the whole 20 m water column. However, the surface concentration (2 m depth) showed a clear decrease in DGM concentration from a maximum at 12:25 to a minimum at 04:20, decreasing from 37 pg L⁻¹ to 28 pg L⁻¹. Diurnal variations of DGM in surface water are due to the balance between photo-reduction, oxidation and evasion processes have previously been observed and described in the literature.^{65,119,125-127}

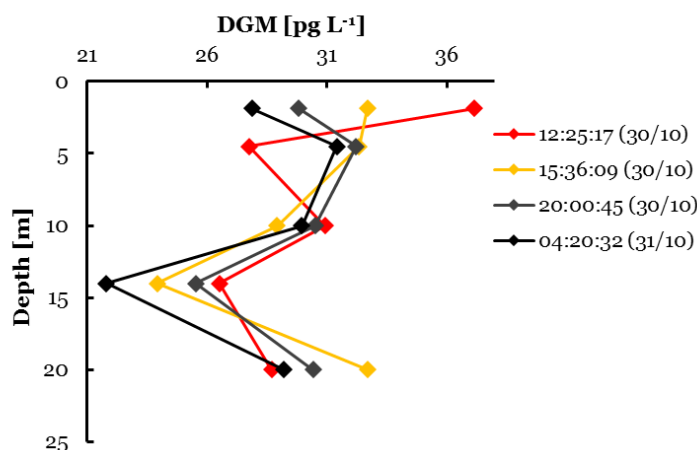


Figure 17. DGM profiles in surface seawater (20 m) sampled at different times of the day at the coastal station S01C (Piombino, Fenice 2011).

The continuous surface measurements of DGM using the continuous equilibrium system showed no diurnal variations (Paper V). However, the water intake for the bow water system is placed at around 4 m depth and as can be observed in Figure 17, the diurnal variations of DGM were only clearly visible in the top 2 m of the water column. Additionally, the diurnal variations of DGM in surface water have previously been found to be more pronounced at coastal stations compared to in the open sea.¹²⁷ Factors that have been proposed in the literature to affect the diurnal variations in the DGM concentration in surface water include the total water depth, wind speed, wave motion and the concentration of DOC.¹²⁷⁻¹²⁹



Measurements in Sweden

The Råö/Rörvik station is situated on the west coast of Sweden close to Onsala (57°23'37.76 N, 11°54'50.73 E), around 50 km south of Gothenburg. The air monitoring station is located in a natural reserve within the area of the Onsala Space Observatory and is one of the GMOS master sites, situated far away from direct emission sources (approximately 150 km). Based on the measuring period the average temperature, humidity and wind speed (± 1 standard deviation) at the site were 9 ± 7 °C, 76 ± 12 % and 6 ± 4 m s⁻¹, respectively. Mercury measurements in air at the site began in the middle of the 1980's and during my PhD studies continuous measurements of GEM, GOM and HgP were performed from 2012 to 2015. Back trajectories were used to study the origin of air masses bringing mercury in air to the site. Surface DGM concentrations in seawater were measured using the in situ purging system (see page 24) during a trial period in spring 2015.

Air measurements

Mercury species in air were measured using the Tekran 1130/35 system (page 19) between 15/5 2012 and 3/7 2013 and between 1/2 2014 and 29/4 2015. The outdoor equipment with the air intake was installed on the roof-top of the measuring station, at approximately 7 m above sea level, and about 20 m from the coast (see Figure 7). The site was cleared of nearby vegetation in order to avoid any vegetal influence. The site primarily measures background concentrations of the three mercury species in air (Paper VI). All results from the air measurements of GEM, GOM and HgP are presented in Figure 18. The average GEM concentration during the measurement periods was 1.41 ng m⁻³ and the average GOM and HgP concentrations were 0.23 and 2.21 pg m⁻³, respectively. These averages were found to be comparable to measurements performed in northern European countries.^{130,131}

Back trajectories were produced using the Hybrid Single-Particle Lagrangian Integrated trajectory (HYSPLIT) 4-0 model that was run together with meteorologically analyzed fields from NCEP/NCAR. The 72-hours back trajectories were created at 5 different heights (10, 50, 100, 250 and 500 m) every four hours to be matched with the sampling cycles of GOM and HgP.

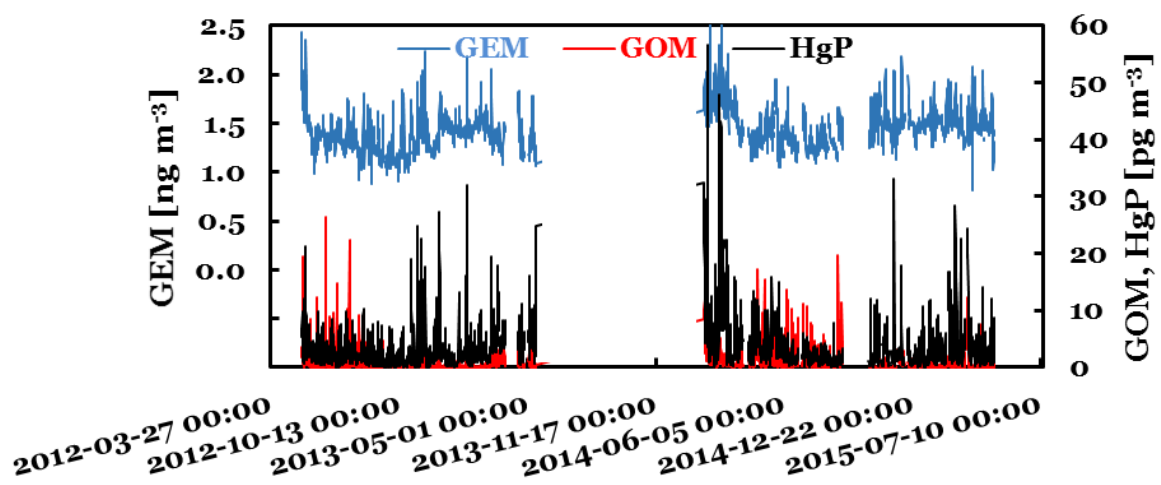


Figure 18. Air measurements of gaseous elemental mercury (GEM), gaseous oxidized mercury (GOM) and particulate mercury (HgP) from 3/7 2013 to 29/4 2015 at the Råö/Rörvik station close to Gothenburg, Sweden.

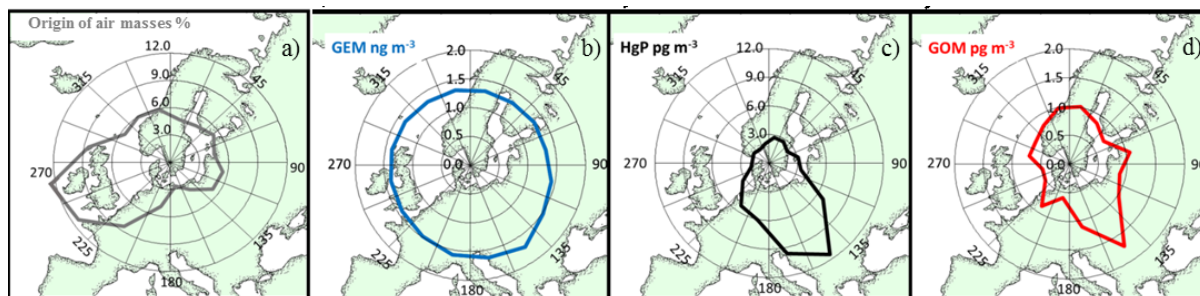


Figure 19. Results from the back trajectory evaluation of the Råö/Rörvik air measurements presented as a) relative frequency of air mass origin within each sector, b) GEM, c) HgP and c) GOM as a function of air mass origin direction arriving at the Råö/Rörvik station.

An imaginary 150 km wide circle with the Råö/Rörvik station centered was divided into 16 geographical sections of 22.5 degrees each ($16 \times 22.5^\circ = 360^\circ$), see Figure 19. The back trajectories were evaluated and matched with the geographical sections using specifically developed Excel VBA software. The concentrations of GEM, GOM and HgP were plotted as a function of air origin direction and only trajectories with limited variations in direction during the last 72 hours were used for the evaluation. The results from the back trajectory analysis is presented in Figure 19.

Figure 19a shows that about one third of the air masses reaching Råö/Rörvik entered from a direction between 202.5° and 270° . As presented in Figure 19b, elevated GEM concentrations (average concentration: 1.51 ng m^{-3}) were observed coming from sectors between 90° and 247.5° , possibly representing polluted air masses (e.g. coal combustion and industrial activities) coming from Poland, Romania, Greece, Bulgaria and other Balkan countries. The average GEM concentration in air coming from the remaining sectors was lower (1.36 ng m^{-3}), and was considered as being associated with the background concentration of GEM in the Northern hemisphere. The anthropogenic contributions to mercury in air coming from between 90° and 247.5° were further supported by the elevated HgP and GOM concentrations found in air coming from these sectors, see Figures 19c and 19d. The finding of high HgP concentrations in air has previously been used as a special marker to denote polluted air masses.¹³² Low concentrations of HgP and GOM from remaining sectors further support that mercury in air entering Råö/Rörvik from the sectors between 0° and 90° and between 247.5° and 360° could be considered as well-mixed background concentrations.

Surface water measurements of DGM

An in situ purging system for measuring DGM concentrations in surface water was developed (described on page 24) and used during a trial period in spring 2015 at the Råö/Rörvik station. The measuring station is situated about 100 m away from the Tekran 1130/35 instrument in the same area. Data from the period 19/3 to 24/3 2015 are presented in Figures 20 and 21.

The average DGM surface concentration during the trial period was $13 \pm 5 \text{ pg L}^{-1}$, which is substantially lower than what has previously been measured in surface water at 16 stations in the North Sea in 1991 ($52 \pm 20 \text{ pg L}^{-1}$).¹³³ The differences could be due to yearly, seasonal or

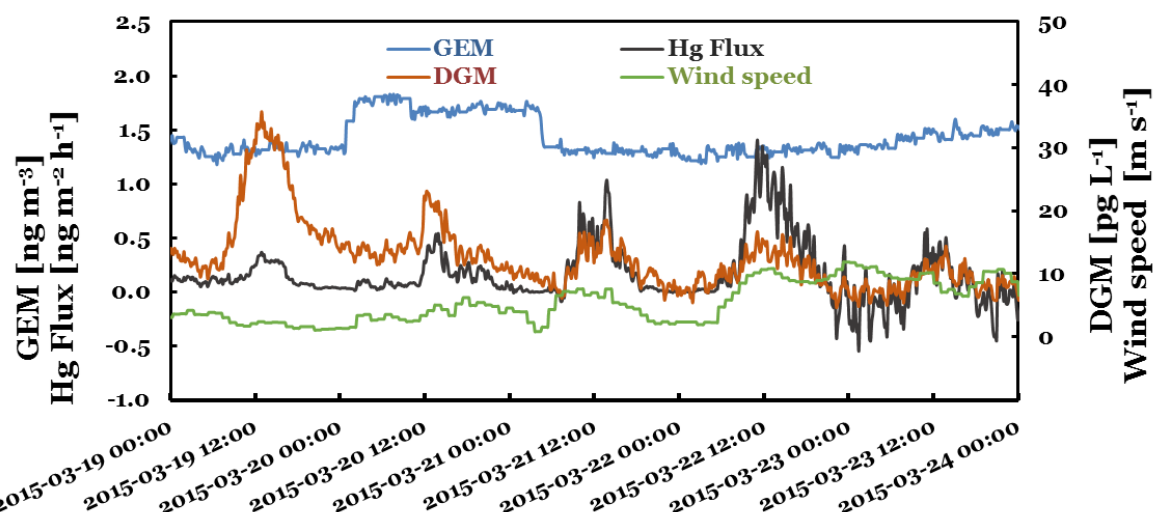


Figure 20. Measurements of GEM in air, DGM in seawater, wind speed and calculated mercury flux for the period 19/3 to 24/3 2015.

spatial variances. It could also be due to the placing of the glass frit in the in situ purging system being only at 20-30 cm depth. As presented in Figure 17, the DGM concentrations in shallow water profiles can vary significantly. DGM in seawater consists of both Hg(o) and DMHg. However, the analysis method of the Lumex RA-915+ instrument only allows the detection of gaseous Hg(o), which also could explain the low values measured in comparison to the literature values.

Mercury flux calculations

The GEM measurements from the Tekran 2537B instrument and the DGM concentrations obtained using the in situ purging system were used to calculate the flux of Hg(o) from the sea surface at the site.

The average Hg flux during the trial period was calculated to be $0.13 \pm 0.25 \text{ ng m}^{-2} \text{ h}^{-1}$, indicating a net evasion of Hg(o) from the coastal waters of the North Sea. Coquery and Cossa (1995) estimated the Hg Flux from the North Sea to be between 0.92 and $1.87 \text{ ng m}^{-2} \text{ h}^{-1}$, calculated based on a similar gas exchange coefficient to that calculated for this study.¹³³ The differences in Hg flux is mainly due to the lower DGM concentrations measured during this study. The calculated Hg fluxes for the period 19/3 to 24/3 2015 are presented in Figure 20, showing a clear relationship to the measured DGM concentrations, as expected from equation 18. The connection between the Hg flux and different measured parameters is further discussed in Paper V.

Solar radiation and Hg(o) in surface seawater

The surface concentrations of DGM are plotted against measured solar radiation in Figure 21. A diurnal variation in surface DGM concentrations was observed, showing a positive correlation with solar radiation ($R^2 = 0.38$). The correlation was especially evident during the solar eclipse on the 20th of Mars 2015 which lead to a sudden decrease in DGM concentration from 19 to 15 pg L^{-1} . Similar observations during a solar eclipse have previously been made by Gårdfeldt et al. (2001).⁶⁶

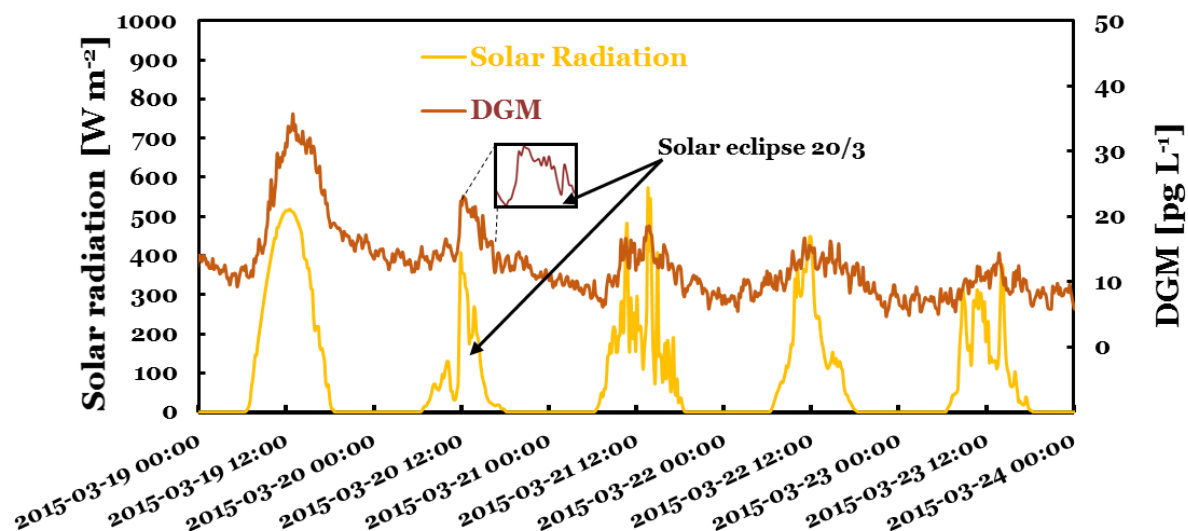


Figure 21. Measurements of surface DGM concentrations and solar radiation at the Råö/Rörvik station from 19/3 to 24/3 2015, showing a decrease in DGM concentration and solar radiation during the solar eclipse on the 20th of Mars 2015.

Measurements in Finland

The Pallas-Matorova station in northern Finland (68°00'N, 24°14'E) is located in a natural park close to the Pallasjärvi Lake. It is situated at the Matorova hilltop at a height of 340 m above sea level, is surrounded by forest and is located far away from potential pollution sources. The station is reached by foot or by snow scooter in winter. The average winter temperature in the area is about -14°C in winter and about 14°C in summer.¹³⁴

Measurements of mercury species in air were performed at the site during a one month long campaign in Spring 2012.

Air measurements

GEM, GOM and HgP were measured at the Pallas-Matorova station from 2/4 to 26/4 2012 using a Tekran 1130/35 system. The aim of the campaign was to monitor mercury species in air during springtime in the Scandinavian Arctic. The average GEM, GOM and HgP concentrations during the entire campaign were $1.4 \pm 0.2 \text{ ng m}^{-3}$, $1.5 \pm 1.4 \text{ pg m}^{-3}$ and $2.2 \pm 1.5 \text{ pg m}^{-3}$, respectively. Ozone was measured during the campaign by Katriina Kyllönen using a Thermo Scientific O₃-analyzer, model 49i, yielding an average concentration of $43 \pm 3 \text{ pptv}$. Selected results of the air measurements are presented in Figures 22a and 22b. On the 7/4 a decrease in GEM from around 1.3 ng m^{-3} to below 1 ng m^{-3} was observed, indicating an detected atmospheric mercury depletion event (see description on page 11). A simultaneous ozone depletion event was detected with concentrations decreasing from around 35 pptv to below 25 pptv, see Figure 22a.

Since no elevated concentrations of HgP and GOM were detected and the depletions of GEM and ozone were minor, the event probably occurred at another location bringing depleted air masses transported over long distances to the Pallas-Matorova station.

To track the origin of the air masses entering the station, 48 h back trajectories were constructed using the NOAA hybrid single-particle Lagrangian integrated trajectory model.

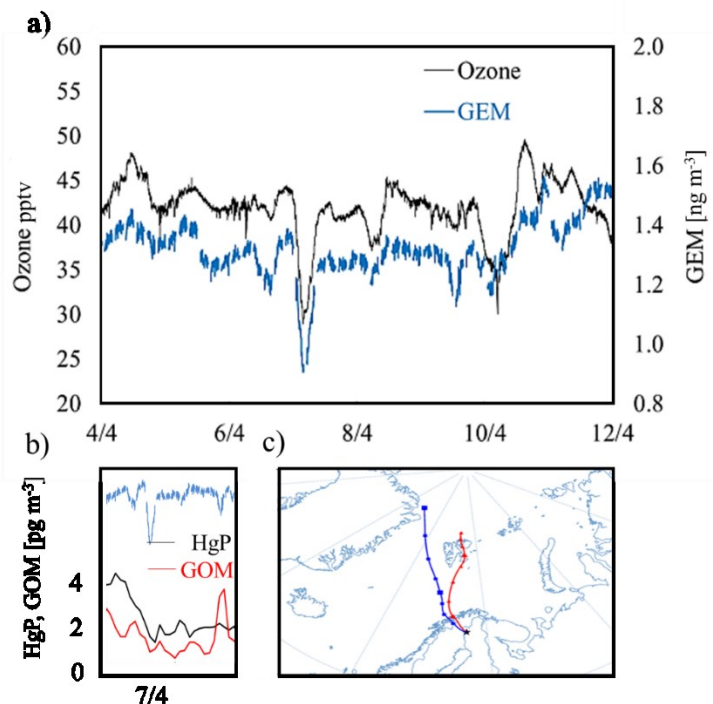


Figure 22. Results from the air measurement campaign at Pallas-Matorova in April 2012. a) Measurements of GEM and Ozone in air from 4/4 and 12/4 showing a clear depletion event on the 7/4. b) Measurements of HgP and GOM during the depletion event on the 7/4. c) 48 h back trajectories calculated for the depletion event detected on the 7/4.

The back trajectories for the 7/4 are presented in Figure 22c, showing that the air masses transporting the GEM and ozone depleted air masses to Pallas originated from Svalbard and the north east coast of Greenland.

BrO that is normally formed during ozone depletions (reaction 6) was detectable with satellite Differential Optical Absorption Spectroscopy (DOAS) measurements. Figure 23a shows the BrO concentrations in the Arctic from the 4/4 to 6/6 2012. High concentrations of BrO were found on the 5/4 in the area in which the air masses originated from, reaching Pallas 48 hours later on the 7/4. This indicates that bromine chemistry was active in the origin area of the air mass.

Furthermore, Br₂ which can form bromine radicals via photolysis (equation 4) is generally released from newly formed sea ice. Sea ice concentration maps from *The Cryosphere Today* show that between 3/4 and 6/4 an increase in sea ice concentration was detectable at the north east coast of Greenland (Figure 23b). This suggests that Br₂ released from the newly formed sea ice was photolyzed by reaction 4 to bromine radicals which destroyed ozone according to reaction 6. The bromine radicals and the BrO formed, could have oxidized GEM in air according to reactions 7-10. Hg(II) (GOM and/or HgP) formed was probably deposited near the area of the depletion event, which could explain why neither elevated GOM nor HgP were detected at the Pallas-Matorova station (Figure 22b).

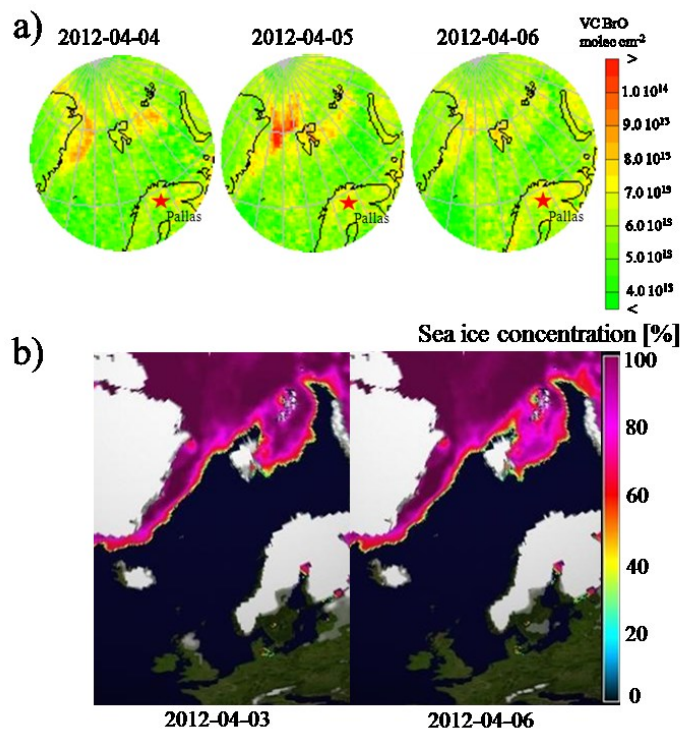


Figure 23. a) BrO maps from the GOME-2/ SCIAMACHY DOAS nadir data browser, University of Bremen (IUP DOAS), showing BrO concentrations in the area of air mass origin of air reaching the Pallas-Matorova station on 7/4 2012. b) Sea ice concentration maps from *The Cryosphere Today* (<http://arctic.atmos.uiuc.edu/cryosphere/>) showing an increase in sea ice extent from 3/4 to 6/4 2012.

Measurements in the Arctic

The Arctic is defined as the area north of the Arctic Circle, drawn along latitude 66.5 degrees north. It has a total area of around 70 million km² and has been inhabited for almost 20 000 years. Indigenous people living in the Arctic are still relying on fish and hunting as their primary source of food.^{23,109} It is estimated that around 80-140 tonnes of mercury are accumulated annually in Arctic food chains, originating from sources in the northern hemisphere.²³ The Arctic is warmer than Antarctica having a winter average temperature of -40°C and a summer average temperature of 0°C. The main differences between the Arctic and Antarctica in terms of temperature is that the Arctic consists of mainly seawater which is surrounded by many continents, and that the Gulf Stream keeps the Arctic warmer.¹⁰⁹

A summer expedition was performed to the Arctic Ocean (AO16) onboard IB Oden departing from Longyearbyen the 8/8 and returning on the 20/9 2016. The route of the expedition is presented in Figure 24. Mercury species in air were measured continuously using the Tekran 1130/35 system (page 19) and the continuous equilibrium system was used to measure DGM concentrations in surface seawater along the cruise track (page 23). Samples from the CTD/Rosette system were collected to obtain deep water profiles of DGM concentrations. Samples of sea ice, snow, brine, under ice water, frost flowers and newly formed sea ice were collected at ice stations mainly reached by helicopter but also at stations on ice floes close to the ship, reached by a mummy chair (Figure 12a). The Hg(o) analyses were performed onboard by Katarina Gårdfeldt and myself. Selected results obtained during the campaign are presented in this section.

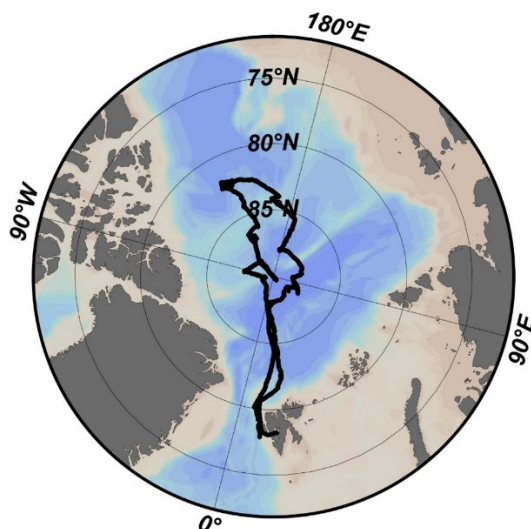


Figure 24. The cruise track of the Arctic Ocean 2016 expedition (AO16) starting and ending in Longyearbyen, Svalbard (8/8 to 20/9 2016).

Air measurements

GEM, GOM and HgP concentrations in air were measured using a Tekran 1130/35 mercury speciation unit. The outdoor equipment with the air intake was installed on the 4th deck in the fore of the ship to avoid influences from the exhaust gases from the ship's funnel. The results from the air measurements are presented in Figure 25.

The average concentrations for the period 9/8 to 18/9 of GEM, HgP and GOM were 1.4 ± 0.2 ng m⁻³, 2.4 ± 2.0 pg m⁻³, and 1.6 ± 2.4 pg m⁻³, respectively. These values are similar in range as what has previously been measured during an oversea campaign in the Arctic in 2004 and estimated by GRAHM modeling for the Arctic Ocean.^{135,136}

Elevated GEM concentrations were found in an area 1 north of Svalbard at around 85°N, 13°E (1.6 ± 0.1 ng m⁻³) and lower concentrations were found in area 2 at 86°N, 135°W (1.1 ± 0.05 ng m⁻³), see Figure 25a. In area 1, a simultaneous smaller increase in HgP concentrations was observed (~ 2 pg m⁻³), see Figure 25c, indicating a possible transportation of polluted air masses. In area 2 where lower GEM concentrations were observed, increased GOM concentrations were also found (~ 10 pg m⁻³). Back trajectories were composed for the two events (area 1 and 2 in Figure 25) and are presented in Figure 26.

Back trajectories for the event in area 1 on the 13/8 (Figure 26a) show that air masses reaching IB Oden were originating from the west, possibly bringing polluted air masses from North America and/or Canada. During the event in area 2 on the 26/8, the air masses bringing decreased GEM concentrations and increased GOM concentrations were found to originate from the south (Figure 26b). Since GOM mainly is formed in the atmosphere via the oxidation of GEM and is not very long-lived, this event was possibly a local phenomenon due to the oxidation of GEM over sea ice.¹³⁷

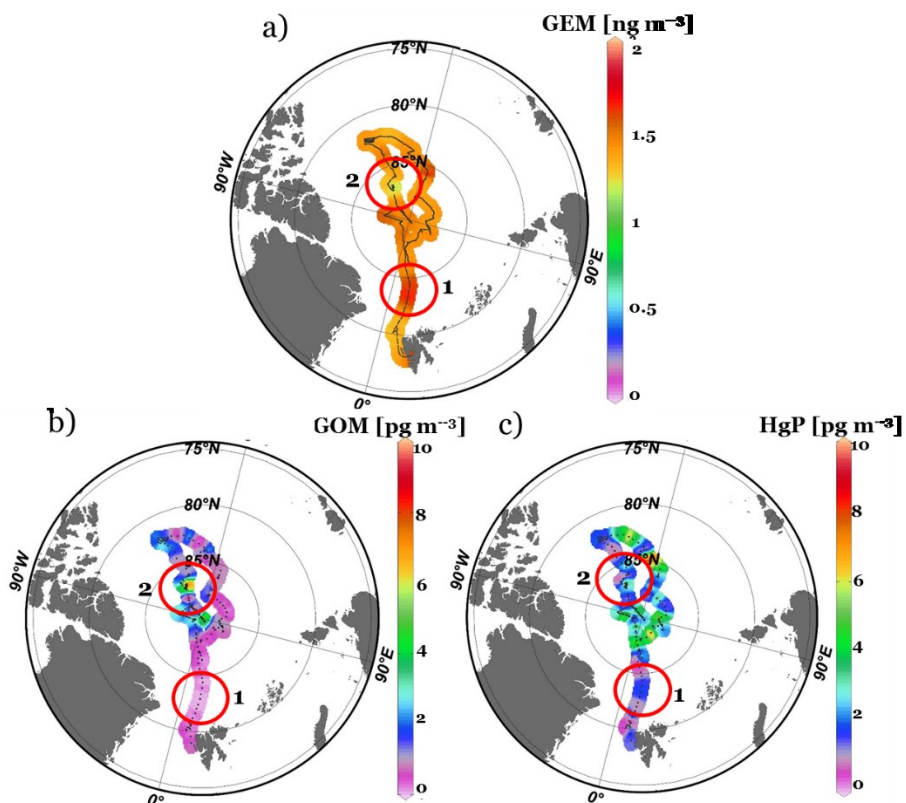


Figure 25. Results from the continuous measurements of a) GEM, b) GOM and c) HgP in air using the Tekran 1130/35 system during the AO16 expedition in the Arctic. (Data from 9/8 to 18/9 2016).

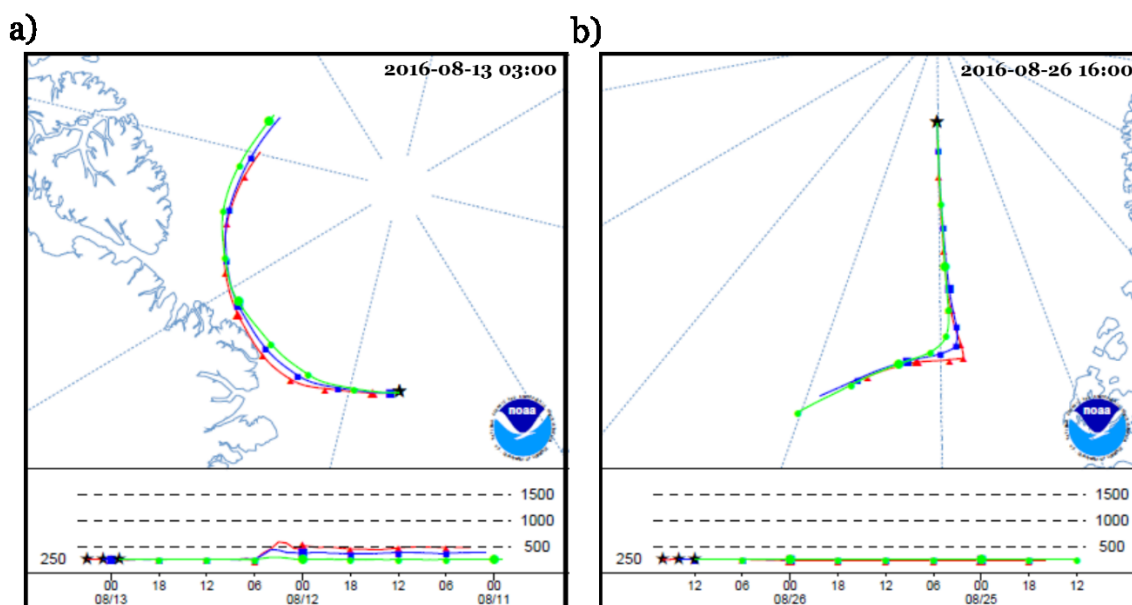


Figure 26. Back trajectories for a) area 1 of Figure 25 (13/8 03:00 at 85°N, 13°E) showing elevated GEM and HgP concentrations, b) area 2 of Figure 25 (26/8 16:00 at 86°N, 135°W), with lower GEM and higher GOM concentrations.

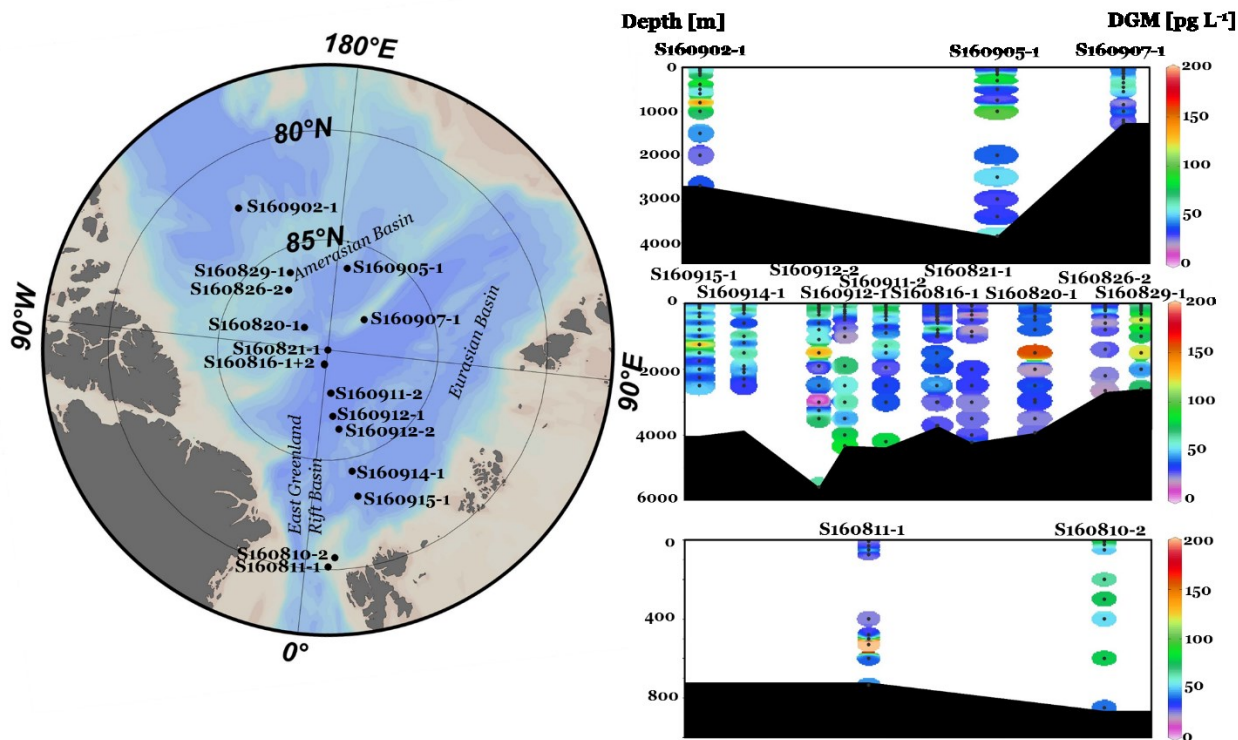


Figure 27. Deep seawater profiles of DGM concentrations in the Arctic Ocean during the AO16 campaign sampled at a total of 16 CTD stations.

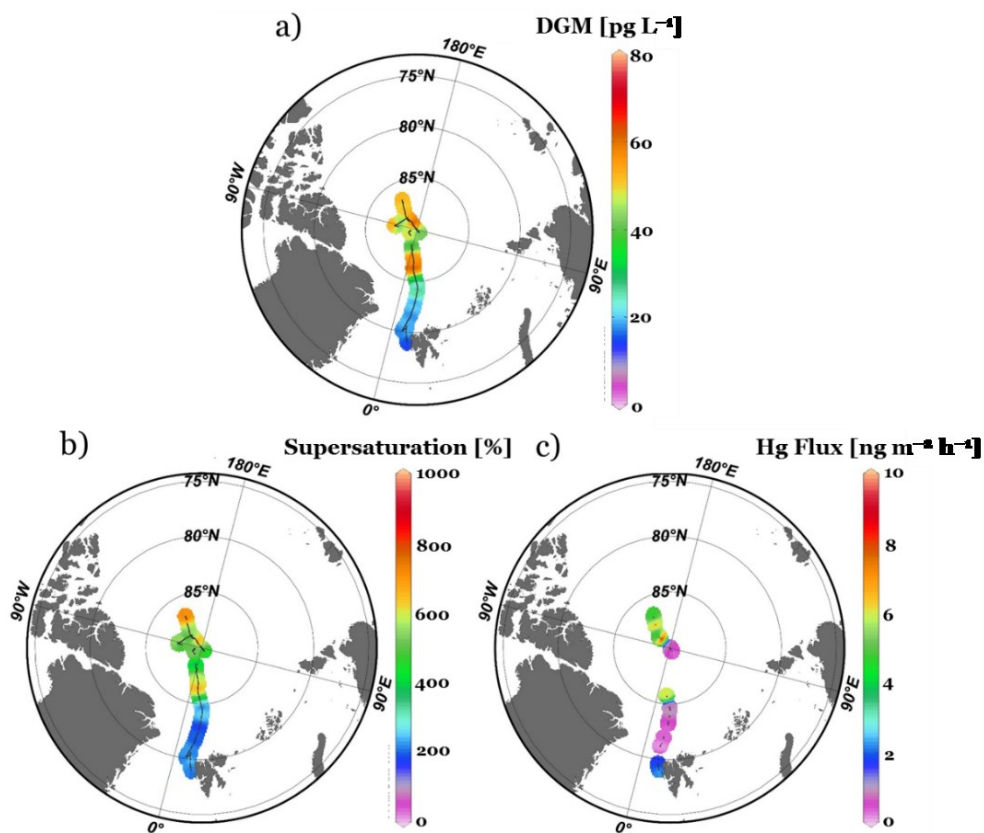


Figure 28. Results from the continuous measurements of a) DGM in surface seawater, b) calculated supersaturation grades and c) calculated Hg Flux in the Arctic Ocean during the AO16 campaign. (Data from 8/8-28/8 2016.)

Water column profiles of DGM

DGM concentrations were measured in discrete seawater samples obtained using the CTD/Rosette system at a total of 16 CTD stations in the Arctic Ocean, see Figure 27.

The results are presented in Figure 27 having an average water column concentration in the Arctic Ocean of $50 \pm 35 \text{ pg L}^{-1}$. No previous studies of DGM concentrations in deep water profiles were found in the literature for comparisons.

The Arctic Ocean is divided into two basins by the Lomonosov Ridge; the Eurasian Basin and the Amerasian Basin, see Figure 27. The spatial differences were studied, showing no significant variations in water column DGM concentrations between the Eurasian Basin ($47 \pm 21 \text{ pg L}^{-1}$) and the Amerasian Basin ($47 \pm 26 \text{ pg L}^{-1}$). However, in the East Greenland Rift Basin the average water column concentration of DGM was found to be significantly higher ($68 \pm 98 \text{ pg L}^{-1}$). The data will be further investigated in terms of different water masses and the circulation of water in the Arctic Ocean. Results will be presented in future publications.

Surface water measurements of DGM

DGM concentrations in surface seawater were measured continuously with 5 min resolution using the continuous equilibrium system (page 23). Results from the expedition are presented in Figure 28, as far as they have been treated when writing this thesis.

The average DGM concentration in surface seawater measured between 8/8 and 28/8 2016 was $40 \pm 19 \text{ pg L}^{-1}$, which is in good agreement with previous measurements using the same equipment in the Arctic during 2005 ($44 \pm 22 \text{ pg L}^{-1}$).¹¹⁶ Surface DGM concentrations were found to be higher when passing through sea ice ($48 \pm 15 \text{ pg L}^{-1}$) compared to when passing through open water ($19 \pm 4 \text{ pg L}^{-1}$). This is due to the capping effect of sea ice which hinders evasion of gaseous mercury from the sea surface, also observed by Andersson et al. (2008).¹¹⁶

Mercury flux calculations

The continuous measurements of DGM in surface seawater and GEM in air were used together with ship data of needed parameters to estimate the supersaturation grade and the Hg flux from the Arctic Ocean for the period 8/8 to 28/8 2016.

The calculated supersaturation grades and Hg fluxes are presented in Figure 28b and 28c, respectively. The average supersaturation grade was calculated to be $438 \pm 196 \%$ and was higher within the sea ice margin ($536 \pm 152 \%$) than in open water ($233 \pm 92 \%$). The average supersaturation grade calculated here, was in good correlation with calculations made by Andersson et al. (2008) ($410 \pm 220 \%$), who used a similar experimental setup in the Arctic Ocean in 2005.¹¹⁶ The high values show that the investigated parts of the Arctic Ocean were supersaturated with respect to Hg(O).

Since sea ice is preventing gaseous mercury from evading directly from the seawater surface to the atmosphere the calculations of the Hg flux are not applicable for periods when the boat is operating in sea ice.¹¹⁶ By studying time lapse videos of the ship's movements in the ice, periods when the ship was operating in open water could be distinguished and used for Hg flux calculations, see Figure 28c. The average Hg flux calculated for the AO16 campaign was $1.52 \pm 2.27 \text{ ng m}^{-2} \text{ h}^{-1}$, indicating a net evasion of Hg(O) from the surfaces of the Arctic Ocean. Previous calculations of the flux rate in the Arctic Ocean in the literature have shown diverse results

ranging from $0.42 \pm 0.36 \text{ ng m}^{-2} \text{ h}^{-1}$ to $5.42 \pm 5.75 \text{ ng m}^{-2} \text{ h}^{-1}$.^{73,117,138} The observed differences are hypothesized to be mainly due to different approaches for Hg Flux calculations.

Hg(o) in the Arctic sea ice environment

Samples for Hg(o) analysis were collected at a total of 26 ice stations whereof 21 stations were reached by helicopter and 5 stations were reached by Mummy chair or via the gangway from the ship. The locations of the ice stations are presented in Figure 29 together with the measured lengths of the obtained ice cores.

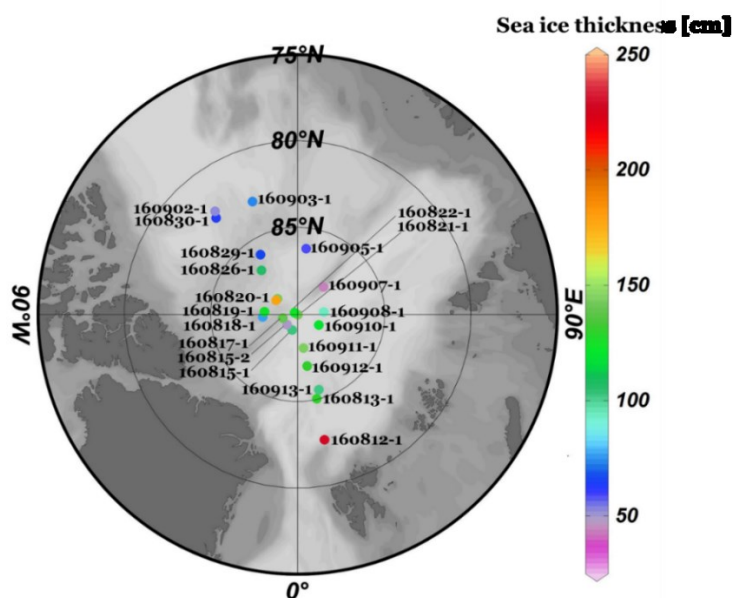


Figure 29. Map showing the locations of the 26 ice stations visited for sampling during the AO16 campaign. The colors represent the sea ice thickness obtained by measuring the length of the obtained ice cores.

All results from the AO16 expedition will be presented in future publications. Selected results from ice station 160911-1 are presented in Table 3, presenting Hg(o) concentrations measured in brine, frost flowers, under ice water, sea ice, snow and new sea ice formed in refrozen sea ice leads.

The highest Hg(o) concentrations were found in sea ice brine. When new sea ice is formed, dissolved species within the brine are being rejected during the freezing process and these form a crystal matrix, leading to an enrichment in brine pockets. According to Chaulk et al. (2011)⁷⁵, mercury is primarily residing within the brine channels in sea ice, which could explain the higher Hg(o) concentrations found brine. However, brine normalization calculations performed and presented in Paper IV indicate that Hg(o) in ice probably exists not only in brine channels, but also in cavities in the bulk phase.

Table 3. Average Hg(o) concentrations (\pm StDev) and salinities in the Arctic sea ice environment in samples collected at ice station 160911-1 during the AO16 campaign.

	Hg(o) [$\mu\text{g L}^{-1}$]	Salinity [ppt]
Brine	358 ± 41	1.75
Frost flowers	86 ± 39	4.40
Under ice water	60 ± 0.2	6.55
Sea ice	24 ± 9	0.56
Snow	9 ± 5	0.04
New ice	38 ± 27	1.9

Gases within sea ice are also, according to Crabeck et al. (2014)¹³⁹, likely to be transported in air bubbles within sea ice cavities. The fraction by volume of air bubbles in sea ice was estimated to be around 0.6-2%.¹³⁹

The brine volume of the ice was calculated from measured temperatures and salinities of the ice according to equation 17. The salinity, temperature and brine volume of an ice core sampled at ice station 160905-1 are presented in Figure 30, having an average brine volume of 0.9%. The low brine volume recorded is mainly due to the low salinity measured, see Table 3 and Figure 30.

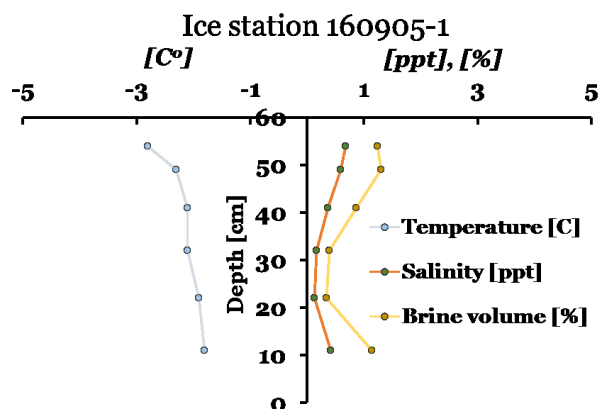


Figure 30. Measured temperatures and salinities and calculated brine volumes [%] in the ice core sampled at ice station 160905-1.

Elevated Hg(O) concentrations were found in frost flowers, however in substantially lower concentrations than what was found during the three campaigns in Antarctica (Paper IV). Frost flowers are normally up to three times more salty than seawater and grow kinetically directly from the vapor phase on frazil young sea ice.¹⁴⁰ However, in this study the salinity of the UIW was higher than in the harvested frost flowers. Frost flowers are considered efficient scavengers of atmospheric mercury due to their large surface area and have been found to be able to accumulate mercury with time.¹⁴¹

Hg(O) in UIW in the Arctic were found to be in the same range as measured during the Antarctic expeditions (Paper IV). However, the Hg(O) concentrations measured in snow and sea ice were found to be 18 times and 4 times lower than concentrations measured in Antarctica, respectively. This could be due to spatial differences in atmospheric deposition of mercury.

The distribution of Hg(O) in the Arctic sea ice environment is visualized in Figure 31, showing the concentrations of Hg(O) in air, snow, meltwater, sea ice and in the deep water column of the sea. The samples were collected at ice station 160905-1 and at the nearby CTD station S160905-1. The highest average Hg(O) concentration was found in melt pond water ($55 \pm 35 \text{ pg L}^{-1}$) followed by the deep water column ($45 \pm 25 \text{ pg L}^{-1}$), sea ice ($22 \pm 18 \text{ pg L}^{-1}$) and snow ($8 \pm 3 \text{ pg L}^{-1}$). The salinity of the meltwater was similar to what was found in the sea ice ($\sim 0.40 \text{ ppt}$), indicating that the meltwater mainly originated from melting sea ice. The higher Hg(O) concentrations found in meltwater compared to sea ice could be due to an in situ photo-reduction in the shallow ponds that probably are more exposed to solar radiation than the sea ice.

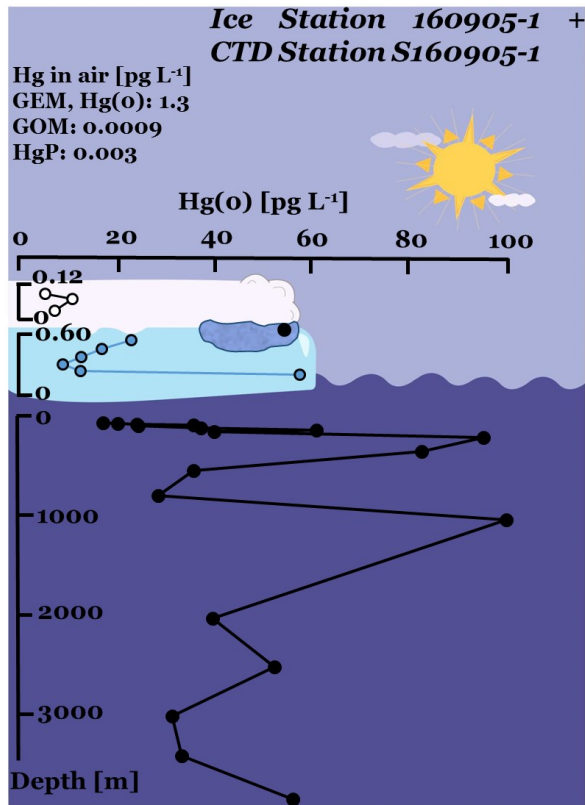


Figure 31. A picture of the distribution of Hg(o) concentrations in the Arctic sea ice environment including measurements in air, snow, sea ice and seawater measured at ice station 160905-1 and CTD station S160905-1.



Chapter 5

“He, who for an ordinary cause, resigns the fate of his patient to mercury, is a vile enemy to the sick; and, if he is tolerably popular, will, in one successful season, have paved the way for the business of life, for he has enough to do, ever afterward, to stop the mercurial breach of the constitutions of his dilapidated patients. He has thrown himself in fearful proximity to death, and has now to fight him at arm's length as long as the patient maintains a miserable existence.”

-Nathaniel Chapman, quoted by William M. Scribner, 'Treatment of Pneumonia and Croup, Once More, Etc,' in *The Medical World* (1885), **3**, 187.

Mercury – The Global picture and Climate change

Global comparisons

Results obtained from measurements performed during my PhD studies are here compared and put in a global perspective. Historic and future changes of the mercury cycle in the marine environment are also discussed. A summary of results, obtained during the measurement campaigns accomplished during my PhD studies, is presented in Figure 32.

Measured mercury species in air

Generally higher GEM concentrations were found in the Northern hemisphere than in the Southern hemisphere, as also presented in the literature study in Table 4, Paper II. The lower GEM concentrations found in Antarctica is mainly due to less emission sources in the Southern hemisphere, and due to the fact that air masses normally do not mix between the two hemispheres. The highest GEM concentrations were found in the Mediterranean region which is acknowledged to be surrounded by many emissions sources, both natural and anthropogenic.^{119,142,143} At the Råö/Rörvik station a seasonality in GEM concentrations was observed with higher average values during winter and spring. This is likely due to anthropogenic influences because of higher electricity demand during winter and spring in Europe. Similar GEM concentrations were found in the Arctic and in Pallas, northern Finland, which implies a well-mixed GEM concentration in the atmosphere in the far north, due to less impacts of direct emission sources.

The highest values of particulate mercury (HgP) concentrations in air were found in Antarctica due to the large production of HgP during observed winter and spring AMDEs (Paper I). At the Råö/Rörvik station on the west coast of Sweden a seasonality in HgP was observed with highest concentrations during winter and spring and lowest during summer, likely due to a seasonality in anthropogenic influences as also observed for GEM (Paper VI). In springtime lower HgP concentrations were found in Pallas compared to the Råö/Rörvik station. This is likely due to Råö/Rörvik being more influenced by anthropogenic emissions but it could also be due to yearly differences.

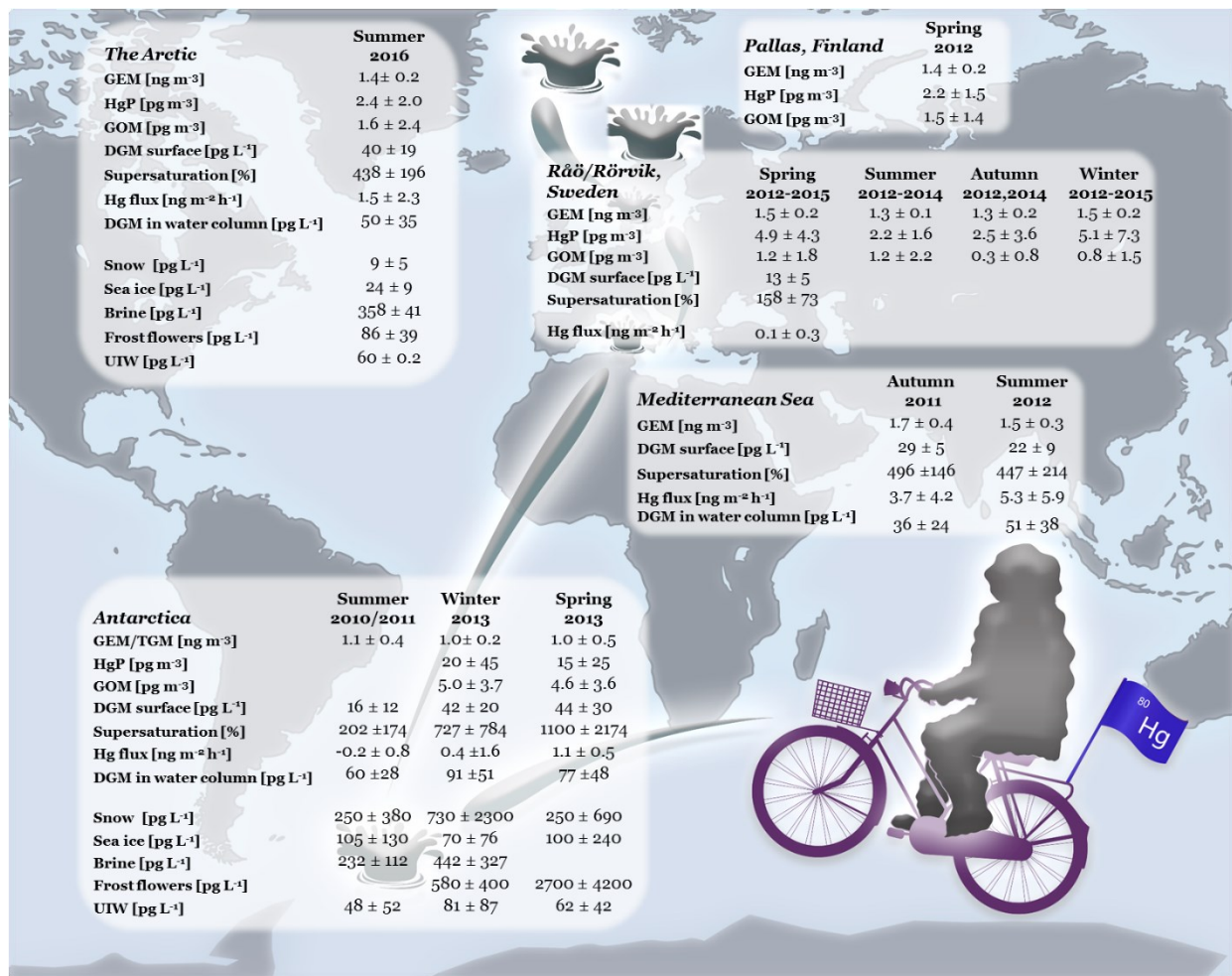


Figure 32. A summary of all measurements of GEM, HgP and GOM in air, DGM in surface and deep waters, calculated supersaturation grades and Hg fluxes, and measured Hg(o) concentrations in polar sea ice environments performed during my PhD studies.

The highest GOM concentrations were found in Polar Regions, indicating a large formation of GOM due to photo-induced halogen chemistry in the atmosphere.⁵¹ The higher concentrations found in Antarctica are likely due to the formation of Hg(II) during detected AMDEs. The average HgP and GOM concentrations in the Arctic and at the Pallas station were found to correlate well, indicating that also the oxidized forms of mercury are well mixed above the north polar circle. However, a seasonality in the concentrations of GEM, HgP and GOM was observed during a study in the Arctic station Ny Ålesund (Svalbard).¹⁴⁴ Steen et al. (2011) measured mercury species in air using the Tekran 1130/35 system from April 2007 to December 2008 and found lower GEM and higher HgP concentrations during spring which was explained by the occurrence of AMDEs. Higher GOM concentrations were found during summer, as also observed at the Råö station, and it was hypothesized that this is due to ozone mediated oxidation in the atmosphere.¹⁴⁴

Measured DGM, supersaturation and fluxes

The highest average surface DGM concentrations were found during winter and spring in Antarctica which is in good agreement with what was measured in the Arctic during summer. This is mainly due to the sea ice cover that hinders evasion of gaseous mercury from the sea surface.¹¹⁶ Substantially lower average DGM concentrations were measured during summer in Antarctica which is probably due to less sea ice coverage or by reason of spatial differences in



Antarctic Seas. The highest open water concentrations of surface DGM were found in the Mediterranean Sea. By studying the global literature comparison in Table 4 (Paper II) it was found that generally higher surface DGM concentrations were found in polluted areas. The low measured DGM concentrations in the surface seawater at the Råö station are believed to mainly be the reason of the measuring depth, further discussed on page 39.

DGM concentrations in deeper water columns were found to be lower in the Mediterranean Sea compared to in Polar Regions. In Antarctica a seasonality in water column DGM concentration was found with highest values during winter and lowest during summer, following a negative correlation to the seasonality in Antarctic sea ice extent.¹⁴⁵ This suggests that sea ice not only influence the surface DGM concentration but also the concentrations deeper in the seawater column. Lower summer column concentrations in the Arctic compared to in Antarctica could be due to spatial differences but could also indicate a higher accumulation of mercury in Antarctic Seas.

In the Mediterranean Sea higher water column concentrations of DGM were found in summer than in autumn, which could be due to spatial variations or due to a seasonality in photo-production of Hg(0). The lower DGM concentrations in the surface water in summer, however, could be the result of higher evasion. Seasonal variations in surface DGM concentrations in the Mediterranean Sea, resulting in variations in calculated supersaturation grades and Hg fluxes, were also found in the literature, see Table 2 (Paper V).

Spatial and seasonal variations of calculated supersaturation grades and Hg flux were found, as presented in Figure 32. The variations are mainly the cause of found variations in concentrations of surface DGM, GEM and measured weather parameters (Paper V).

Measured Hg(0) in the sea ice environment

Large variations in Hg(0) concentrations were found in the sea ice environment between Antarctica and the Arctic.

The high concentrations found in snow in Antarctica are likely due to the atmospheric deposition and reduction of Hg(II), formed during AMDEs. However, the concentrations of Hg(0) in snow during summer in Antarctica were almost 30 times higher than during the same season in the Arctic, which shows that also the summer atmospheric deposition and/or reduction is higher in Antarctica.

Hg(0) concentrations in under ice water were found to be in the same range in both Polar Regions, see Figure 32. The concentrations of both Hg(0) and HgTot, however, were found to be substantially lower in the Arctic than in Antarctica, which implies existing geographical differences in the uptake and reduction of mercury in polar sea ice (Table 2, Paper IV). The reasons for the found differences need further investigation.

Implications for global modelling

Chemistry models have been widely used in the literature to, for example, try to estimate the total yearly emissions of mercury from the ocean surfaces globally. The models often take into account the whole cycle of mercury in the environment including, for example, emissions



(natural and anthropogenic), oxidation processes, atmospheric deposition, cloud chemistry and variations in meteorological conditions. The cycling of mercury in seawater also includes processes such as biological and chemical methylation/demethylation processes, riverine inputs, remineralization and sedimentation.^{3,4,8,59,146} The results of the different used models have been found to vary extensively, presenting a yearly net evasion of mercury from sea surface varying between 800 to 3000 tonnes.^{3,4,8,59}

No modeling was performed in this study. However, the calculated flux rates obtained from the different campaigns were used to estimate the annual net evasion of Hg(o) from the different study areas. The results are presented in Figure 33.

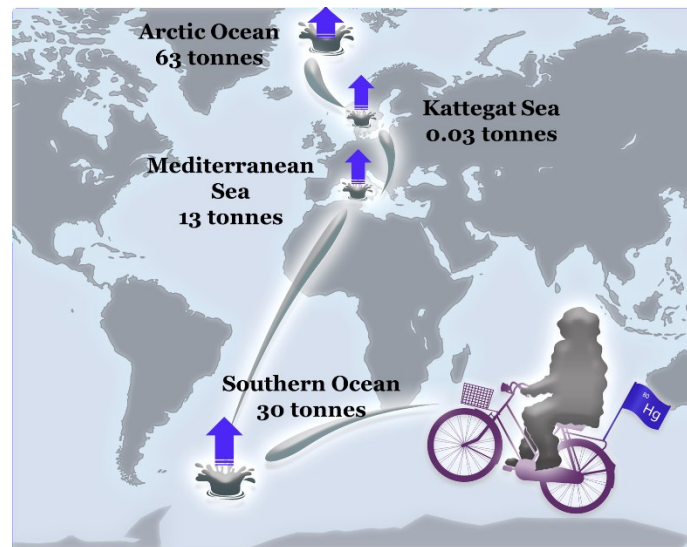


Figure 33. Estimations of the annual net evasion of Hg(o) from the Southern Ocean, the Mediterranean Sea, the Kattegat coast and the Arctic Ocean, calculated from obtained flux rates presented in Figure 32.

The procedures for calculating the annual fluxes from the Southern Ocean and the Mediterranean Sea are described in Paper II and Paper V, respectively.

The area of the Kattegat Sea was estimated to be 30 000 km² and was not considered to be particularly covered by sea ice in winter time¹⁴⁷. By excluding any sea ice coverage and seasonal variation in Hg flux rate, the yearly net evasion of Hg(o) from the Kattegat Sea was calculated to be 0.03 tonnes.

The total area of the Arctic Ocean is 14 060 000 km², and the sea ice extent has in recent years varied from a low summer extent of approximately 4 000 000 km² to a maximum extent in winter of about 13 000 000 km².¹⁴⁵ By accounting for the seasonality in sea ice extent, and using the calculated flux rate for summer, extended for the whole year, the total annual net evasion of Hg(o) from the Arctic Ocean was estimated to be 63 tonnes. The total area of the studied oceans and seas presented in Figure 33 (36 568 000 km²) represents about 10% of the area of the world's seas and contributes to between 3.5-13% of the modeled annual emissions.^{3,4,8,59} This shows that the estimations made in this study are in good agreement with previous modeled results.

By modeling the mercury cycle in the environment, a larger understanding of the dynamics of mercury can be achieved. Modeling can also provide information about possible future changes due to, for example, climate change and changes in natural and anthropogenic emissions.



Models are thus very useful tools to fill the gaps in our knowledge. However, models used in the literature are often complex and can bring uncertainties due to made approximations of different parameters.¹⁴⁸ For instance, Dastoor and Dunford (2013) used two different models to estimate mercury deposition and evasion to and from the Arctic Ocean, leading to considerably different results. The GEOS-Chem model estimated a net evasion of mercury of 45 tonnes year⁻¹ while the GRAHM model showed a net atmospheric deposition of 75 tonnes year⁻¹.¹³⁸

The models are often based on limited measurements and, as also pointed out by Strode et al. (2007)³, more measurements are needed to be able to also account for spatial and seasonal variations in the global marine environment. Results presented in this thesis bring new insights about spatial and seasonal variations from areas previously considered inaccessible and could be of importance for future modeling.

Changing climate – changing mercury cycle

Historic changes

The effects of climate change are more visible in Polar Regions. The surface temperature in the Arctic has increased due to global warming. As an effect, the sea ice extent decreased by 17% between 1980 and 2005. A minimum in sea ice extent was found in 2012 and another minimum was recently observed in summer 2016.¹⁴⁹ Expanding vegetation in the lower Arctic has led to more trapping of snow that has isolated the ground, giving a positive feedback to the increasing temperatures. The Arctic has also experienced more storms and melting permafrost.¹⁵⁰ Also in Antarctica the winter sea ice extent recently (2016) reached its lowest point since 1979.¹⁵¹

In 1985, when mercury measurements were initiated in Antarctica, low concentrations of GEM in air were recorded (0.23 ng m⁻³). Within the short time frame between 1987 and 1988 measurements showed an increase in GEM concentrations from 0.52 ± 0.14 ng m⁻³ to 0.60 ± 0.4 ng m⁻³. Between 1990 and 1995 an increase in mercury emissions from the African continent, Australia and South America was recorded, leading to observed increased mercury concentrations in air. Since 1995, however, the background concentrations have been relatively constants and in 2003 the levels of GEM in the Southern hemisphere was estimated to be 1.2 ng m⁻³.^{34,110} Despite the large increase in concentration since 1985, the background levels of GEM are still lower in Antarctica compared to the Arctic.

Generally, more mercury studies have been conducted in the Arctic than in Antarctica, likely because the Arctic is more accessible and closer to civilization and research centers. Between 1995 and 2007 at Alert (Canada), a negative trend in GEM concentrations of 0.6%/year was observed.¹⁵² Similar decreasing trends have also been observed at other sites in the Arctic.^{136,153}

A negative trend in GEM concentrations, with rates between 1-2% year⁻¹, have also been observed in North America and Europe from the 1990's to 2016.¹⁵⁴ Long-term monitoring of TGM in the Mediterranean region was initiated in 1998. Between 1998 and 1999 the average concentration was between 1.3 to 2.4 ng m⁻³. Measurements performed from year 2000 to 2007 showed no significant increasing or decreasing trend.¹¹⁹ Among studies presented in Table 2 (Paper V) a decreasing trend in GEM concentrations of -1.244% year⁻¹ was calculated



for the time period 1998 to 2012 (Paper V).

At the Råö/Rörvik station an 8% increasing trend in TGM concentration (~ 1.5 to ~ 1.6 ng m⁻³) was observed between the two time periods 1995-1998 and 1999-2002.⁴¹ However, the measurements of GEM performed at the site between 2012 and 2015 showed no significant trend.

Not enough measurements of surface DGM concentrations, in the study areas presented in Figure 32, were found in the literature to study any historical changes in concentrations. A summary of performed surface DGM measurements in the Mediterranean Sea are presented in Table 2, Paper V. From reported data for the time period 1998 to 2012 a decreasing trend was found having a rate of -1.243% year⁻¹.

Future changes

Also in the future the effects of climate change will probably be most evident in Polar Regions. Increasing temperatures would lead to higher rates of sea ice and land ice melts, melting of permafrost and glaciers and more riverine outflow to the oceans. More open sea surface areas would lead to albedo changes, which would cause a negative spiral with increased accumulation of heat in polar oceans.¹⁵⁵

The sea ice extent is important for the cycling of mercury in Polar Regions since it is believed to partly reduce the re-emission of mercury from the sea surface to the atmosphere.^{116,156} Decreasing sea ice extent would therefore initially lead to a larger re-emission of Hg(O) from sea surfaces, which would cause an increased global spread due to the long life-time in air.⁸ Sea ice is also believed to reduce the amount of solar radiation available for photo-chemical reactions in under ice water, such as the primary production and breakdown of MeHg.^{23,108}

Sea ice is believed to play an important role during springtime atmospheric mercury depletion events. It influences the timing and magnitude of atmospheric deposition into aquatic systems by slowing down the uptake of mercury in marine ecosystems.^{8,79,157} Cole and Steffen (2010) observed a time shift in the occurrence of AMDEs from before starting in May to later have been observed as early as in April at Alert, Canada. They also found a negative correlation between AMDEs and temperature and increasing temperatures due to climate change, which suggest a change in atmospheric oxidation rates of GEM and a lower frequency of AMDEs in Polar Regions in the future, possibly leading to less deposition of atmospheric mercury to polar oceans.^{152,156}

In this study it was found that significant amounts of mercury are presently stored in the polar sea ice environment. The melting of sea ice and snow (and also land ice and glaciers) would thus lead to an increased input of mercury into polar oceans.^{156,155} In the Arctic the ongoing transition from multiyear old ice to first year old ice will probably continue, possibly leading to an increased volume of brine in the ice, in which a large part of mercury is accumulating.^{75,156} Many melt ponds were observed during summer 2016 in the Arctic, which were found to contain elevated concentrations of Hg(O). However, in a study by Aspmo et al. (2006), low HgTot concentrations were found in melt ponds in the North Atlantic Ocean.¹³⁵ It could imply that mercury is depleted in melt ponds by reduction and evasion processes. However, more research is needed to study the effects of increasing melt ponds and how they will affect the mercury cycling in the marine environment in a warming climate.



Climate change might affect the global marine cycling of mercury in other ways. Higher winds would increase the circulation and transportation velocity of mercury in air. Higher precipitation could lead to higher rates of wet deposition, increasing the input of mercury to land and oceans. Larger run-off and erosion would lead to a larger movement of terrestrial mercury to the oceans and a suggested increase in wild-fires would increase the emissions of Hg(O) and HgP to air.^{155,158}

Concentrations of different mercury species in water columns were in this study found to vary in different Antarctic water masses and were also suggested to be affected by the water circulation in the Southern Ocean (Paper III). Climate change could cause changes in oceanic circulations worldwide and could also lead to changes in productivity and methylation rates and affect the future distribution of mercury in the water column.¹⁵⁸

Future possible changes in anthropogenic emissions could also influence the cycling of mercury in the global marine environment. In a global anthropogenic emission scenario it was estimated in a best-case scenario that anthropogenic sources could decrease to about 800 tonnes year⁻¹ in 2050 from present-day yearly emissions of about 2000 tonnes year⁻¹.¹⁵⁹ It is however unknown how future technologies will develop.

The largest future non-anthropogenic contributor to atmospheric mercury, in the scenario of a warming climate, is here hypothesized to be the re-emission of previously emitted and deposited mercury through Hg evasion from land and oceans. Increased number of storms and escalated winds would highly affect the Hg flux disregarding the choice of gas exchange model used for calculations, see Figure 5, Paper V. The heating of the surface oceans would also affect the Hg flux. The almost linearly dependence ($R^2=0.99$) of the seawater temperature to the calculated flux rate was in this study found to cause an increase of almost 9%/°C increase of the water temperature.

Many environmental effects of climate change have been suggested, leading to several hypotheses of how the global marine mercury cycle will be affected. However, too many uncertainties exist in the predictions to fully draw any conclusions on how future marine ecosystems will be influenced by these possible changes.



Chapter 6

“Learning is like mercury, one of the most powerful and excellent things in the world in skilful hands; in unskilful, the most mischievous.”

-Alexander Pope, Thoughts on various Subjects', The Works of Alexander Pope (1806), Vol. 6, 406.

Mercury – The Conclusions and Future work

Research questions – The answers

A number of research questions were stated in the beginning of this thesis which are here tried to be answered:



What are the concentrations of mercury species in air in different parts of the world?

The concentrations of different mercury species in air were found to be well-mixed in the Northern hemisphere. Measurements in Sweden, Finland and the Arctic showed average concentrations of GEM, HgP and GOM of 1.3 - 1.5 ng m⁻³, 2.2 - 5.1 pg m⁻³ and 0.3-1.6 pg m⁻³, respectively. Higher GEM concentrations were found in the Mediterranean due to local emission sources. The lowest GEM (1.0-1.1 ng m⁻³) and highest HgP (15-20 pg m⁻³) and GOM (4.6-5.0 pg m⁻³) concentrations were found in Antarctica. This was due to observed AMDEs during winter and spring.



Are there any spatial or seasonal variations of elemental mercury (Hg(0)) in surface seawater? Is surface seawater generally over-saturated or under-saturated with respect to Hg(0)?

Spatial variations of DGM concentrations in surface waters were found, having the highest average concentrations in Polar Regions. This is due to that sea ice acts as a cap, preventing re-evasion of Hg(0) from sea surfaces. It was found that the measuring depth influence the results, yielding lower concentrations in the top 30 cm of the water column.

The seawater surfaces in the studied areas were nearly all found to be over-saturated with respect to Hg(0), having saturation grades varying between 158 and 1100%. Parts of the Amundsen and Ross Seas in summer were found to be under-saturated.



What is the estimated mercury flux between the air-seawater interphase and how is this varying with season and location?

Mercury flux rates were found to vary spatially and seasonally ranging from -0.2 to 5.3 $\text{ng m}^{-2} \text{h}^{-1}$. The highest flux rates were found in the Mediterranean Sea during summer and the lowest rate was found during summer in Antarctic Seas. The calculated flux rates were mainly depending on the spatial and seasonal variations of measured DGM and GEM concentrations. Local variations in temperature and wind speed were also found to influence the calculated flux rates.



How does the choice of flux model affect the estimate of mercury re-evasion from sea surfaces in global modelling?

The consequences of the choice of gas exchange model to estimate the Hg flux were studied and discussed in Paper V. Depending on the gas exchange model, the results in Hg flux could differ as much as 43% even at lower wind speeds (7 m s^{-1}). At higher wind speeds (25 m s^{-1}) the differences between models resulted in large diversities in calculated flux rates of up to about 700%.



Which parameters influence the distribution of different mercury species in seawater columns?

DGM, HgTot and MMHg concentrations were measured in the water columns of the Weddell, Amundsen and Ross Seas (Paper III). The DGM concentrations in the water column were found to vary seasonally, possibly due to changes in sea ice extent, seawater temperature and solar radiation. The general DGM profile showed an increase along the thermocline with lowest concentrations in the Antarctic Surface Water (AASW).

The concentrations of HgTot in seawater columns showed to be relatively well-mixed with variations mainly visible in the surface layer and close to the bottom. This was hypothesized to be due to processes such as re-evasion from sea surfaces and sediment fluxes. A seasonality was observed for HgTot with higher values in spring than in winter, which could be because of meltwater discharge from sea ice floes.

The concentrations of MMHg in the water columns showed no seasonal variations. The largest variations were found in the top 500 m of the water column. The lowest concentrations were found in the AASW, possibly because of photo-induced demethylation. Highest MMHg concentrations were found close to the Dotson and Getz ice shelves in the MCDW water layer, which contains water from melted sea ice and snow and is associated with high phytoplankton blooms.



How is the sea ice environment affecting the global budget of mercury?

Sea ice was found to act as a cap preventing gaseous mercury at the surface to evade. Since a higher average water column concentration of DGM was observed in winter in Antarctica it was suggested that the sea ice also affects the DGM concentrations further down in the water column.

Sea ice also act as a barrier for atmospheric deposition, as was observed during AMDEs when high concentrations of mercury were found in surface snow. The high concentrations of mercury found in the sea ice environment (especially in Antarctica) suggest that sea ice could be a present significant reservoir of mercury. It has also been found in previous studies that sea ice can influence the timing of AMDEs which have an impact of the atmospheric deposition of mercury in Polar Regions.



How can the cycling of mercury in marine environments be affected by climate change?

Many different changes have been proposed in the literature to happen in the future due to climate change such as increased surface temperatures, higher winds and precipitation, larger run-off, more erosion, increased wild fires, melting sea ice, land ice, permafrost and glaciers. These changes might affect the global marine cycling of mercury in several ways. Previously stored mercury in the sea ice environment, land ice and glaciers could initially increase the input of mercury into polar oceans. On the contrary; increased winds and temperatures could lead to a larger re-evasion of gaseous mercury from sea surfaces. On one hand, this is leading to an increased spread of mercury in the atmosphere. On the other hand, it is decreasing the load of mercury in the world's oceans.



Outlook

More measurements of GEM, GOM and HgP at different geographical locations would be beneficial to further study interannual variations and to monitor future atmospheric trends. The performed measurements of mercury species in air over sea ice during winter and spring in Antarctica showed a large production of HgP during observed AMDEs. These observations have previously not been detected at coastal stations in Antarctica. It is therefore suggested that more measurements of GEM, GOM and HgP over sea ice are needed in Polar Regions to further study the formation and deposition of Hg(II) species occurring within the sea ice margin.

Measurements of mercury in sea ice are sparse and to our knowledge no previous studies have presented Hg(o) concentrations in the sea ice environment. Speciation of mercury in sea ice provides valuable information of how mercury enters, transforms and transports within the ice and more field measurements are therefore needed in both Polar Regions. Laboratory experiments are necessary to examine and further support the field experiments performed in this work, to study the uptake of mercury in newly frozen sea ice and the photo-production of Hg(o) within sea ice. The study of mercury in polar sea ice environments are important for future modelling and for the predictions of how the approaching melting of sea ice will affect the load of mercury in polar marine ecosystems.

Spatial and seasonal variations of measured DGM concentrations in surface and deep waters were found to be substantial in this study. The variations cause large fluctuations in calculated mercury flux rates, which in turn affect the global estimates of mercury evasion from sea surfaces globally. Previous global models have been based on limited measurements of DGM and GEM in different parts of the world. It is therefore suggested to expand the measurements to support future modelling. Surface DGM could be measured continuously during oceanographic campaigns or by permanently installing, for example, a continuous equilibrium system (page 23) or an in situ purging system (page 24) on board cargo and passenger ships or installing them on oil rigs, at wind power station platforms at sea or at coastal stations.



Acknowledgements

During my five years as a PhD student I have shared uncountable good moments with many people in my life. I have mainly shared my journey with my two supervisors Katarina Gårdfeldt and Ingvar Wängberg who have given me support, good advices and great friendships. Katarina and I have visited the world's both extremes together and I will never forget the fun we had on the ice. The many trips back and forth to the Råö station together with Ingvar have resulted in many valuable discussions, both work-related and non-work-related. Thanks for all the wonderful moments!

I would like to thank my examiner Jan-Erik Svensson for all support and help during my studies and for always looking so happy, even though we often pass each other in a hurry. I have changed offices and office mates several times during my studies, so not to forget anyone, thanks to all previous and present colleagues for many fun moments shared together during department activities. Special thanks are addressed to Esa Väänänen and his team for all the things you have helped me with in the workshop!

I have met many people during my travels and research campaigns and I would like to thank you all for good companionships and fun moments together. Big thanks to the crew and fellow colleagues and friends on R/V Urania. Thank you Katriina for a good time at the Pallas-Matorova station. I would like to thank the crew and all friends that I met on R/V Polarstern for the four enjoyable months on board. Special thanks to my Swedish co-workers Katarina A, Martin and my cabin-mate Anna for all the help on the ice, and for the nice time spent on board together. Big thanks to the crew and new found friends on board IB Oden for a nice trip to the top of the world! Special thanks to my wonderful 'heavy metal team' Katarina, La Daana and Sofi for all the happy days in the lab and on the ice. Thanks to all the people that have helped us a bit extra e.g. Per, Lennart, Robert (thanks also for reading through my thesis!), Axel, Bengt, Ted, Åsa, Piotr and Nicke. Hans-Martin, I am very grateful for all the help in the lab and on the ice and for all the support when writing my thesis. Thanks also for the very useful time laps videos and for always being there for me.

I would like to thank friends and colleagues within the GMOS project that I have met during meetings, training courses and conferences. Thanks to the project coordinator Nicola Pirrone and Francesca Sprovieri for organizing campaigns with R/V Urania and for lending us the Tekran 1130/35 instrument used on board R/V Polarstern. Thanks also to Aurélien Dommergue and Hans-Werner Jacobi for making the campaign on R/V Polarstern possible and for lending us a Tekran 2537A instrument.

I'm thankful to the GMOS colleagues at the IVL Swedish Environmental Institute for nice meetings together and good support.

Thanks to the Swedish Polar Research Secretariat for financial support and for organizing the expedition on board IB Oden. Financial support was also appreciated from ÅF and 'Bengt Lundquist Minne'.

In spring 2015 I took a course at the University of Svalbard (UNIS). I had a wonderful time there, meeting new friends and learning more about how contaminants spread to the Arctic.

Thanks to Professor Mark Hermansson who let me come back to UNIS and teach about mercury for students in autumn 2015 and in spring 2016.

Thank you Mikael Östblom for inviting me to Unverseum to present my work to the common public. It was a great deal of fun and I learned a lot!

Most of all I would like to thank people who in some way or another have been close to me the last five years, giving me support and shared with me highs and lows: Hanna, Pan-Pan, Johan, Sebastian, Jenny (and Chef) and many more. My biggest thanks to Robin who has shared his life with me the last four years. I am so grateful for all the support and advices you have given me during the years and thanks also for your big understanding when I have been disappearing for long periods of time.

Last but not least, endless gratitude to my family who have always been there for me, giving me love and support. You know me better than anyone. Special thanks to my dear brother Donnie who has helped me with many pictures presented in various papers, posters, presentations and in this thesis.

References

1. Schroeder, W. H., Anlauf, K. G., Barrie, L. a, Lu, J. Y. & Steffen, A. Arctic Springtime Depletion of Mercury. *Nature* **394**, 331–332 (1998).
2. UNEP. *Global Mercury Assessment 2013: Sources, Releases and Environmental Transport*. (2013).
3. Strode, S. A. *et al.* Air-sea exchange in the global mercury cycle. *Global Biogeochem. Cycles* **21**, 1–12 (2007).
4. Mason, R.P., Sheu, G-R. Role of the ocean in the global mercury cycle. *Glob. Biogeochem. Cycles*. **16**, 40-1-40–14 (2002).
5. Lew, K. *Understanding the elements of the periodic table – Mercury*. (The Rosen publishing group, Inc., 2009).
6. Atkins, P., Jones, L. *Chemical principles - The quest for insight*. (W. H. Freeman and Company, 2005).
7. Raofie, F. & Ariya, P. A. Product Study of the Gas-Phase BrO-Initiated Oxidation of Hg⁰: Evidence for Stable Hg¹⁺ Compounds. *Environ. Sci. Technol.* **38**, 4319–4326 (2004).
8. Schroeder, W. H. & Munthe, J. Atmospheric mercury—An overview. *Atmos. Environ.* **32**, 809–822 (1998).
9. Brown, I. D., Gillespie, R. J., Morgan, K. R., Tun, Z. & Ummat, P. K. Preparation and crystal structure of mercury hexafluoronioabate (Hg₃NbF₆) and mercury hexafluorotantalate (Hg₃TaF₆): mercury layer compounds. *Inorg. Chem.* **23**, 4506–4508 (1984).
10. National Research Council (U.S.) – Board on Environmental Studies and Toxicology. *Toxicological Effects of Methylmercury*. (National Academies Press).
11. Landis, M. S., Stevens, R. K., Schaedlich, F. & Prestbo, E. M. Development and characterization of an annular denuder methodology for the measurement of divalent inorganic reactive gaseous mercury in ambient air. *Environ. Sci. Technol.* **36**, 3000–9 (2002).
12. Sprovieri, F. *et al.* Atmospheric Mercury Concentrations observed at ground-based monitoring sites globally distributed in the framework of the GMOS network. *Atmos. Chem. Phys. Discuss.* 1–32 (2016). doi:10.5194/acp-2016-466
13. WHO. *Environmental health criteria 118. Inorganic mercury. International program on chemical safety*. (1991).
14. Ferracane, J. L. *Materials in Dentistry: Principles and Applications*. (Lippincott Williams & Wilkins, 2001).
15. Bjørklund, G. [The history of dental amalgam]. *Tidsskr. den Nor. lægeforening Tidsskr. Prakt. Med. ny række* **109**, 3582–5 (1989).
16. Czarnetzki, A. . E. S. Re-dating the Chinese amalgam-filling of teeth in Europe. *Int. J. Anthropol.* **5**, 325–332 (1990).

17. Edlich, R.F., Rhoads, S.K., Cantrell, H.S., Azavedo, S.M., Newkirk, A. T. *Banning mercury amalgam. Report. FDA, U.S. Food and Drug Administration.* (2014).
18. Baek, H.-J. *et al.* Dental amalgam exposure can elevate urinary mercury concentrations in children. *Int. Dent. J.* **66**, 136–143 (2016).
19. Mutter, J., Naumann, J., Walach, H. & Daschner, F. Amalgam: Eine Risikobewertung unter Berücksichtigung der neuen Literatur bis 2005. *Das Gesundheitswes.* **67**, 204–216 (2005).
20. Vähäsarja, N. *et al.* Neurological disease or intellectual disability among sons of female Swedish dental personnel. *J. Perinat. Med.* **44**, (2016).
21. Carty, A.J., Malone, S. F. *The chemistry of mercury in biological systems. The biochemistry of mercury in the Environment.* (Elsevier/North Holland Biomedical Press, 1979).
22. Philbert, M.A., Billingsley, M.L., R. K. R. Mechanisms of injury in the central nervous system. *Toxic Pathol.* **28**, 45–53 (2000).
23. Monitoring, A. & Amap, A. P. *Arctic Pollution 2011.* (2011).
24. Emsley, J. *The elements of murder – A history of poison.* (Oxford University Press, 2005).
25. Bakir, F. *et al.* Methylmercury Poisoning in Iraq. *Science (80-).* **181**, 230–241 (1973).
26. Center for Environmental Health Sciences, D. C. Mercury – Element of the ancients. (2012). Available at: <http://www.dartmouth.edu/~toxmetal/mercury/history.html>. (Accessed: 5th July 2016)
27. Environment Canada, F. G. of C. Mercury and the environment – Basic facts. (2004). Available at: <http://www.ec.gc.ca/mercure-mercury/default.asp?lang=En&n=9A4397AD-1>. (Accessed: 5th July 2016)
28. Selin, N. E. Global Biogeochemical Cycling of Mercury: A Review. *Annu. Rev. Environ. Resour.* **34**, 43–63 (2009).
29. Sunderland, E. M. & Mason, R. P. Human impacts on open ocean mercury concentrations. *Global Biogeochem. Cycles* **21**, n/a-n/a (2007).
30. EUR-lex. Europa – Summaries of EU legislation. Export and storage of Mercury. Regulation (EC) No 1102/2008. (2010). Available at: <http://eur-lex.europa.eu/legal-content/EN/TXT/?uri=URISERV:l28184>. (Accessed: 5th July 2016)
31. Brooks, W. *Mercury. Minerals Yearbook – Metals and Minerals. Volume 1.* (United States Government Printing Office, 2010).
32. Edlich, R.F., Rhoads, S.K., Cantrell, H.S., Azavedo, S.M., Newkirk, A. T. *Banning mercury amalgam.* (2014).
33. UNEP. Minamata Convention on Mercury. (2014). Available at: <http://www.mercuryconvention.org/Convention/tabid/3426/Default.aspx>. (Accessed: 5th July 2016)
34. Slemr, F. *et al.* Worldwide trend of atmospheric mercury since 1977. *Geophys. Res. Lett.* **30**, n/a-n/a (2003).
35. Zhang, L. *et al.* Assessment of modeled mercury dry deposition over the Great Lakes

- region. *Environ. Pollut.* **161**, 272–283 (2012).
36. Hall, B. The gas phase oxidation of elemental mercury by ozone. *Water, Air, Soil Pollut.* **80**, 301–315 (1995).
 37. Pal, B. & Ariya, P. A. Gas-phase HO-initiated reactions of elemental mercury: kinetics, product studies, and atmospheric implications. *Environ. Sci. Technol.* **38**, 5555–66 (2004).
 38. Ariya, P. a., Khalizov, A. & Gidas, A. Reactions of gaseous mercury with atomic and molecular halogens: Kinetics, product studies, and atmospheric implications. *J. Phys. Chem. A* **106**, 7310–7320 (2002).
 39. CALVERT, J. & LINDBERG, S. Mechanisms of mercury removal by O and OH in the atmosphere. *Atmos. Environ.* **39**, 3355–3367 (2005).
 40. Obrist, D. *et al.* Bromine-induced oxidation of mercury in the mid-latitude atmosphere. *Nat. Geosci.* **4**, 22–26 (2010).
 41. Munthe, J., Wängberg, I., Shang, L. *The origin and fate of mercury species in the environment.* (2008).
 42. Gårdfeldt, K., Munthe, J., Strömberg, D. & Lindqvist, O. A kinetic study on the abiotic methylation of divalent mercury in the aqueous phase. *Sci. Total Environ.* **304**, 127–136 (2003).
 43. Alexandre Renard. Identification des sources printanières de méthylmercure dans le manteau neigeux arctique. (l'École Doctorale Terre Univers Environnement, 2006).
 44. Barrie, L. A., Bottenheim, J. W., Schnell, R. C., Crutzen, P. J. & Rasmussen, R. A. Ozone destruction and photochemical reactions at polar sunrise in the lower Arctic atmosphere. *Nature* **334**, 138–141 (1988).
 45. Tarasick, D. W. & Bottenheim, J. W. Surface ozone depletion episodes in the Arctic and Antarctic from historical ozonesonde records. *Atmos. Chem. Phys. Discuss.* **2**, 339–356 (2002).
 46. Fan, S.M., Jacob, D. J. Surface ozone depletion in Arctic spring sustained by bromine reactions on aerosols. *Nature* **359**, 522–524 (1992).
 47. Foster, K. L. *et al.* The role of Br₂ and BrCl in surface ozone destruction at polar sunrise. *Science* **291**, 471–4 (2001).
 48. Stefan Fickert, Jonathan W. Adams, and J. N. C. Activation of Br₂ and BrCl via uptake of HOBr onto aqueous salt solutions. *J. Geophys. Res.* **104**, 23,719–23,727 (1999).
 49. Oum, K. W., Lakin, M. J. & Finlayson-Pitts, B. J. Bromine activation in the troposphere by the dark reaction of. *Geophys. Res. Lett.* **25**, 3923 (1998).
 50. Eneroth, K., Holmén, K., Berg, T., Schmidbauer, N. & Solberg, S. Springtime depletion of tropospheric ozone, gaseous elemental mercury and non-methane hydrocarbons in the European Arctic, and its relation to atmospheric transport. *Atmos. Environ.* **41**, 8511–8526 (2007).
 51. Skov, H. *et al.* Fate of elemental mercury in the Arctic during atmospheric mercury depletion episodes and the load of atmospheric mercury to the Arctic. *Environ. Sci. Technol.* **38**, 2373–82 (2004).
 52. Ebinghaus, R. *et al.* Antarctic springtime depletion of atmospheric mercury. *Environ.*

- 798 (1995).
69. Gårdfeldt, K., and Jonsson, M. Is biomolecular reduction of Hg(II) complexes possible in aqueous systems of environmental importance. *J. Phys. Chem. A* **107**, 4478–4482 (2003).
 70. Allard, B. & Arsenie, I. Abiotic reduction of mercury by humic substances in aquatic system — an important process for the mercury cycle. *Water Air Soil Pollut.* **56**, 457–464 (1991).
 71. Mason, R. P. & Fitzgerald, W. F. The distribution and biogeochemical cycling of mercury in the equatorial Pacific Ocean. *Deep. Res. Part I* **40**, 1897–1924 (1993).
 72. Kotnik, J. *et al.* Mercury speciation in surface and deep waters of the Mediterranean Sea. *Mar. Chem.* **107**, 13–30 (2007).
 73. Andersson, M. E., Sommar, J., Gårdfeldt, K. & Jutterström, S. Air–sea exchange of volatile mercury in the North Atlantic Ocean. *Mar. Chem.* **125**, 1–7 (2011).
 74. Poulain, A. J. *et al.* Redox transformations of mercury in an Arctic snowpack at springtime. *Atmos. Environ.* **38**, 6763–6774 (2004).
 75. Chaulk, A., Stern, G. a, Armstrong, D., Barber, D. G. & Wang, F. Mercury distribution and transport across the ocean-sea-ice-atmosphere interface in the Arctic Ocean. *Environ. Sci. Technol.* **45**, 1866–72 (2011).
 76. Durnford, D. & Dastoor, A. The behavior of mercury in the cryosphere: A review of what we know from observations. *J. Geophys. Res.* **116**, D06305 (2011).
 77. Larose, C., Ferrari, C. & Schneider, D. Interactions entre composition chimique et populations microbiennes de la neige : quelles sont les conséquences sur le cycle du mercure en Arctique ? **Doctorat**, 164 (2010).
 78. Weeks, W. . On sea ice. *Univ. Alaska Press Fairbanks, AK* 664 (2010).
 79. Beattie, S. a *et al.* Total and methylated mercury in arctic multiyear sea ice. *Environ. Sci. Technol.* **48**, 5575–82 (2014).
 80. Fitzgerald, W. F. & Gill, G. A. Subnanogram determination of mercury by two-stage gold amalgamation and gas phase detection applied to atmospheric analysis. *Anal. Chem.* **51**, 1714–1720 (1979).
 81. Ebinghaus, R., Jennings, S. G., Schroeder, W. H., Berg, T., D., T., Ferrara, R., Guentzel, J., Kenny, D., Kock, H. H., Kvietkus, K., Landing, W., Mazzolai, B., Muhleck, Munthe, J., Prestbo, E. M., Schneeberger, D., F., S., Sommar, J., U. & A., Wallschlager, D., and Xiao, Z. International field intercomparison measurements of atmospheric mercury species at Mace Head, Ireland. *Atmos. Environ.* **33**, 3063–3073 (1999).
 82. Munthe, J., Wangberg, I., Pirrone, N., Iverfeldt, A., Ferrara, R., Ebinghaus, R., Feng, X., Gardfeldt, K., Keeler, G., L., E., Liundberg, S. E., Lu, J., Mamane, Y., Prestbo, E., S., S., Schroeder, W. H., Sommar, J., Sprovieri, F., Stevens, R. K. & Stratton, W., Tuncel, G., and Urba, A. Intercomparison of methods for sampling and analysis of atmospheric mercury species. *Atmos. Env.* **35**, 3007–3017 (2001).
 83. Aspomo, K., Gauchard, P.-A., Steffen, A., Temme, C., Berg, T., Bahlmann, E., Banic, C., Dommergue, A., Ebinghaus, R., F. & C., Pirrone, N., Sprovieri, F., and Wibetoe, G. Measurements of atmospheric mercury species during an international study of mercury depletion events at Ny-Alesund, Svalbard, spring 2003. How reproducible are

- Sci. Technol.* **36**, 1238–44 (2002).
53. Brooks, S., Lindberg, S., Southworth, G. & Arimoto, R. Springtime atmospheric mercury speciation in the McMurdo, Antarctica coastal region. *Atmos. Environ.* **42**, 2885–2893 (2008).
 54. Xie, Z.-Q., Sander, R., Pöschl, U. & Slemr, F. Simulation of atmospheric mercury depletion events (AMDEs) during polar springtime using the MECCA box model. *Atmos. Chem. Phys. Discuss.* **8**, 13197–13232 (2008).
 55. Calvert, J. G. & Lindberg, S. E. The potential influence of iodine-containing compounds on the chemistry of the troposphere in the polar spring. II. Mercury depletion. *Atmos. Environ.* **38**, 5105–5116 (2004).
 56. Calvert, J. G. & Lindberg, S. E. A modeling study of the mechanism of the halogen-ozone-mercury homogeneous reactions in the troposphere during the polar spring. *Atmos. Environ.* **37**, 4467–4481 (2003).
 57. Durnford, D. a. *et al.* How relevant is the deposition of mercury onto snowpacks? – Part 1: A statistical study on the impact of environmental factors. *Atmos. Chem. Phys.* **12**, 9221–9249 (2012).
 58. Steffen, A. *et al.* A synthesis of atmospheric mercury depletion event chemistry in the atmosphere and snow. *Atmos. Chem. Phys.* **8**, 1445–1482 (2008).
 59. Fitzgerald, W. F., Lamborg, C. H. & Hammerschmidt, C. R. Marine biogeochemical cycling of mercury. *Chem. Rev.* **107**, 641–662 (2007).
 60. Cossa, D., Martin, J.-M., Takayanagi, K. & Sanjuan, J. The distribution and cycling of mercury species in the western Mediterranean. *Deep Sea Res. Part II Top. Stud. Oceanogr.* **44**, 721–740 (1997).
 61. Batrakova, N., Travnikov, O. & Rozovskaya, O. Chemical and physical transformations of mercury in the ocean: A review. *Ocean Sci.* **10**, 1047–1063 (2014).
 62. Qureshi, A., O’Driscoll, N. J., MacLeod, M., Neuhold, Y.-M. & Hungerbühler, K. Photoreactions of Mercury in Surface Ocean Water: Gross Reaction Kinetics and Possible Pathways. *Environ. Sci. Technol.* **44**, 644–649 (2010).
 63. Hui, R. . in (ed. Barker, J. .) 374–419 (World Scientific Publishing Co, 1995).
 64. Gårdfeldt, K., Sommar, J., Strömberg, D. & Feng, X. Oxidation of atomic mercury by hydroxyl radicals and photoinduced decomposition of methylmercury in the aqueous phase. *Atmos. Environ.* **35**, 3039–3047 (2001).
 65. Dill, C., Kuiken, T., Zhang, H. & Ensor, M. Diurnal variation of dissolved gaseous mercury (DGM) levels in a southern reservoir lake (Tennessee, USA) in relation to solar radiation. *Sci. Total Environ.* **357**, 176–93 (2006).
 66. Gårdfeldt, K., Feng, X., Sommar, J. & Lindqvist, O. Total gaseous mercury exchange between air and water at river and sea surfaces in Swedish coastal regions. *Atmos. Environ.* **35**, 3027–3038 (2001).
 67. O’Driscoll, N. J., Siciliano, S. D., Lean, D. R. S. & Amyot, M. Gross Photoreduction Kinetics of Mercury in Temperate Freshwater Lakes and Rivers: Application to a General Model of DGM Dynamics. *Environ. Sci. Technol.* **40**, 837–843 (2006).
 68. Xiao, Z. F., Strömberg, D. & Lindqvist, O. Influence of humic substances on photolysis of divalent mercury in aqueous solution. *Water, Air, Soil Pollut.* **80**, 789–

- our present methods? *Atmos. Env.* **39**, 7607–7619 (2005).
84. OhioLumex Co. Inc. User's manual Ra-915 + Mercury Analyzer.
 85. Tekran. Model 2537X Ambient Mercury Vapor Analyzer User Manual. (2014).
 86. Temme, C., Einax, J. W., Ebinghaus, R. & Schroeder, W. H. Measurements of atmospheric mercury species at a coastal site in the Antarctic and over the south Atlantic Ocean during polar summer. *Environ. Sci. Technol.* **37**, 22–31 (2003).
 87. Slemr, F. *et al.* Gaseous mercury distribution in the upper troposphere and lower stratosphere observed onboard the CARIBIC passenger aircraft. *Atmos. Chem. Phys.* **9**, 1957–1969 (2009).
 88. Gustin, M. & Jaffe, D. Reducing the Uncertainty in Measurement and Understanding of Mercury in the Atmosphere. *Environ. Sci. Technol.* **44**, 2222–2227 (2010).
 89. Steffen, A., Schroeder, W. H., Bottenheim, J., Narayan, J., and Fuentes, J. D. Atmospheric mercury concentrations: measurements and profiles near snow and ice surfaces in the Canadian Arctic during Alert 2000. *Atmos. Env.* **36**, 2653–2661 (2002).
 90. Hynes, A. J., Donohoue, D. L., Goodsite, M. E. & Hedgecock, I. M. in *Mercury Fate and Transport in the Global Atmosphere* 427–457 (Springer US, 2009). doi:10.1007/978-0-387-93958-2_14
 91. Ariya, P. A., Peterson, K., Snider, G., Amyot, M. in *Mercury Fate and Transport in the Global Atmosphere* (ed. Mason, R., Pirrone, N.) (N., Eds.; Springer, 2009).
 92. Lindberg, S. E. & Stratton, W. J. Atmospheric Mercury Speciation: Concentrations and Behavior of Reactive Gaseous Mercury in Ambient Air. *Environ. Sci. Technol.* **32**, 49–57 (1998).
 93. Gustin, M. S. *et al.* Do We Understand What the Mercury Speciation Instruments Are Actually Measuring? Results of RAMIX. (2013).
 94. Wilson, D. S., Pollard, D., DeConto, R. M., Jamieson, S. S. R. & Luyendyk, B. P. Initiation of the West Antarctic Ice Sheet and estimates of total Antarctic ice volume in the earliest Oligocene. *Geophys. Res. Lett.* **40**, 4305–4309 (2013).
 95. Gårdfeldt, K. *et al.* Comparison of procedures for measurements of dissolved gaseous mercury in seawater performed on a Mediterranean cruise. *Anal. Bioanal. Chem.* **374**, 1002–8 (2002).
 96. Wängberg, I., Schmolke, S., Schager, P., Munthe, J., Ebinghaus, R., Iverfeldt, I. Estimates of air-sea exchange of mercury in the Baltic Sea. *Atmos. Env.* **35**, 5477–5484 (2001).
 97. Andersson, M. E., Gårdfeldt, K. & Wängberg, I. A description of an automatic continuous equilibrium system for the measurement of dissolved gaseous mercury. *Anal. Bioanal. Chem.* **391**, 2277–82 (2008).
 98. Andersson, M. E., Gårdfeldt, K., Wängberg, I. & Strömberg, D. Determination of Henry's law constant for elemental mercury. *Chemosphere* **73**, 587–92 (2008).
 99. Frankenstein, G., Garner, R. Equations for determining the brine volume of sea ice from -0.5 C to -22.9 C. *J. Glaciol.* **6**, 943–944 (1967).
 100. Fantozzi, L., Manca, G. & Sprovieri, F. A comparison of recent methods for modelling

- mercury fluxes at the air- water interface. **23004**, 2010–2012 (2013).
101. Andersson, M. E. *et al.* Seasonal and daily variation of mercury evasion at coastal and off shore sites from the Mediterranean Sea. *Mar. Chem.* **104**, 214–226 (2007).
 102. Sharif, A. *et al.* Comparison of Different Air–Water Gas Exchange Models to Determine Gaseous Mercury Evasion from Different European Coastal Lagoons and Estuaries. *Water, Air, Soil Pollut.* **224**, 1606 (2013).
 103. Liss, P.S., Slater, P. G. Flux of gases across the air-sea interface. *Nature* **247**, (1974).
 104. Johnson, M. T. A numerical scheme to calculate temperature and salinity dependent air-water transfer velocities for any gas. *Ocean Sci.* **6**, 913–932 (2010).
 105. Kuss, J., Holzmann, J. & Ludwig, R. An elemental mercury diffusion coefficient for natural waters determined by molecular dynamics simulation. *Environ. Sci. ...* **43**, 3183–3186 (2009).
 106. Fuller, E. N., Schettler, P. D. & Giddings, J. C. A new method for prediction of binary gas-phase diffusion coefficients. *Ind. Eng. Chem.* **16**, 551 (1966).
 107. Tsilingiris, P. Thermophysical and transport properties of humid air at temperature range between 0 and 100 °C. *Energ. Convers. Manag.* **49**, 1098–1110 (2008).
 108. Joyner, C. . *Antarctica and the Law of the Sea*. (Martinus Nijhoff Publishers, 1992).
 109. Polar Discovery. Polar Discovery – Woods hole oceanographic institution. (2006). Available at: <http://polardiscovery.whoi.edu.html>. (Accessed: 9th May 2015)
 110. Dommergue, A. *et al.* and Physics Overview of mercury measurements in the Antarctic troposphere. 3309–3319 (2010).
 111. Bargagli, R., Monaci, F. & Cateni, D. marine coastal food web. **169**, 65–76 (1998).
 112. Angot, H., Barret, M., Magand, O., Ramonet, M. & Dommergue, a. A 2 year record of atmospheric mercury species at a background Southern Hemisphere station on Amsterdam Island. *Atmos. Chem. Phys. Discuss.* **14**, 14439–14470 (2014).
 113. Slemr, F. *et al.* Comparison of mercury concentrations measured at several sites in the Southern Hemisphere. *Atmos. Chem. Phys.* **15**, 3125–3133 (2015).
 114. Haag, W.R., Hoigné, J. Ozonation of bromide-containing waters: Kinetics and formation of hypobromous acid and bromate. *Environ. Sci. Technol.* **17**, 261–267 (1983).
 115. Cossa, D. *et al.* Mercury in the Southern Ocean. *Geochim. Cosmochim. Acta* **75**, 4037–4052 (2011).
 116. Andersson, M. E., Sommar, J., Gårdfeldt, K. & Lindqvist, O. Enhanced concentrations of dissolved gaseous mercury in the surface waters of the Arctic Ocean. *Mar. Chem.* **110**, 190–194 (2008).
 117. Kirk, J. L., St. Louis, V. L., Hintelmann, H., Lehnerr, I., Else, B., Poissant, L. Methylated mercury species in marine waters of the Canadian high and sub-Arctic. *Environ. Sci. Technol* **42**, 8367–8373 (2008).
 118. Loset, S., Shkhinek, K.N., Gudmestad, O.T., Hoyland, K. V. *Actions from ice on Arctic offshore and coastal structures*. (LAN, 2006).

119. Kotnik, J., Sprovieri, F., Ogrinc, N., Horvat, M. & Pirrone, N. Mercury in the Mediterranean, part I: Spatial and temporal trends. *Environ. Sci. Pollut. Res.* **21**, 4063–4080 (2014).
120. Gibičar, D. *et al.* Human exposure to mercury in the vicinity of chlor-alkali plant. *Environ. Res.* **109**, 355–367 (2009).
121. Fantozzi, L., Manca, G., Ammoscato, I., Pirrone, N. & Sprovieri, F. The cycling and sea-air exchange of mercury in the waters of the Eastern Mediterranean during the 2010 MED-OCEANOR cruise campaign. *Sci. Total Environ.* **448**, 151–62 (2013).
122. Gårdfeldt, K. *et al.* Evasion of mercury from coastal and open waters of the Atlantic Ocean and the Mediterranean Sea. *Atmos. Environ.* **37**, 73–84 (2003).
123. Wängberg, I. *et al.* Atmospheric mercury at mediterranean coastal stations. *Environ. Fluid Mech.* **8**, 101–116 (2007).
124. Astraldi, M. *et al.* The role of straits and channels in understanding the characteristics of Mediterranean circulation. *Prog. Oceanogr.* **44**, 65–108 (1999).
125. Gårdfeldt, K. *Transformation of Mercury Species in the Aqueous Phase.* (Intellecta Docusys AB, Göteborg, Sweden, 2003).
126. Andersson, M. E. *Transport of Mercury species in the Environment.* (Intellecta Docusys AB, Göteborg, Sweden, 2008).
127. Fantozzi, L., Ferrara, R., Frontini, F. P. & Dini, F. Factors influencing the daily behaviour of dissolved gaseous mercury concentration in the Mediterranean Sea. *Mar. Chem.* **107**, 4–12 (2007).
128. Lanzillotta, E., Ceccarini, C. & Ferrara, R. Photo-induced formation of dissolved gaseous mercury in coastal and offshore seawater of the Mediterranean basin. *Sci. Total Environ.* **300**, 179–87 (2002).
129. Ferrara, R. *et al.* Profiles of dissolved gaseous mercury concentration in the Mediterranean seawater. *Atmos. Environ.* **37**, 85–92 (2003).
130. Kentisbeer, J., Leeson, S. R., Clark, T., Malcolm, H. M. & Cape, J. N. Influences on and patterns in total gaseous mercury (TGM) at Harwell, England. *Environ. Sci. Process. Impacts* **17**, 586–595 (2015).
131. Kentisbeer, J. *et al.* Patterns and source analysis for atmospheric mercury at Auchencorth Moss, Scotland. *Environ. Sci. Process. Impacts* **16**, 1112–1123 (2014).
132. Wängberg, I., Munthe, J., Ebinghaus, R., Gårdfeldt, K., Iverfeldt, Å., Sommar, J. Distribution of TPM in Northern Europe. *Sci. Total Environ.* **304**, 53–59 (200AD).
133. Coquery, M. & Cossa, D. Mercury speciation in surface waters of the north sea. *Netherlands J. Sea Res.* **34**, 245–257 (1995).
134. Pallas fells - topography, climate and history. *FINNISH METEOROLOGICAL INSTITUTE* (2016). Available at: <http://en.ilmatieteenlaitos.fi/pallas-fells>. (Accessed: 5th October 2016)
135. Aspomo, K. *et al.* Mercury in the atmosphere, snow and melt water ponds in the North Atlantic Ocean during Arctic summer. *Environ. Sci. Technol.* **40**, 4083–9 (2006).
136. Dastoor, A. *et al.* Atmospheric mercury in the Canadian Arctic. Part II: Insight from modeling. *Sci. Total Environ.* **509–510**, 16–27 (2015).

137. Bieser, J. *et al.* A diagnostic evaluation of modeled mercury wet depositions in Europe using atmospheric speciated high-resolution observations. *Environ. Sci. Pollut. Res.* **21**, 9995–10012 (2014).
138. Dastoor, A. P., Durnford, D. A. & Accepted, J. Arctic Ocean : Is it a sink or a source of atmospheric mercury ? (2013).
139. Crabeck, O. *et al.* First ‘in situ’ determination of gas transport coefficients (DO₂, DAr, and DN₂) from bulk gas concentration measurements (O₂, N₂, Ar) in natural sea ice. *J. Geophys. Res. Ocean.* **119**, 6655–6668 (2014).
140. Douglas, T. a. *et al.* Frost flowers growing in the Arctic ocean-atmosphere–sea ice–snow interface: 1. Chemical composition. *J. Geophys. Res.* **117**, D00R09 (2012).
141. Douglas, T. a. Elevated mercury measured in snow and frost flowers near Arctic sea ice leads. *Geophys. Res. Lett.* **32**, L04502 (2005).
142. Gencarelli, C. N., De, S. F., Hedgecock, I. M., Sprovieri, F. & Pirrone, N. Development and application of a regional-scale atmospheric mercury model based on WRF/Chem: a Mediterranean area investigation. *Environ.Sci.Pollut.Res.Int.* **21**, 4095–4109 (2014).
143. Žagar, D. *et al.* Mercury in the Mediterranean. Part 2: processes and mass balance. *Environ. Sci. Pollut. Res.* **21**, 4081–4094 (2014).
144. Steen, A. O. *et al.* Natural and anthropogenic atmospheric mercury in the European Arctic: A fractionation study. *Atmos. Chem. Phys.* **11**, 6273–6284 (2011).
145. J. C. Comiso, C. L. Parkinson, T. Markus, D. J. C. and R. G. Current State of the Sea Ice Cover. *NASA Cryosphere Science Research Portal* Available at: <http://neptune.gsfc.nasa.gov/csb/index.php?section=234>. (Accessed: 29th September 2016)
146. Zhang, Y., Jaeglé, L. & Thompson, L. Natural biogeochemical cycle of mercury in a global three-dimensional ocean tracer model. *Global Biogeochem. Cycles* **28**, 553–570 (2014).
147. Jouni Vainio, Patrick Eriksson, Natalija Schmelzer, Jürgen Holfort, Jan Tegtmeier, Magnus Larsson, Sian Petersen, Andris Viksna, I. S. and M. S. THE BALTIC SEA ICE SEASON 2011-2012 THE BALTIC SEA ICE SEASON 2011-2012. *HELCOM Baltic Sea Environment Fact Sheets* Available at: <http://www.helcom.fi/baltic-sea-trends/environment-fact-sheets/>.
148. Sorensen, A. L. *Gaseous mercury in the marine boundary layer: measurements and modeling.* (2011).
149. Viñas, M.-J. Arctic sea ice annual minimum ties second lowest on record. *NASA Earth Science News Team* (2016). Available at: <http://climate.nasa.gov/news/2496/arctic-sea-ice-annual-minimum-ties-second-lowest-on-record/>. (Accessed: 4th October 2016)
150. Turner, J., Overland, J.E., Walsh, J. E. An Arctic and Antarctic perspective on recent climate change. *Int. J. Clim.* **27**, 277–293 (2007).
151. J. C. Comiso, C. L. Parkinson, T. Markus, D. J. C. and R. G. Current State of the Sea Ice Cover. *NASA Cryosphere Science Research Portal* Available at: <http://neptune.gsfc.nasa.gov/csb/index.php?section=234>. (Accessed: 4th October 2016)

152. Cole, a. S. & Steffen, a. Trends in long-term gaseous mercury observations in the Arctic and effects of temperature and other atmospheric conditions. *Atmos. Chem. Phys.* **10**, 4661–4672 (2010).
153. Cole, a. S. *et al.* Ten-year trends of atmospheric mercury in the high Arctic compared to Canadian sub-Arctic and mid-latitude sites. *Atmos. Chem. Phys.* **13**, 1535–1545 (2013).
154. Zhang, Y. *et al.* Observed decrease in atmospheric mercury explained by global decline in anthropogenic emissions. **113**, 1–6 (2015).
155. Fisher, J. A. *et al.* Factors driving mercury variability in the Arctic atmosphere and ocean over the past 30 years. *Global Biogeochem. Cycles* **27**, 1226–1235 (2013).
156. Stern, G. A. *et al.* How does climate change influence arctic mercury? *Sci. Total Environ.* **414**, 22–42 (2012).
157. Lalonde, J. D., Poulain, A. J. & Amyot, M. The role of mercury redox reactions in snow on snow-to-air mercury transfer. *Environ. Sci. Technol.* **36**, 174–8 (2002).
158. Krabbenhoft, D. P. & Sunderland, E. M. Global Change and Mercury. *Science (80-.)*. **341**, 1457–1458 (2013).
159. Rafaj, P., Cofala, J., Kuenen, J., Wyrwa, A. & Zyśk, J. Benefits of European climate policies for mercury air pollution. *Atmosphere (Basel)*. **5**, 45–59 (2014).

Paper I

Paper II

Paper III

Paper IV

Paper V